Characterisation of complex polymer mixtures

A thesis submitted to the
UNIVERSITY OF MANCHESTER

For the degree of
DOCTOR OF PHILOSOPHY

In the
FACULTY OF ENGINEERING AND PHYSICAL SCIENCE

2010

NASSER M ALHARBI

SCHOOL OF CHEMISTRY

Contents

List of Figures

List of Tables

Abbreviations

BHT	Butylated hydroxytoluene
CH	Cyclohexane
CF	Chloroform
DCM	Dichloromethane
DMAc	Dimethylacetamide
DMF	Dimethylformamide
DP	Degree of Polymerization
HDPE	High-density polyethylene
LLDPE	Linear Low-density polyethylene
LDPE	Low-density polyethylene
MALDI-TOF	Matrix Assisted Laser desorption/ionization time of flight
M	Molecular mass
PIM	Polymer of Intrinsic Microporosity
ppm	Parts per million
PS	Poly(styrene)

PE	Polyethylene
PP	Polypropylene
SFE	Supercritical fluid extraction
THF	Tetrahydrofuran
THSB	5,5’,6,6’-Tetrahydroxy-3,3,3’,3’ tetramethyl-1,1’-spirobisindane
UV-Vis	Ultraviolet-Visible
TCTPN	1,4-dicyanotetrachlorobenzene
TFPN	1,4-dicyanotetrafluorobenzene
UAE	Ultrasonic-assisted Extraction
PDI	Polydispersity Index

Abstract

The polymer of intrinsic microporosity PIM-1 was synthesized following various procedures: (i) from fluoro-monomer by the conventional method, (ii) from fluoro-monomer by a high temperature, high shear mixing method and (iii) from chloro-monomer. For a more complete understanding of the structure of the resultant products of a series of polymerizations under different reaction conditions, a multi-detector gel permeation chromatography (GPC) method was established and validated. A procedure for fractionating PIM-1 using chloroform methanol solvent mixtures was established and validated. A combination of multi-detector GPC and matrix-assisted laser desorption/ionization – time of flight (MALDI-ToF) mass spectrometry was used for the determination of molar mass distribution and to identify structural differences between fractions and between the products from different synthetic procedures. High molar mass samples tended to have broader molar mass distributions. Both Mark-Houwink plots and hydrodynamic volume plots showed deviation from linearity at Mw = 200000 g mol^{-1}, which was attributed to branching. A low cost route for the preparation of PIM-1 from chloro-monomer was successfully established, though samples prepared by this route had broader polydispersities than those prepared from fluoro-monomers. It was found that stable flexible membranes were formed from samples with Mw > 83000 g mol $^{-1}$.

In addition, a comparison of two analytical methods for extraction and determination of additives in HDPE, LLDPE and PP polymers of interest to Saudi Basic Industries Corporation was performed. A comparison of dissolution with ultrasonic assisted extraction methods for the determination of anti-oxidant additives in polyolefins was performed. Ultrasound assisted extraction methods were found to be superior for HDPE and LLDPE, where conventional dissolution was preferred for PP.

Copyright

Copyright and ownership of intellectual property rights

Declaration

I declare that no portion the work referred to in the thesis has been submitted in support of an application for another degree or qualification of this or any other university or institute of learning.

Acknowledgements

First of all, I would like to express my sincere gratitude to Professor Yeates, for his direction, continuous encouragement, valuable suggestions and ideas in this work.

I would like to thank Professor Peter Budd who although has a demanding schedule, never ceased to be able to provide myself and other students with helpful advice and always seemed to take our needs as paramount, for which I am eternally grateful.

I would like to thank the Saudi Basic Industries Corporation, Chemical Research Department, for their support in my Higher Education Program at the University of Manchester.

I have had the pleasure of working with Professor. Peter Budd's group. I have found them energetic contributors to the success of the group as a whole. I can recommend students without reservation to work with this group. Louise Maynard-Atem and Christopher Mason are gratefully acknowledged for provision of a range of PIM-1 samples for analysis. Special thanks for Mr. Keith Nixon for his technical support during my work in the GPC lab.

To Dr. Amjad Yakhoul, UK & International Service Manager, Polymer Laboratories Ltd, and Mrs Kariman Yakhoul for their advice, support, encouragement and their help during my time in Great Britain.

To my parents and my dear wife, Mashael for their patience and support and a special thank to my lovely children, my daughter Atharee and my son Alwaleed for their love and patience.

Chapter 1: Introduction

1.1 Aims and objectives

In this study, the first aim was to establish a reliable characterization method to study the effect of the reaction conditions on the products of PIM-1, a polymer of intrinsic microporosity, made by a series of polymerizations under different reaction conditions, and the effect of the nature of the product on its application, such as film forming ability. Specific objectives were (i) to prepare a sample of PIM-1 within the detection limits of a combination of two analytical techniques, multi-detector GPC and MALDI-ToF mass spectrometry, and (ii) to establish a procedure for fractionating high molar mass PIM-1 using solvent/non-solvent mixtures.

A second aim was to investigate low cost routes to high molar mass PIM-1. To achieve this, PIM-1 was prepared using a relatively cheap chloro-monomer instead of a fluoro-monomer.

In addition, a third aim was to establish an inexpensive, rapid and simple method to measure quantitatively the additives contained in different grades of polyethylene (PE) and polypropylene (PP) samples. The initial plan to achieve such objectives is to establish a reliable HPLC method in order to separate different types of pure additives by high resolution chromatographic separation and then to focuses on simple and an inexpensive analytical methods, such as ultrasonic bath techniques and refluxing, with subsequent direct determination by LC-UV diode array.

1.2 General Introduction

It is very important for a customer or any end user to have a product of high quality; therefore the structure of a polymer and the amount of any additives added to it during the manufacturing process must be well known and understood to avoid an unacceptable finished product. Such information is important for a polymer under investigation, to provide an understanding of the relationships between the synthesis and molecular properties of polymers, and between their molecular and bulk properties. For example, if two samples of the same polymer are similar in melt viscosity, it may nevertheless not be possible to use them for the same application because of differences in manufacturing, causing significant divergence in the molecular weight distributions of the two resin samples, which is known to affect a large number of properties. Such differences will affect the quality of the finished product. The resolution of this issue requires a powerful technique to measure this parameter.[1,2,3] As this work can be done by using gel permeation chromatography, it has become one of the most critical techniques in the polymer industry as the principal method of molecular weight analysis in many polymer laboratories.[4] Its power lies in its ability not only to give rapid analysis with high resolution[5] but also to provide information on the whole molecular weight distribution.[6] The multi-detection GPC system is a more advanced form of GPC which utilizes additional detectors to provide a complete picture: not only to determine the absolute molecular weight with high precision directly, without GPC column calibration in advance,[7,8] but also structure information over the whole molecular weight range,[9] characterizing long chain branching in polymers[10,11] and to overcome the limitations of conventional GPC,[12] which only detects differences in hydrodynamic size. In multi-detector GPC, the column is connected to a differential refractive index detector or UV detector as a concentration detector, a capillary viscometer and a static laser light-scattering photometer as a molecular mass-sensitive detector to assess the molecular weight distribution and molecular

weight structure of polymers without having a column calibration, while in the conventional GPC system it is connected only to a single concentration detector, such as a differential refractive index detector.[13]

In this study we are aiming to characterize the polymer of intrinsic microporosity PIM-1 prepared under different reaction conditions, to determine the optimum reaction conditions which will be suitable for different applications. In addition to that, we aim to investigate a low cost route for the preparation of PIM-1. As PIM-1 is solution processable, it can be cast into robust freestanding films. The ease of processing, good stability and high internal surface area of PIM-1 make it a promising material for use in organophilic separation membranes, which leads to the need to understand of the resultant polymer structure to investigate its effect in such an important application. Research related to PIM-1 is reported in chapters 2-6 of this thesis.

In addition, we are aiming to establish an inexpensive, rapid and simple method to measure quantitatively the additives contained in different grades of PE such as high density polyethylene, low density polyethylene, and linear low density polyethylene and in PP samples.

Polymers today constitute one of the most widely used groups of materials, indispensable to people all over the world. They are essential in the manufacture and provision of clothing, shelter, transport and communication, as well as to many conveniences of modern living. Appropriately selected additives are vital in improving their properties.[14] The main goal of adding these additives, such as plasticizers, antioxidants and ultraviolet (UV) light absorbers, is to alter the properties or prolong the life of the polymer.[15] If additives are not incorporated, polymers would not be able to perform such diverse functions, as some would degrade, oxidize, cross-link, discolour, lose molecular weight or become brittle with time and exposure to air, heat, radiation, metals or other chemicals. Without the direct assistance of

additives, polymers such as polyethylene are very susceptible to air oxidation.[16] Additives as a whole are considered to be very important in improving the performance and stability of most polymer resins.

The most widely used thermoplastic polymers are polyolefins, which are employed in an extremely wide range of applications.[17] Unless they are protected with efficient antioxidants, polyolefins are subject to thermal and oxidative degradation and cannot be used in practical applications, such as automobile parts.[18] Suitable amounts of additives must be added to commercial polyolefins so as to prevent their degradation both during processing and their lifetime and to achieve optimal performance in specific applications.[17] Polyolefins are stabilized by antioxidants mainly composed of sterically hindered phenols in combination with phosphites, to ensure non-degradative processing and long-term stability.[19] These antioxidants themselves undergo many chemical transformations and yield numerous transformation products as a consequence of their interceding to protect polymers against the chemical effects of oxygen, heat and light. Similarly, the physical loss of stabilizer can result from diffusion, photochemical reactions and degradation to smaller fragments, evaporation or washing out, and this physical loss of stabilizers accelerates the aging of polymers more than thermal oxidation or photo-oxidation.[20] Failures in polymeric materials can in the same way be attributed mostly to the leaching of antioxidants from the polymer or their chemical transformation. Developing methods to determine the amount of un-reacted antioxidants present to guarantee non-degradation of polyolefins during use is thus deemed a necessity.[19]

As the properties of a polymer product are affected by the purity and amount of additives incorporated into it, there is increasing need for reliable, rapid and accurate analytical methods to characterize such additives and to determine the amounts present. Manufacturers and regulators need to know the level of these materials in the polymer in order to ensure a product's fitness for its intended purpose.[15] There are several methods that can be utilized for

the extraction of additives from polymers; this thesis concerns the principal points of such methods. Research on the analysis of additives in polyolefins is reported in chapter 7 of this thesis.

1.3 Introduction to Polymers of intrinsic microporosity (PIMs)

A porous material is defined as a material having cavities, channels or interstices that have greater depth than width.[21] it is classified as follows ; a microporous material which contains interconnected pores of less than 2 nm in diameter, mesoporous material which contains interconnected pores between 2 and 50 nm; and macroporous material which contains interconnected pores greater than 50 nm.[22] The accessible surface area for the microporous materials is measured by gas adsorption and is found to be large (300-2000 m^2 g^{-1}). In addition to the zeolites and activated carbons, which are considered to be the conventional microporous materials, the recently developed and emerging materials, including metal organic frameworks (MOFs) and polymers of intrinsic microporosity (PIMs) are most widely used as adsorbent materials as such materials have characteristically high surface area. It could be used in different applications, such as molecular separations and storage and heterogeneous catalysis.[23,24,25,26] The success of these materials has resulted in opportunities for advances in such technological areas as hydrogen storage. The creation of microporous materials from organic components is particularly interesting, because such materials are expected to allow a high degree of control over the chemical nature of the large accessible surface area.[27]

Polymers of Intrinsic Microporosity (PIMs), which are novel porous materials, can be prepared as insoluble networks [28-30] or soluble polymers.[31] They have attracted great interest in different potential applications, including membrane-based gas separation, adsorption of small molecules, and heterogeneous catalysis.[32] Due to a contorted zig-zag structure these polymers show inefficient chain packing, generating very high free volume.[33-35] Polymers

with no single bonds in the spine, and with sites of contortion such as spiro-centres, have a random molecular structure with a large amount of interconnected free volume in the glassy state. Such polymers containing interconnected pores of less than 2 nm are microporous materials according to the International Union of Pure and Applied Chemistry (IUPAC) definition. Recently, a range of polymers with intrinsic microporosity has been developed for use in various applications, such as insoluble network-PIMs, which contain catalytic centres, and soluble PIMs for forming membranes, such as PIM-1.[34,35]

PIM-1 is an example of a non-network ladder polymer of intrinsic microporosity that will be presented in more detail. The microporosity of this polymer is a result of its unique structure: it has inefficient chain packing in the solid state due to its highly rigid and contorted molecular structure, generating a very high free volume **(Fig. 1)**, which is why it is said to have intrinsic microporosity. PIM-1 is prepared by a nucleophilic aromatic substitution reaction between 1,4-dicyanotetraflurobenzene (TFPN) or 1,4-dicyanotetrachlorobenzene (TCTPN) and 5,5',6,6'-tetahydroxy-3,3,3',3'-tetramethyl-spirobisindane (THSB), using anhydrous potassium carbonate as a base and anhydrous dimethylformamide (DMF) as the solvent **(Fig. 2)**.[35] The conventional method comprises polymerization at 8% monomer concentration (monomer/DMF: w/w) at 65 °C for 72 hours.[31, 34, 36-38] Under similar reaction conditions to the conventional conditions,[39,40] Kricheldorf and coworkers[41] concluded that the majority of the product was cyclic, which results in low molecular weight polymer and high polydispersity.[41] More recently, a Canadian research group optimized the conditions, using a high-speed homogenizer at about 155 °C to provide a high molecular weight PIM-1 ladder polymer in high yield within a few minutes which is almost free of crosslinking and cyclic species.[33] The synthesis of PIM-1 by the nucleophilic aromatic substitution reaction between TCTPN and THSB, using anhydrous potassium carbonate as a base and anhydrous DMF as the solvent was investigated and reported by Kevin Reynolds. He concluded that the majority

of the product was a large amount of low molecular weight oligomeric material due to the lower reactivity of the chlorinated monomer.[42]

PIM-1 is a thermally stable, amorphous and glassy polymer which has a surface area, as measured by nitrogen adsorption at 77 K, greater than 700 $m^2 g^{-1}$ and is soluble in some organic solvents such as tetrahydrofuran and chloroform. In membrane form, the performance of the highly microporous and rigid PIM-1 **(Fig. 1)** in the separation of a number of important gases was investigated in terms of the selectivity ($\alpha = P_i/P_j$) and permeability (P_i) of the desired component. Compared with other polymers, it shows high permeability coupled with a high selectivity for O_2/N_2 and other important gases such as CH_4/CO_2.[38] It also shows a significant adsorption of H_2 (1.7% by mass) at relatively low pressure and adsorption of organic materials such as phenol from aqueous solution.[27, 32, 38, 43]

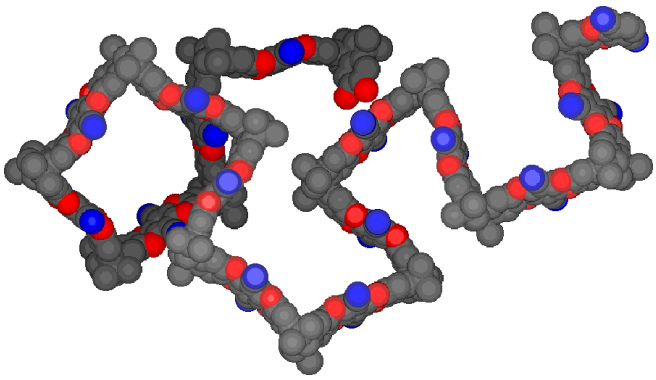

Figure 1 The molecular model of a random fragment of PIM 1 showing its highly rigid and contorted structure[42]

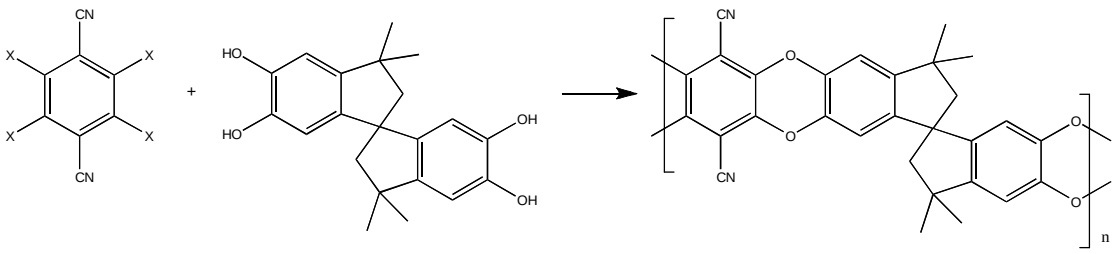

Figure 2 Synthesis of PIM 1. Reagents and conditions: x = Cl or F, K_2CO_3, DMF, 65°C

1.4 Step-growth polymerization reactions

In step-growth polymerization, the reactive functional groups present in the monomers are linked to each other, forming a polymer. In such polymerization, chain growth occurs when any suitable combination of molecular species present in the reaction mixture (monomer with monomer, monomer with polymer, and polymer with polymer).[41,44] The molecular weight and the polymer size of the product both depend on the conversion percentage: as this increases, both polymer size and molecular weight will gradually increase with time, which makes extent of reaction a critical factor influencing the degree of polymerization and consequently the molecular weight of polymers. The process is also often described as condensation polymerization if synthesis involves the elimination of a low molecular weight by-product[45] such as small molecules like water, methanol or hydrogen halides.[41] The absence of the termination step in step-growth polymerization makes it different from chain-growth polymerization and the ends of the polymer chains remain reactive.[46]

The relationship between the degree of polymerization ($\bar{x}_n$) and the extent of the reaction (p) is given by Carothers in the following equation:

$$\bar{x}_n = \left(\frac{1}{1-p} \right)$$

With reference to this equation, a very high (>0.99) extent of reaction is required to achieve a high molecular mass polymer in step-growth polymerization reactions. In other words, more than 99% of the end groups must react.[46-48]

1.5 Introduction to Gel Permeation Chromatography

Gel permeation chromatography (GPC) was invented by Grant Henry Lathe and Colin R Ruthven, who were working at Queen Charlotte's Hospital in London,2 and later in 1959, J. Porath and P. Flodin demonstrated that columns packed with cross-linked polydextran gels could be used for aqueous media to separate many water-soluble macromolecules.[49] The use

of cross-linked polystyrene gels was disclosed in 1964, by J.C. Moore for separating synthetic polymers soluble in organic solvents.[3,49] The column materials that were used by Porath and P. Flodin for gel filtration and by J.C.Moore for gel permeation was limited to relatively low flow rates and pressures, <250 psi, because they were made of lightly cross-linked, porous, semirigid, organic-polymer networks. The development of small and more rigid porous particles results in the modern high-performance size-exclusion chromatography (HPSEC). µ-Styragel was the first small particles introduced commercially by Waters Associates, Milford, Massachusetts. These particles were semirigid, 10 µm in size, and could be used at relatively high pressure, 2000-3000 psi, providing performance 10 times better than that of the cross-linked polystyrene macroparticles, 70-150 µm in size, that previously had a wide use.[50] It is considered a powerful analytical technique, widely accepted and used for the characterization of molecules differing in size and molar mass,[51] compared with other methods of analysis, such as, for example, osometry and static light scattering, and the only proven one for providing the complete molecular weight distribution of natural and synthetic polymers and proteins.[49, 52] In its conventional form using a single concentration detector, it gives only relative molecular masses. For this reason, and for characterisation of increasingly complex polymers, there was a strong push to extend the capability of conventional GPC not only to obtain absolute molecular weights, but also information on structure and conformation. The procedure is known as gel filtration chromatography (GFC) when an aqueous solution is used as a mobile phase to separate water soluble polymers[52] and gel permeation chromatography when the mobile phase is an organic solution.[53]

1.5.1 Conventional Gel Permeation Chromatography

1.5.1.1 GPC Principle

The principle of GPC is very straightforward: particles of different sizes dissolved in a suitable solvent will pass through a stationary phase at different rates, which results in the separation of the particles according to their effective size in solution, which could be quite different for different polymers of the same molecular weight.[53, 54] Thus, the technique does not depend on molecular weight or chemical differences to achieve separation. By this means, particles of the same size will be eluted together. Since separation depends on the size of the particles in solution, there should be no interaction with the stationary phase material. The process takes place in an apparatus called a column, which is an open tube filled with a material of controlled porosity and particle size. This material, which has millions of highly porous, rigid particles of different sizes, acts as a molecular filtration system.[49] The smaller particles permeate more deeply into the porous matrix and so are retained in the column for a longer time, while the larger ones cannot permeate so readily and hence are eluted first.[49] The stationary phase material is usually crosslinked polystyrene for polymer applications and polyacrylamide, dextran or agarose for biological polymers.[55]

1.5.1.2 GPC application

The application of GPC is limited to the separation of macromolecules or particles of different sizes, as it does not discern differences among particles of the same size very well. GFC can be used to separate large molecules such as proteins and other water-soluble polymers, while determination of the size and polydispersity of synthesised organic-soluble polymers is achieved by using GPC. The absolute molecular weights can be measured without need for a column calibration by coupling techniques such as light scattering and/or viscometry with GPC. This is a desirable method because of the difference in size of two polymers with identical molecular weights.[2] Several important parameters can be determined

by GPC, such as number average molecular weight (M_n), weight average molecular weight (M_w) and the molecular weight distribution of a polymer, which is considered its most fundamental characteristic.[56]

Indeed, all of these parameters are of great importance because they are correlated to significant differences in the physical properties of polymers, such as adhesive strength, impact strength, hardness and melt viscosity. For example, both adhesion and hardness will be lower in a polymer with a narrow molecular weight distribution. The distribution shape depends on how polymerization is carried out, so that it will be fairly narrow for a condensation or step-growth polymer such as polyester and very broad for a polyolefin or other polymer formed by free radical polymerization. Obtaining the desired molecular weight distribution depends on controlling the kinetics of polymerization, which makes GPC a powerful analytical instrument for the polymer chemist.[56]

1.5.1.3 GPC instrumentation

The basic GPC instrument (**Fig. 3**) consists of an injector, either manual or automated, to introduce the sample solution into the mobile phase, the column and a detector. The column must be heated to some elevated temperature in order to enhance the solubility of the sample and maintain dissolution, to increase the resolution and in some cases to reduce the viscosity of the solvent and hence the backpressure across the column. A high-pressure pump is also required to overcome the resistance of the column material to the flow and to deliver the solution into system.[49] A degasser is sometimes used to remove air bubbles, mainly when using tetrahydrofuran (THF) solvent with a refractive index detector; this can also be achieved by purging the mobile phase with helium, which is insoluble in almost all solvents. The final elements are a detector to monitor the separated particles[50, 56,49] and a computer with suitable software to analyze and report the output.[55] However, in its conventional form,

i.e. using a single concentration detector, the performance of the pump is a critical issue in the separation process, because the system is calibrated by plotting the logarithm of the molecular weight against retention time or volume, so any fluctuation in the flow rate will result in a large error in molecular weight determination. It is also important for the results to be kept independent of viscosity differences by delivering the same flow rates, because different polymers produce solutions of different viscosities. When the mobile phase is changed the system should be flushed with the new one and the mobile phase reservoir should be full enough to allow for continuous running of the apparatus. The injector used for molecular weight measurement will have a relatively small capacity, which will be large if fraction collecting is desirable. The column must provide repeatable and reproducible results, while the detector must be nondestructive to allow the eluted particles to be collected and used in further analysis, if required.[49, 56]

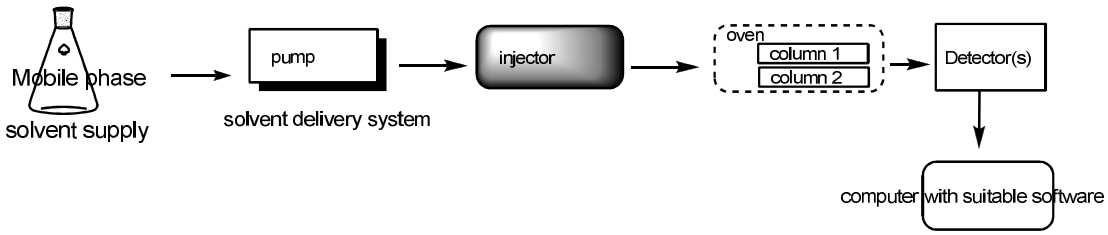

Figure 3 The basic components of a GPC instrument

1.5.1.4 GPC Columns

There are three types of column: "the linear" or "mixed bed" column,[52,57] which covers a broad molecular weight range with fairly linear calibration,[58] and the single pore size column, which is sensitive to a narrow range. Each type has its limitations, the former giving poor resolution, while the latter covers only a limited molecular range; therefore, it is often better to use a series of columns rather than a single one of either type. In cases where the molecular

weight range of the sample polymer is very broad, or where the values are very uncertain, it is recommended to use a series of columns to give an acceptably wide molecular weight range, such as using three mixed bed columns or two mixed bed and a single column of 500 Å pore size. The reason for using a single pore size column with two mixed bed ones is to provide some pore volume and so to ensure that the low molecular weight tail of the sample is resolved from the impurity peaks that usually appear at the end of the chromatogram.[56] The third type is named "multipore" column composed of a single gel type, but each bead contains a wide range of pore sizes. Consequently, such a column has very wide resolving range, which results in a better resolution.[52]

1.5.1.5 GPC Detectors

In its simplest form (conventional GPC), either a refractive index detector (RF), which also referred as a Differential Refractometer, or a UV detector[49] is used to obtain a concentration profile of the eluted polymer sample, that is converted into a relative molecular weight. Since all compounds refract light[49] and many polymers have no chromophores[50] the differential refractometer has become the detector most often used to screen molecular weight distribution, especially for polymers above 1000 M_w which have a constant refractive index (RI), so that detector response is directly proportional to concentration only. It measures the difference in refractive index between the mobile phase and the mobile phase containing the sample, hence measuring the concentration of the solution.[49, 55] The RI signal represents the concentration of the sample solution eluting from the GPC column, not the polymer molecular weight or size.

$$RI(signal) = K \bullet \left(\frac{dn}{dc} \right) \bullet c$$

Where K is a constant, dn/dc is the refractive index increment and c is the concentration in mg/ml.[59]

Besides information about molecular weight averages and distribution obtained with RI, information about composition can be obtained by coupling the GPC with UV absorbance detectors. The use of light-scattering and viscometer " molecular-weight-sensitive" detectors [60] provides information about polymer structure by offering a way to obtain not only the intrinsic viscosity [η] of the polymer, but also the absolute molecular weight and estimation of long-chain branching in a single analysis.[8, 58, 61, 62]

1.5.1.6 Sample preparation

The samples should be completely dry to be accurately weighed. The polymer samples were dried in a vacuum oven at 100 °C to obtain an accurate concentration measurement because the solvent residue will result in inaccurate calculated weights which will directly result in inaccurate calculated concentration. Such uncertainty will affect the determination of the concentration across the molecular weight distribution which directly affects the determination of the intrinsic viscosity by the viscometer and/or the determination of the molecular weight by light scattering. The concentration of the injected polymer solution was optimized due to the difference in sensitivity between the refractometer, a mass-sensitive detector, and the molecular-weight sensitive detectors (viscometer or light scattering) in order to reduce the noise level in the resultant raw chromatograms.[63, 64]

It is important for the sample solution to be filtered under vacuum before use in GPC. A fluorocarbon filter (0.45 µ) is commonly used for organic solutions, while an acetate filter is used for aqueous solutions.[56] The elution volume is affected by the concentration and the viscosity, so that the column should not be loaded with a sample solution which is too highly concentrated. If the sample solution is more viscous than the mobile phase, then the mobile phase will take a long time to dilute it, resulting in a broad peak, long retention time and hence incorrect measurement.[53, 65] The sample concentration should therefore not be too high,

to avoid overloading the column, but it must be high enough to yield an acceptable signal-to-noise ratio. Generally, the ideal concentration of the sample solution depends on the molecular weight, so for a polymer whose average molecular weight is more than 10^6 it is 0.01% (w/v), while for a polymer of average molecular weight between 20 000 and 10^6 it is 0.1% (w/v). The exact concentration is required if viscometry or light-scattering analysis is being performed, so that it is important to multiply the sample weight by density when the analysis is being done at elevated temperature. The preferred instrument flow rate is often 1 ml/min, which is considered a compromise between resolution and speed.[50] Polar solvents such as methanol, isopropanol and ethanol are not compatible with a stationary phase composed of polystyrene gel, because such solvents will damage the column bed by causing extreme shrinkage in the polystyrene gel. The selected mobile phase should therefore be compatible with both the detector and column used.[53] it also needs to be a good solvent to dissolve the sample at appropriate temperature and sufficiently long before running it to allow the polymer coil to swell in the solvent or to break down aggregates, so as to avoid nonexclusion effects. In some cases an additive is required in the mobile phase to prevent certain interactions that might otherwise occur between the solution and the stationary phase material. For example, 0.05 M of lithium bromide is added to polar solvents such as DMF, which is used to analyze polar polymers such as polyamides, to avoid a dipole interaction resulting in the appearance of a front tailing at the high molecular weight end of the distribution, while in high temperature analysis of polyolefins, an antioxidant is added to reduce oxidation of the sample.[56] Hence, solvents such as THF and toluene, which reduce hydrophobic interactions, are widely used for polymer applications. The mobile phase boiling point should be about 25-50 °C greater than the column temperature to maintain high resolution and to avoid bubble formation, which would interfere with detection.[50]

1.5.1.7 Calibration methods

The calibration process depends not only on the column set, as it is usually known, but also on the sample solvent, all external tubing connected to the instrument and the detector. Calibration is not greatly affected by small fluctuations in the temperature or flow rate, but should be done when changing solvent, columns, or the nature of the sample being analyzed.[50] Calibrating the system is important to give a molecular weight to each retention time slice for the eluted particles. The calibration procedure involves the determination of retention volumes of standards of known molecular weight, assuming that all the polymers will elute in a similar way, so that their mass distribution can be determined by reference to the calibration established with polymer standards which are commercially available.[9] There are three different calibration methods by using different detection techniques: The range of approaches includes broad standard or multiple narrow standards to create a calibration curve of log M vs. elution volume (conventional calibration)[49, 54, 66, 67] utilized by using size exclusion chromatography with a single concentration detector. This method has a limitation as it only measures relative molecular weight and molecular weight distribution values but not information about molecular conformation or size. [67, 68] In addition to that, unfortunately, only a few standards are commercially available, so that the universal calibration method[3] (2) suggested by Grubisic *et al*, [9] which uses a plot of the logarithm of the product of intrinsic viscosity and molecular weight against retention volume, is the method most widely used and has been widely demonstrated[12] to obtain an accurate molecular weight. It is utilized using size exclusion chromatography with a single concentration detector when Mark-Houwink constants of the standard and sample are known, or by GPC systems with dual detectors (concentration and viscosity) when the Mark-Houwink constants are unknown. It is applied if the separation occurs according to the size exclusion mechanism but not if there are significant polymer-stationary phase interactions, which are also known as nonsize-exclusion

effects, such as hydrogen bonding, or hydrophobic interactions.[49, 67, 68] Assuming that molecules of the same molecular size (hydrodynamic volume) elute at the same retention volume; for different polymer types, the hydrodynamic volume, which is given as $M[\eta]$ will be equal, so that the absolute molecular weight averages of sample, conformation and size information could be obtained using the universal calibration method through the Mark-Houwink relationship.[9, 67]

$$M_1[\eta]_1 = M_2[\eta]_2$$

Through the Mark-Houwink relationship,

$$M[\eta] = KM^{a+1}$$

By arranging these relationships, the molecular weight of the unknown sample can be obtained using the following equation:

$$LogM_2 = \left(\frac{1}{1+a_2}\right) Log\left(\frac{K_1}{K_2}\right) + \left(\frac{1+a_1}{1+a_2}\right) LogM_1$$

Where K_1, a_1 are Mark-Houwink constants for polymer standards and K_2, a_2 are those of the polymer under investigation.[49, 50]

The third method is called absolute molecular weight calibration. It is utilized by using size exclusion chromatography with a concentration detector coupled with a molecular weight sensitive detector, such as light scattering detector. The molecular weight result is generated without need to resort to external standards.[58, 67, 69]

1.5.1.8 Factors affect the separation

The passage of particles of different sizes through the column may be impeded by a pore which is not of the standard size. The particles of the stationary phase and the pores may also vary in size because they are not well defined, so the elution curves will resemble a Gaussian

distribution.[2] Any fluctuation in the flow rate can produce serious errors in molecular weight determination, so the flow rate must be constant and reproducible.[49] The retention time is influenced by unwanted interactions between the stationary phase and the particles passing through; therefore, much work has been done by column manufacturers to minimise this effect. The resolution is increased by increasing the column length, while the column capacity is augmented by increasing its diameter. The column should be well packed to avoid the collapse of the pores of the beads in an overpacked column or a reduction in the relative surface area of the stationary phase in an underpacked one. Filtering the sample may not be appropriate in all cases, as it may remove a significant amount of ultrahigh molecular weight polymer.[49] Temperature can have a significant effect on column resolution by causing a slight shift in the retention volume, but this effect is relatively minor when the sample is dissolved in a good solvent.[50] Adsorption is more noticeable with smaller particles because they penetrate many pores;[2] therefore, an increase in temperature is required to reduce this adsorption, which can be expected mainly with low molecular weight samples. Impurities may generate baseline noise, so the solvent and the mobile phase must be of high purity. To provide optimum baseline stability, the mobile phase should be used not only for the chromatograph but also to dissolve the standards and the sample being analysed. The adsorption or the degradation of the sample on the column may cause a low sample recovery by inhibiting the elution of the whole sample from the column.[50] Furthermore, the necessity of using diluted solution for macromolecules is quite difficult to achieve even with a good solvent. For example, a polymer such PVC may form strong aggregates in solution, which complicates the precise measurement of molecular weight.[9]

1.6 Multiple-detector GPC

1.6.1 Introduction

In conventional GPC, the system has to be calibrated with standards of a narrow molecular weight distribution having known molecular weight and the same structure as the unknown samples in order to determine the absolute molecular weight and the molecular weight distribution of the unknown polymer sample.[13] Unfortunately, there is a limited number of standards available in the market, so that the calibration step is usually the basic problem in conventional GPC. Coupling the GPC system with a differential RI detector and a capillary viscometer detector solves that problem,[70] as the calibration can be achieved by using standard polymers which are different in their chemical structure from the unknown samples. The system can also be calibrated using the sample itself with no need for a standard material, if the GPC system is coupled with a differential RI detector and a static laser light-scattering photometer. The use of molecular weight-sensitive detectors such as capillary viscometers and static laser light-scattering photometers offers the great advantage of obtaining several important parameters such as the intrinsic viscosity, molecular weight distribution and the Mark-Houwink coefficients. [13]

1.6.2 Principle of multi detection system

A UV spectro-photometric detector or refractometer detector, which give molecular weights that are not relative to the molecular weight of the unknown sample, but to calibrated standards, were used in the first twenty-five years of GPC development to measure molecular size, but the limited ability of the refractometer detector to distinguish between the effects of molecular weight and structural differences in changing the molecular size motivated work on improving GPC performance by developing two specialised detectors, using the scattering

of laser light and viscometry to provide more information[56] and so to meet the growing need for the characterization of new complex polymers.[59] The response of the light-scattering detector (equation [1.1]) is proportional to molecular weight and concentration, while that of the viscometer detector (equation [1.2]) is proportional to the intrinsic viscosity and concentration. These detectors will perform just as well, but the data can not be analysed without a concentration detector, so the GPC is normally coupled to three detectors.[59]

$$LS(signal) = K \bullet \left(\frac{dn}{dc}\right)^2 Mw \bullet c \qquad (1.1)$$

$$K = \left(\frac{4\pi^2 n_0^2}{\lambda_0^4 N_A}\right)$$

Where n_0 is the refractive index of the solvent, λ_0 is the wavelength of the incident light in a vacuum and N_A is Avogadro's number.[71]

$$Visc.(signal) = K \bullet \eta \bullet c \qquad (1.2)$$

Equation (1.1) shows that concentration and $\frac{dn}{dc}$ value must be known to determine the molecular mass. Because the refractive index increment, $\frac{dn}{dc}$ appears squared in the equation, any error in the determination of the refractive index increment will lead to a large inaccuracy in the reported results. In terms of sensitivity, the viscosity detector is more sensitive at low molecular weights than the light-scattering detector, which makes the viscosity detector more useful in applications with a polymer of low molecular weight.[59]

1.6.3 Light scattering detector

Light scattering is considered one of the few techniques available for the determination of the absolute molecular weight of macromolecules.[53] There are two types of light-scattering technique: static light or Rayleigh scattering, in which the scattered light intensity is measured as a function of angle, is used to determine the weight average molar mass, the square radius of gyration and the second virial coefficient, A_2, while dynamic light scattering, in which the fluctuation in the scattered light is measured as a function of time, is used to determine the hydrodynamic radius of macromolecules. It covers a wide range of molecular weights and is a nondestructive technique, so that the sample can be collected to be used in further analysis. For this reason, it is more widely used than some other traditional physiochemical techniques for the determination of molar mass, such as mass spectrometry, membrane osmometry and sedimentation equilibrium.[72]

Lord Rayleigh established the science of light scattering at the end of the 19th century. Since that time, the technique has been used within the limitations of the technology available until monochromatic, polarized lasers appeared in the early 1970s, when light scattering technology became applicable in research. In the early 1990s, some economical devices such as laser diodes of sufficient power, digital signal processors (DSPs) and avalanche photo-diodes (APDs) appeared on the market to help in making light-scattering detectors more reliable and stable, so that the use of such techniques became more widespread in research laboratories.[55] The different types of detectors available include low-angle laser light-scattering, multi-angle light-scattering and right-angle laser light-scattering photometers.[7] In order to determine molecular weight, all commercial light scattering detectors utilize the Rayleigh equation, which simply states that the intensity of the scattered light is equal to an optical constant times the concentration times the molecular weight. The way of measuring molecular weight is that a beam from a laser light source being focused on a cell holding the

sample solution, results in an interaction with the molecules of the sample, which induces a temporary dipole moment and thus scatters the light in different directions. The intensity of scattered light is proportional to the weight-average molar mass multiplied by the concentration of the macromolecules. When used as a GPC detector, the MW obtained does not depend on the Stokes radius of the macromolecule or the calibration curve, which depends upon running several standards of known molecular weight. The refractive index detector then measures the concentration of the sample eluting from the light-scattering detector. By assuming that the two instruments see the same chromatographic profile, the molecular weight profile is then computed slice-by-slice by dividing the light scattering signal by the concentration signal and including the appropriate constants.[55]

1.6.4 Light Scattering Theory

To understand the relationship between scattered light intensity and the weight average molecular weight, we need to apply the Rayleigh equation:

$$\frac{KC}{R_0} = \left(\frac{1}{M_w}\right) + 2A_2c \qquad [1.3]$$

Where R_0 is the Rayleigh factor at zero scattering angle, M_w is the weight-average molecular weight, c is the concentration of the solution, KC is an optical constant which includes $\frac{dn}{dc}$ and A_2 is the 2nd virial coefficient. The concentration on the right-hand side of the above equation [1.3] reflects the polymer-polymer interaction in the solution. In GPC this interaction is negligible,[55, 66] because the polymer is prepared as a dilute solution in the eluent and injected into the system, so that in the above expression, the scattered light is proportional to M_w in terms of the scattered light at zero degrees of angle, which is impossible due to the presence of the incident laser beam. For this reason, the scattered light

has to be measured at some other angles, which further complicates the process because the amount of scattered light is dependent on both the scattering angle and the size of the molecules being measured. This does not have a significant effect in the case of very small molecules, where it can be ignored. There are three ways to overcome such problems, using a multi-angle light-scattering (MALS) detector, in which the scattered light is measured at two or more angles, then extrapolating the data to a zero angle,[73] using a right-angle light scattering detector (RALS), in which the scattered light is measured at 90°, or using a low-angle light scattering (LALS) detector, where the angular effects are negligible because the scattered light is measured at a low angle, close to zero. [8] The third method is regarded as the only absolute method and has opened the possibility of using GPC-LS to measure molecular weights directly because it requires no extrapolation or correction.[55]

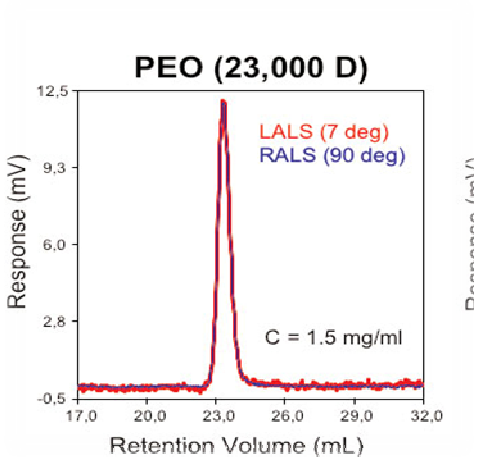

Figure 4 LALS and RALS signals for low molecular weight polyethylene oxide[55]

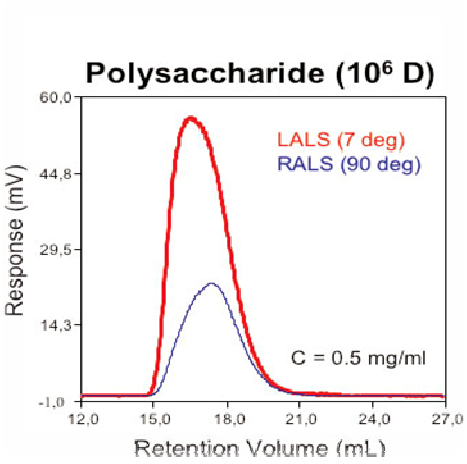

Figure 5 LALS and RALS signals for high molecular weight polysaccharide.[55]

A comparison of RALS and LALS is shown in **Figs. 4 & 5,** which illustrates the angular dependence effect on the accuracy of the calculated results, especially at high molecular weight (large molecular sizes). Both RALS and LALS detectors give the same signal for the low molecular weight polymer in the absence of angular effects, while the LALS gives an excellent signal-to-noise ratio for the high molecular weight polymer compared with the same ratio in the case of the RALS.[55]

1.6.5 Determination of d*n*/d*c* by multi-point RI method

The refractive index detector measures the change in the eluted sample concentration so the measurement of $\frac{dn}{dc}$ is required. This is also a requirement for determining the light-scattering constant K.[70] For a homopolymer, the measurement of dn/dc is mostly dependent on the monomer and weakly or even independent of molecular weight. For this reason, for a given polymer-solvent system it is a characteristic constant dependent on the temperature, T, and the light wavelength.[69] There are two ways to determine the $\frac{dn}{dc}$ for the polymer: either plotting RI detector peak area vs. sample concentration at constant injection volume, or

plotting RI detector peak area vs. injection volume at fixed sample concentration. The slope in both cases will be equal to the value of d*n*/d*c*. This method will help in estimating the precision of measurement to confirm the linear response of the RI detector. For example, using the first method, with fixed injection volume, $\frac{dn}{dc}$ can be calculated from the measured slope (RI peak areas were measured and plotted against sample concentration) equation below, assuming that the values for *RI.Cal*, n_0 and Conc. are known.

$$Slope = \left(\frac{RI_{cal}}{n_0}\right) \bullet \left(\frac{dn}{dc}\right) \bullet Vinj.$$

Where n_0 is the refractive index of the solvent at the detector temperature, $RI._{\text{Cal}}$ is the detector calibration constant and *V* inj. is the volume of sample injected in ml.[55, 69, 74]

1.6.6 Viscometer Detector

The viscometer detector was introduced by Ouano[55] in 1972, since when it has become one of the techniques applied to determine the molecular weight, intrinsic viscosity and Mark-Houwink parameters of polymers. The principle of the detector is that the change in the pressure when the polymer solution travels through a single capillary tube is compared with the same measurement for solvent alone. The pressure drop of the eluent across the capillary is measured using a variable transducer. The Hagen- Poiseuille equation is applied to transform this pressure drop signal to viscosity.[55]

$$\Delta P = KC \bullet Q \bullet \eta$$

Where ΔP is the pressure drop across the capillary, Q is the solution flow rate, η is the viscosity of the solution and KC is the capillary constant. Since the viscosity of a polymer solution depends on the ambient temperature, the viscosity of the solution is altered by any

variation in temperature. In addition, according to the Hagen-Poiseuille law, any fluctuations in the flow rate will result in an altered viscosity reading. For these reasons, the viscometer detector was not considered a reliable technique until multiple capillary tubes were employed by Haney[12] in the early 1980s. The pure solvent with viscosity η0 flows through all four capillaries (**Fig. 6**) with no change in the recorded differential pressure, ΔP, while the resistance in the capillaries R1, R2 and R3 will increase as the polymer solution travel through them. Thus, the increase in the differential pressure will be proportional to the solution viscosity.[12]

$$\eta_{sp} = \left(\frac{\eta - \eta_0}{\eta_0}\right) = \left(\frac{4\Delta P}{P_{in} - 2\Delta P}\right)$$

Where P_{in} is the inlet pressure and ΔP is the differential pressure recorded. Since the polymer is prepared in a very dilute solution, it can be assumed that its concentration is very close to zero; hence at infinite dilution intrinsic viscosity is determined by the formula[55]:

$$\left.\frac{\eta_{sp}}{c}\right|_{c\to 0} = [\eta]$$

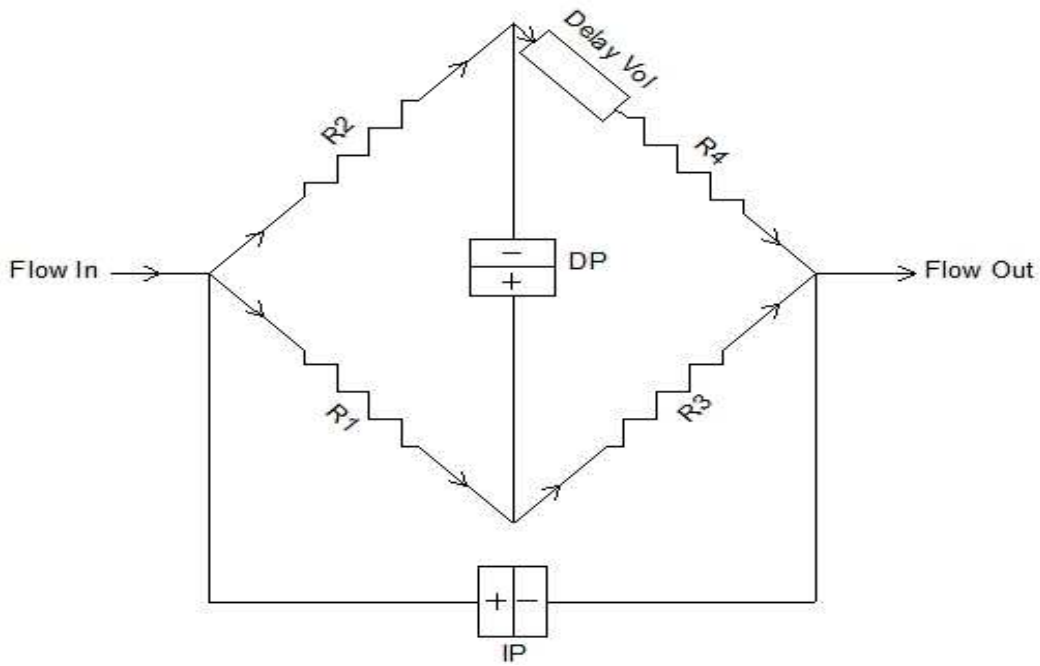

Figure 6 diagram of differential viscometer

1.6.7 Determination of the polymer structure

Determination of the polymer structure is more accurate and reproducible using a viscosity detector that measures the difference in the structure directly and can be applied to samples of a wide range of molecular weights. As the intrinsic viscosity is directly sensitive to structural differences, the polymer structure can be determined using the Mark-Houwink equation by plotting the double logarithmic plot of intrinsic viscosity vs. molecular weight. It reflects changes in the polymer structure, such as branching and chain rigidity.[59] The slope, described by the Mark-Houwink exponent a, is equal to 0, 0.5-0.8, and 1.8 for polymers in sphere, random coil, and rod shape, respectively.[59,75] This method provides the ability to determine how branched a polymer is, relative to a known linear polymer standard. It is important to know how a branched polymer will process in comparison to the linear counterpart. This method is quite sensitive to long chain branching, but it is insensitive to short chain branching.[76]

Another form of polymer structure analysis is described by the conformation plot of log *Rg* vs. log M_w that is constructed from light scattering data. Its slope varies from 0 to 1.[59] Furthermore, the value of *Rg* is equal to the slope of the plot of the inverse light-scattering intensity vs. $\sin^2(\theta/2)$. However, for a polymer with a coil diameter smaller than 1/20 of the wavelength of the light, the determination of *Rg* is not possible, because of the appearance of angular dependence in such polymers. The *Rg* approach is also unreliable for large polymers, which present a nonlinear angular dependence of the inverse scattering intensity. Therefore, for structural properties of polymers, determination of the polymer structure is more accurate and reproducible by means of viscosity detection, which is very sensitive to structural difference, rather than by light scattering.[59]

1.7 Introduction to HPLC

In high performance liquid chromatography (HPLC), the sample is introduced as a liquid onto the chromatographic column, which contains the stationary phase that is used to effect a separation. Unlike GPC, sample analyte mixtures are separated by distributing them between the mobile phase and the stationary phase in the column. The mobile phase can be a mixture or a single solvent such as water or hexane and the stationary phase can be packed porous silica particles.[77]

1.7.1 A brief history

Classical liquid chromatography (LC) was discovered in 1903 by Mikhail Tswett,[77] who separated plant pigments on chalk ($CaCO_3$) packed in glass columns. Later, in 1952, A.J.P. Martin and co-workers[77] from the United Kingdom invented gas chromatography and the successful applications of this new technique encouraged chemists to work on developing LC. The first use of a column of small particles was in the late 1960s and since that time LC has been developed to become high performance liquid chromatography (HPLC) because the use of such columns requires high pressure pumps. Horvath, Kirkland, and Huber[77] were the researchers who developed the first generation of high performance liquid chromatography. The development of in-line detectors and a reliable injector in the 1980s makes it a sensitive and quantitative technique. It has come to be considered one of the most critical analytical techniques, as it is capable of rapid and precise quantitative analysis and high sensitivity detection.[77]

1.7.2 Modes of HPLC

There are four main separation modes of HPLC: ion-exchange chromatography, gel permeation chromatography, normal phase chromatography and reversed-phase chromatography. The last two will be discussed in this chapter in some detail. Normal phase chromatography is also known as liquid-solid chromatography or adsorption chromatography. The separation process is based on the adsorption/desorption of the analyte onto a polar stationary phase, which is typically silica or alumina. Hence, polar analytes will be retained longer, due to strong interactions with the stationary phase material. For this reason, this mode is very useful for the separation of non-polar analytes. Reversed-phase chromatography is simply the opposite of the normal phase mode. Here, the separation process is based on the partition of the analyte between a polar mobile phase and less polar stationary phase. The stationary phase comprises solid particles coated with non-polar liquids, or octadecyl (C_{18}) bonded groups on silica supports, which are more permanently bonded hydrophobic groups. Hence, the polar analytes elute first, while the non-polar analytes are retained longer, due to strong interactions with the stationary phase material.[77]

1.7.3 Mobile phase

It is the solvent that moves the analyte down the column. It has a powerful influence on analyte retention and separation, as it interacts with both the analyte and the stationary phase. The selected mobile phase should therefore be non-corrosive to components of the HPLC system, highly pure, low in cost, viscosity and toxicity, non-flammable and of zero absorbance.[77]

1.7.4 Solvent strength and selectivity

The strength of a solvent is its ability to interact with the analyte, eluting it from the column. For example, in normal phase chromatography the non-polar hexane is described as a weak solvent, whereas water is a strong solvent. In reversed phase, water is a weak solvent and the organic solvents are strong, so that solvent strength increases from water to methanol to acetonitrile to THF.[77]

1.7.5 Isocratic and gradient analysis

The analysis can be performed under two basic elution modes: either isocratic or gradient. In the isocratic mode, the mobile phase used to elute the analytes remains the same throughout the run, making it useful for the separation of a single analyte or simple mixture of analytes of similar polarities, while in gradient elution the composition of the mobile phase changes during separation, which causes the ability of the solvent to interact with the analytes to increase with time throughout the run, making it preferable for the separation of more complex samples containing analytes of different polarities.[77, 78]

1.7.6 HPLC column

The HPLC column in which the stationary phase material is held is the heart of the system. It is usually protected from particles or contaminants associated with the eluted sample by a small column placed before the main column, called a guard column. It is classified in different ways: by column hardware, like stainless steel; by chromatographic modes, as noted above; by dimensions such as prep, semi-prep, analytical and fast LC; or by support types such as silica or polymer. Silica (SiO_2) is considered to be the dominant support material, with excellent physical and chromatographic performance, and is bonded to groups such as

C_{18}, which is very hydrophobic, retentive and stable, making it the first choice for most separations, or C_8, which has similar selectivity but is less retentive.[77]

1.7.7 HPLC instrumentation

The HPLC instrument consists of an injector, either manual or automated, to introduce the sample solution into the mobile phase, a pump, an online degasser to eliminate dissolved gaseous molecules for accurate pump blending and gradient operation, a column, a column oven, a detector and a data-handling device.[77]

1.7.8 UV/Vis absorbance detector

A UV/Vis detector measures the absorbance of those analyte molecules which absorb ultraviolet or visible light. These analytes have at least: (a) a double bond adjacent to an atom with an electron pair, (b) bromine, iodine or sulphur, (c) a carbonyl group, (d) a nitro group, (e) two conjugated double bonds, (f) an aromatic ring. Since most analytes of interest have UV absorbance, the UV/Vis absorbance detector has become the type most often used to measure the concentration or the mass of eluting analytes by monitoring the absorption of UV or visible light in the HPLC eluent. The absorption measurements can be at a single wavelength using the UV/Vis absorbance detector, or over an extended spectral range using a photo diode array detector. The UV/Vis detector consists of a monochromator in which a prism allows the selected wavelength to pass through the exit slit, a deuterium lamp, and a small flow cell. The most common design is a dual-beam optical one in which only the sample beam passes through the sample flow cell. Here the generated light is split into a sample and a reference beam, and their light intensity is measured by separate photodiodes

after the former has passed through the sample. The concentration of analytes of interest is then assessed by measuring the absorbance at a set wavelength or wavelengths.[77]

1.7.9 Photodiode array detector

The photodiode array detector, also known as a diode array detector, is the preferred detector for method development because of its ability to measure the intensity of light at each wavelength.[77]

1.7.10 Quantitation analysis

There are three popular strategies to measure quantitatively the amount of an analyte of interest in the eluted sample solution. In the normalized area percentage method, which is most often used for measuring the level of impurities, the area of each peak is divided by the total area of all peaks and multiplied by 100. In the external standardization method, which is used for most quantitative assays, standard solutions of known concentrations of the analytes of interest are run to calibrate the HPLC system. Finally, the internal standardization method is commonly used for complex samples; here, the internal standard is added before sample work-up and to the prepared standard solutions.[79]

Chapter 2: Synthesis of PIM-1

2.1 Introduction

The initial objective of the work described in this chapter was to synthesise a well defined sample of PIM-1 with a molecular weight within the detection limits of both MALDI-ToF mass spectrometry and triple detector GPC. This well defined sample was subsequently used (see chapter 5) together with other samples of higher molar mass to establish a reliable GPC method for determining the molar mass distribution of PIM-1 and to determine the differences in molecular weight and the structure for samples of PIM-1 prepared under different reaction conditions. The second objective was to prepare PIM-1 using a relatively cheap chloro-monomer.

The polymer of intrinsic microporosity PIM-1 was synthesized following various procedures: (i) from fluoro-monomer by the conventional method, in which PIM-1 was prepared on both a large scale and a small scale , (ii) from fluoro-monomer by a high temperature, high shear mixing method and (iii) from chloro-monomer in which three methods were applied, conventional method (method A) (130 ^{o}C, 24 hours, DMF), dual solvent method B (155-160 ^{o}C, 8 hours, DMF/Toluene), dual solvent method C (155-160 ^{o}C, 8,17 hours, DMAc/Toluene).

2.2 Materials and Equipment

2.2.1 Materials

All materials were purchased from Sigma-Aldrich, Avocado, Lancaster or BDH and used as received except the monomers. Samples were dried in a Binder vacuum oven at 100 °C and purified water was obtained from a Millipore Elix 3 water purification system. All glassware and needles was oven dried at 100 °C for at least 24 hours and cooled to room temperature under nitrogen before use to ensure anhydrous conditions.

2.2.2 Purification of Monomers

23.5 g of 1,4-dicyanotetrachlorobenzene (TCTPN) was heated under reflux in 330 ml of dichloromethane (DCM) for 1 hour. Then the solution was allowed to cool. After the solution was cooled (at room temperature), the white solid was passed through a vacuum filter and dried overnight at 100 °C in a vacuum oven. This gave the purified product as a white solid (17.63 g, 75% yield).

20.5 g of 5,5',6,6'-tetrahydroxy-3,3,3',3' tetramethyl-1,1'-spirobisindane (THSB) was dissolved in 400 ml of hot methanol, and then half of the methanol was evaporated by heating, after which DCM was added slowly whilst the solution was still hot. The solution was then allowed to cool (at room temperature) for about 2 hours. The off-white precipitate that formed was isolated by vacuum filtration and left to dry overnight. The purified product was still off-white in colouring and so the re-crystallization steps were repeated, this gave a pure white monomer (11.96 g, 58% yield).

21.14 g of 1,4-dicyanotetraflurobenzene (TFPN) was heated under reflux in ~120 ml methanol in a conical flask and heated until the monomer had completely dissolved. The solvent was then reduced in volume by evaporation until the solid began to precipitate out.

The solution was then removed from the heat to cool (at room temperature) and the precipitate was collected by vacuum filtration. It was then dried in a vacuum dessicator over P_2O_5 over the weekend to yield TFPN as a white crystalline solid (13.22g, 62.5% yield).

2.2.3 Equipment

A Viscotek GPC max VE 2001 instrument (conventional GPC system) was used with a Viscotek VE 3580 RI detector and two 30 cm 10 micron PLGel columns (2 x Mixed B and 1 x 500 Å), eluting with THF at 1 ml/min at 35 °C. For this system, calibration was carried out with a series of polystyrene standards, using a dodecane marker.

A Viscotek GPC max 302 TDA instrument (LAlS-RAlS-UV-RI-Viscometer) (Multiple-detector GPC system) was used with two 30 cm 10 micron PLGel columns (2 x Mixed B), eluting with Chloroform at 1 ml/min at 35 °C.

MALDI-ToF analysis was carried out on a Micromass Tof Spec 2E equipped with a nitrogen laser at 337 nm. Dithranol was used as the matrix doped with sodium bromide (0.1 μL). Samples of approximately 5 mg were dissolved in chloroform.

2.3 High shear mixing condition route

2.3.1 Synthesis of low molecular weight PIM-1

The purpose of this work was to prepare a low molecular weight PIM-1 sample that could be characterized within the detection limits of both the triple detector GPC and MALDI, to prove the present structure and to help in interpretation of the structure of PIM-1. This could be achieved by reducing the amount of base, changing molar ratio (imbalance the molar ratio of the monomers), or it could be done by reducing the reaction time.[42] The first approach was used in this work to repeat the Canadian group method [33] in order get a linear low molecular weight PIM-1 sample.

2.3.1.1 Synthesis procedure for PIM-1-20

The calculated amounts of THSB (5.106 g, 0.015 mol), TFPN (3.003 g, 0.015 mol), K_2CO_3 (2.073 g, 0.015 mol) and DMAc (25 ml) were added to a two-necked round-bottomed flask (50 ml), with a reflux condenser on one side under a flow of nitrogen and a high-speed homogenizer (T 18 basic ULTRA-TURRAX®, 7000 rpm, IKA®) on the other side. The flask was then lowered into the heated (155 °C) oil bath to a level just above the level of the DMAc in the flask. The solution was stirred vigorously for 2 minutes and 20 ml toluene was then added to the reaction mixture to increase the solubility of the resultant polymer. After 2 minutes, when a precipitate appeared and the reaction mixture became viscous, another 20 ml toluene was added and the reaction allowed to continue for 4 minutes. The flask was then lifted above the oil bath and allowed to cool to room temperature without stirring. Methanol was then added to precipitate the dissolved polymer and the precipitate was recovered by filtration through a vacuum filter (sintered filter). The resultant product was dissolved in chloroform and re-precipitated in methanol, boiled in hot water for four hours to remove the salt, then passed through a vacuum filter and dried overnight at 100 °C in a vacuum oven.[33]

2.3.2 Synthesis of high molecular weight PIM-1

Polymerizations were carried out as for **2.3.1.1** but with increased ratio of base (6.2 g, 0.045 mol) K_2CO_3 for reaction of 8 minutes (NMH01), and for 13 minutes (NMH03) following the procedure detailed in **2.3.1.1**

2.4 Conventional route

2.4.1 Introduction

PIM-1 was prepared on a large scale and small scale under the conventional reaction conditions[31, 42] using different setups. For the large scale preparation (100-150 g), a LARA reactor was used, where mixing was achieved using a PTFE anchor stirrer. For the small scale preparation, a round-bottomed flask was used, where mixing was achieved using a magnetic stirrer bar. In addition, the possibility was investigated of forming homogeneous films that are suitable for use as membranes (Chapter 6).

2.4.2 Large scale preparation of PIM-1 (JDS057)

The preparation was achieved in a Radleys LARA™ reactor, equipped with an anchor-type stirrer **(Fig. 7)**. A 5 L reaction vessel was dried overnight at 100 ^oC before use, then charged with a mixture of 5,5',6,6'-tetrahydroxy-3,3,3',3'-tetramethyl-1,1'-spirobisindane (108.4899 g, 0.319 mol) and 1,4-dicyanotetrafluorobenzene (TFPN) (63.7651 g, 0.319 mol). The reactor vessel was flushed with nitrogen for 1 hour and then anhydrous DMF (2.5 L) was added. The mixture was heated to 65 ^oC with stirring (300 rpm) under nitrogen gas and then anhydrous K_2CO_3 (373 g, 2.70 mol) was added in one portion and the reaction allowed to continue for 60 hours. The reacted mixture was then cooled to room temperature. The product was collected by vacuum filtration and washed with an excess of water and with acetone.

Purification of the yellow solid (PIM-1) was achieved by rewashing the crude product with an excess of water, acetone and 1,4 dioxane. This step was carried out twice to remove oligomers and low molecular weight product. Finally, the purified product was dried in a vacuum oven at 100 ^{o}C (100 g, 40 % yield).[42] It was later discovered that the house nitrogen had a high level of moisture at this time.

Figure 7 a Radleys LARA reactor, equipped with an anchor-type stirrer. [80]

2.4.3 Small scale preparation of PIM-1

The calculated amounts of THSB (10.25 g, 0.0301 mol), TFPN (6.02 g, 0.0301 mol), and DMF (200 ml) were added to a round bottomed flask with a reflux condenser under a flow of nitrogen. The flask was then lowered into a temperature controlled oil bath (65 °C) to a level just above that of the DMF in the flask and the reaction temperature was maintained while the solution was stirred. The calculated amount of K_2CO_3 (10.25 g, 0.074 mol) was then added and the reaction allowed to continue for 72 hours. The flask was then lifted above the oil bath and allowed to cool to room temperature without stirring. The product was collected by vacuum filtration and washed with an excess of water. Next, methanol was added to precipitate the dissolved polymer, which was then recovered by filtration through a vacuum filter. The resultant product was dissolved in chloroform, re-precipitated in methanol and

boiled in hot water for four hours to remove the salt, then passed through a vacuum filter to be dried overnight at 100 °C in a vacuum oven. Polymers were prepared by Louise Maynard-Atem.

2.5 Low cost route

The aim of this work was to obtain PIM-1 via a low cost route using the chlorinated monomer TCTPN instead of TFPN.

2.5.1 Synthesis procedure (method A): T= 130 °C, solvent DMF, 24 hours

The calculated amounts of THSB (10.25 g, 0.0301 mol), TCTPN (6.02 g, 0.0301 mol), and DMF (200 ml) were added to a round bottomed flask with a reflux condenser under a flow of nitrogen. The flask was then lowered into a temperature controlled oil bath (130 °C) to a level just above that of the DMF in the flask and the reaction temperature was maintained while the solution was stirred. The calculated amount of K_2CO_3 (10.25 g, 0.074 mol) was then added and the reaction allowed to continue for 24 hours. The flask was then lifted above the oil bath and allowed to cool to room temperature without stirring. The product was collected by vacuum filtration and washed with an excess of water. Next, methanol was added to precipitate the dissolved polymer, which was then recovered by filtration through a vacuum filter. The resultant product was dissolved in chloroform, re-precipitated in methanol and boiled in hot water for four hours to remove the salt, then passed through a vacuum filter to be dried overnight at 100 °C in a vacuum oven.

2.5.2 Synthesis procedure (method B): T= 155 °C, solvent DMF/Toluene, 8 hours

The calculated amounts of THSB, TCTPN and DMF **(Table 1)** were added to a round bottomed flask connected to a reflux condenser under a flow of nitrogen. The flask was then lowered into a temperature controlled oil bath (155 °C) to a level just above that of the DMF in the flask and the reaction temperature was maintained while the solution was stirred. The calculated amount of K_2CO_3 **(Table 1)** was then added. Once it had become viscous, 5 ml toluene was added to the reaction mixture to increase the solubility of the resultant polymer. This step was repeated when a precipitate appeared and the reaction mixture become viscous. The reaction was continued for 8 hours, which was found to be the typical time required to form a high molecular weight sample of PIM-1. The flask was then lifted above the oil bath and allowed to cool to room temperature without stirring. Next, methanol was added to precipitate the dissolved polymer, which was then recovered by filtration through a vacuum filter. The resultant product was dissolved in chloroform, re-precipitated in methanol and boiled in hot water for four hours to remove the salt, then passed through a vacuum filter to be dried overnight at 100 °C in a vacuum oven.

Polymerization was carried out at 155 °C, at which temperature the chloro-monomer is soluble. Toluene was added to the reaction mixture when a precipitate appeared and the reaction mixture become viscous, in order to increase the solubility of the polymer as it formed; otherwise, stirring could not be continued easily. The reaction was continued for 8 hours.

Table 1 Amounts of TCTPN, THSB, DMF, K_2CO_3 and Toluene used in synthesis of PIM-1 by Method B.

	T	TCTPN		THSB		DMF	K_2CO_3		Toluene
	(°C)	(g)	(mol)	(g)	(mol)	(ml)	(g)	(mol)	(ml)
NEW09	155	2.8757	0.0108	3.6659	0.0108	18	4.5611	0.0330	20*
10	155	0.8602	0.0032	1.0991	0.0032	5	1.7033	0.0123	15**

*4 ml (Toluene) was added immediately, 6 ml after 1 hour and 50 minutes, 6 ml after 1 hour and 57 minutes and 4 ml after 2 hours and 25 minutes.
** 5 ml (Toluene) was added immediately, 5 ml after 2 hours and 15 minutes and 5 ml after 6 hours and 44 minutes.

2.5.3 Synthesis procedure (method C): T= 155-160 °C, solvent DMF/Toluene, 8 hours

To a two neck round bottom flask, equipped with condenser and under an inert atmosphere of N_2, was added TCTPN (0.80 g, 0.030 mol), THSB (1.02 g, 0.030 mol) and anhydrous DMAc (5 ml). The reaction was sealed with a septum and placed into a preheated oil bath between 155-160 ^oC. The reagents were stirred at this temperature for approximately 15 minutes after which they had dissolved. To the reaction was then added anhydrous K_2CO_3 (2.49 g, 0.0180 mol). As the molecular weight of the polymer increased the solution became viscous and a precipitate started to form. For that reason, toluene (5 ml) was added to the reaction, to dilute the reaction mixture and to re-dissolve some of the precipitate. Each time this reaction was carried out, the timing of the 3 toluene additions varied (**Table 2**). The reaction was left for a period of time (**Table 2**), after which it was allowed to cool. The reaction mixture was then poured into vigorously stirred methanol (300 ml). The precipitate was collected by vacuum filtration and partially dried on the funnel for approximately 30-40 minutes. The solid was then washed by stirring in hot water (300 ml) for 2 hours to remove the inorganic salts produced in the reaction. The solid was then collected by filtration and dried in a Buchi vacuum oven for about 4 hours.

Table 2 Amounts of Toluene and the total reaction time for synthesis of PIM-1 by method C

sample #	1st addition	2nd addition	3rd addition	Total reaction time (hour)
DNM46B	2 minutes	22 minutes	1 hour 52 minutes	17
DNM48B	1 minute	12 minutes	1 hour 44 minutes	17
DNM32A	1 hour	1 hour 15 minutes	4 hours	8

2.6 Characterization results

2.6.1 Low molecular weight PIM-1

Table 3 shows the average molar masses from multi-detector GPC for a low molecular weight sample of PIM-1 (PIM-1-20), prepared as described in **Section 2.3.1.1** The molar mass distribution and Mark-Houwink plot are shown in **Fig. 8**. The same sample was analysed at different concentrations (**Table 3**) to obtain the relative standard deviation for the M_w, M_n values, which can be considered as the experimental uncertainty for this measured value.

Table 3 Average molar masses for PIM-1-20

PIM-1-20	Molar mass	
Sample Conc. (mg/ml)	M_n	M_w
2.22	4426	7653
2.24	4508	7732
1.34	4332	7552
RSD %	2	1.1

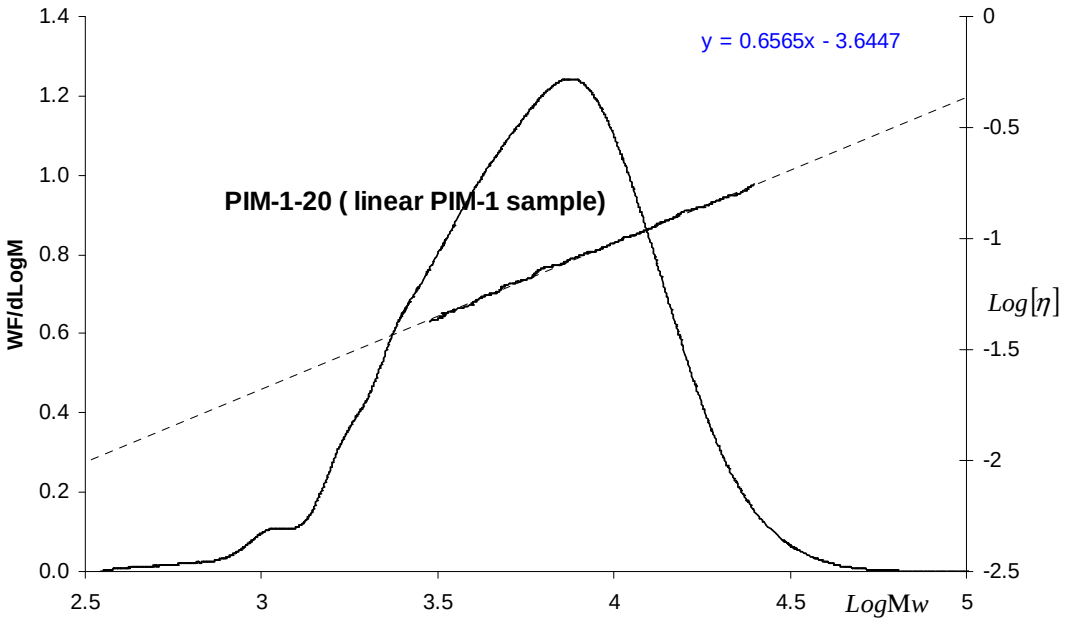

Figure 8 Weight distribution of log (molar mass) (left hand axis) and Mark-Houwink plot (right hand axis) for PIM-1-20, prepared under high shear mixing conditions, reagent molar ratio THSB: TFPN: K_2CO_3 (1:1:1), DMAc/Toluene as solvent, 150-155 °C, 8 minutes.

The MALDI-TOF mass spectrum (**Fig. 9**) obtained for this sample shows the presence of only linear species. It shows a series of different linear species distributions (**Table 4**). The dominant distribution AB (THSB and TFPN-terminated material) in the spectrum has masses consistent with linear chains having both THSB and TFPN end units (**Fig. 10**). There is another distribution in the MALDI spectrum denoted BhB. This distribution has masses consistent with the termination of the polymers with the TFPN followed by hydrolysis of any two of the fluoride endgroups to form terminal hydroxyl groups as per **Scheme 1**. The dominant distribution BhBh in the spectrum has masses of which are equal to fully hydrolysed TFPN-terminated PIM-1 **(Fig. 10)**. It is worth mentioning that the difference in masses between a fluorine atom and a hydroxyl group is a mass of two, which is within the error margin for detector calibration and so the number of fluorines hydrolysed cannot be reliably surmised. The dominant distribution AA in the spectrum represents the termination

of the polymers with the TFPN and THSB and furthermore the fluorine endgroups appear to have remained intact showing no signs of the hydrolysis **(Fig. 10)**. The dominant distribution ABh in the spectrum represents series of two peaks with masses correspond to hydroxyl (1,2-diol) terminated linear PIM-1 chains **(Fig. 10)**. Finally, the dominant distribution BB in the spectrum represent series of peaks with masses consistent with the structures shown in **Fig. 10** respectively.[81]

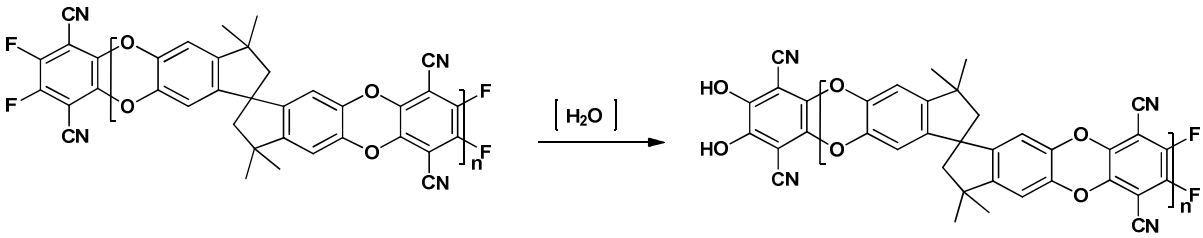

BhB

Scheme 1

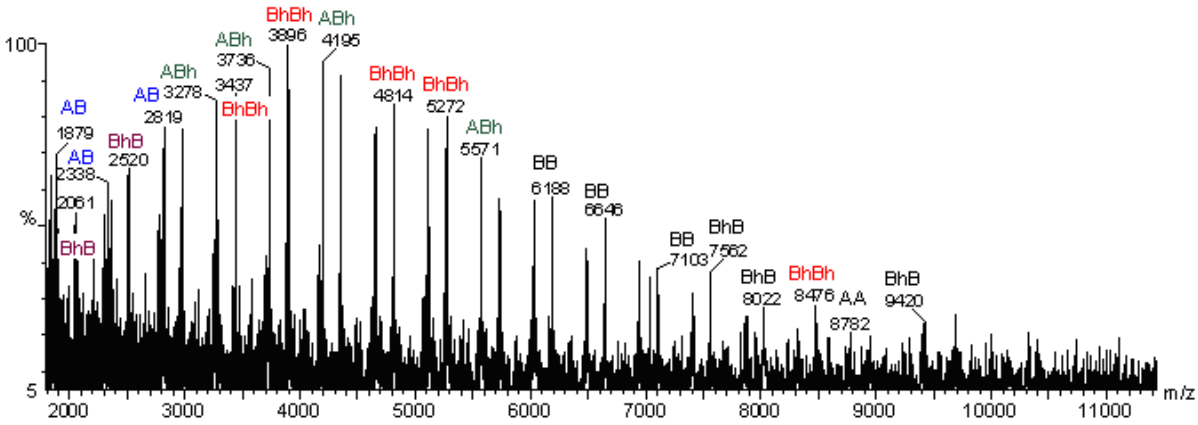

Figure 9 MALDI-ToF mass spectrum of sample PIM-1-20:

Table 4 The calculated and the observed mass for the dominant distributions

Endgroup Type	Endgroup formula	Repeat unit	N	Cation	Overall formula	Mass (calc.)	Mass (obs.)
AB	H_2, F_2	$C_{29}H_{20}O_4N_2$	4	H^+	$(C_{29}H_{20}O_4N_2)_4H_3F_2^+$	1881	1879
ABh	H_2, $(OH)_2$	$C_{29}H_{20}O_4N_2$	7	Na+	$(C_{29}H_{20}O_4N_2)_7H_3(OH)_2^+$	3279	3279
BhBh	$(OH)_2$, $C_8N_2(OH)_2$	$C_{29}H_{20}O_4N_2$	7	Na+	$(C_{29}H_{20}O_4N_2)_7$ $C_8N_2(OH)_2(OH)_2^+$	3439	3437
BhB	F_2, $C_8N_2(OH)_2$	$C_{29}H_{20}O_4N_2$	4	Na+	$(C_{29}H_{20}O_4N_2)_7$ $C_8N_2(OH)_2$ F_2^+	2061	2061
BB	F_2, $C_8N_2F_2$	$C_{29}H_{20}O_4N_2$	15	H^+	$(C_{29}H_{20}O_4N_2)_7$ $C_8N_2F_2$ F_2^+	7102	7103
AA	H_2, $C_{20}O_2H_{18}$	$C_{29}H_{20}O_4N_2$		H^+	$(C_{29}H_{20}O_4N_2)_7$ $C_{20}O_2H_{18}H^+$	8783	8782

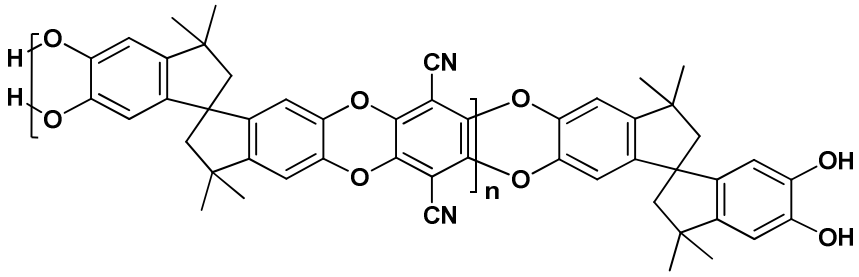

AA

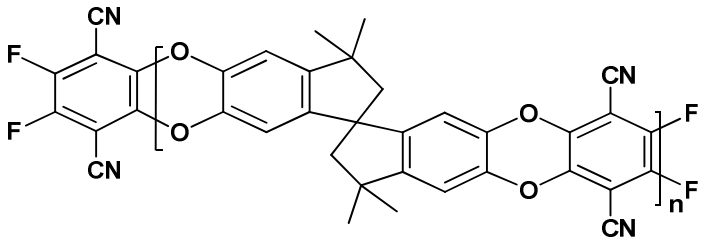

BB

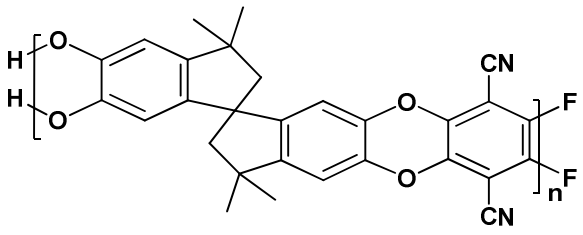

AB

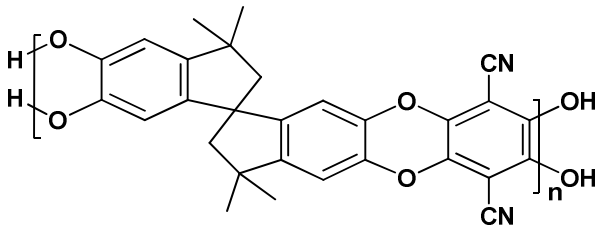

ABh

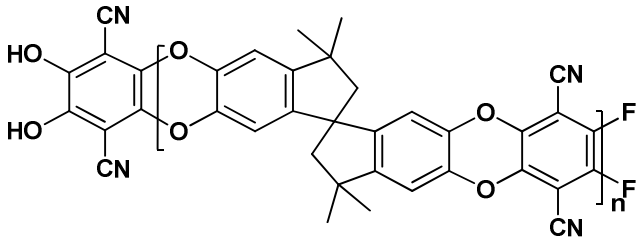

BhB

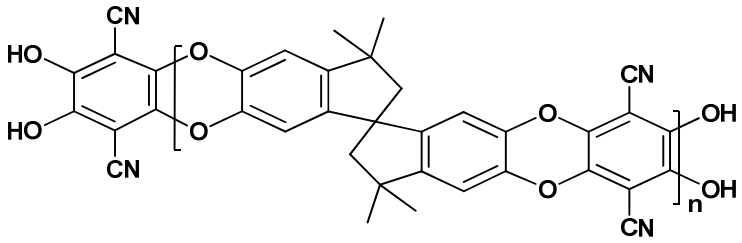

BhBh

Figure 10 Structures consistent with peaks observed in the MALDI-ToF mass spectrum of sample PIM-1-20

2.6.2 High molecular weight PIM-1

Average molar masses and reaction times for samples of PIM-1 prepared from TFNP and THSB under high shear mixing conditions are summarized in **Table 5.** A comparison of the molar mass distributions of the prepared samples is shown in **Fig. 11**, and **Fig.12** shows the Mark-Houwink plots. The results show that molecular weight increases with increasing reaction time. It was observed that shortly after the reaction was started by addtion of K_2CO_3 to the monomer solution, the reaction mixture turned bright yellow.

Table 5 Average molar masses and reaction times for PIM-1 samples prepared under high shear mixing conditions.

Sample ID	M_w	M_n	M_w / M_n	Reaction time (minutes)
NMH01	38000	19000	2	8
NMH03	80000	29000	2.8	13

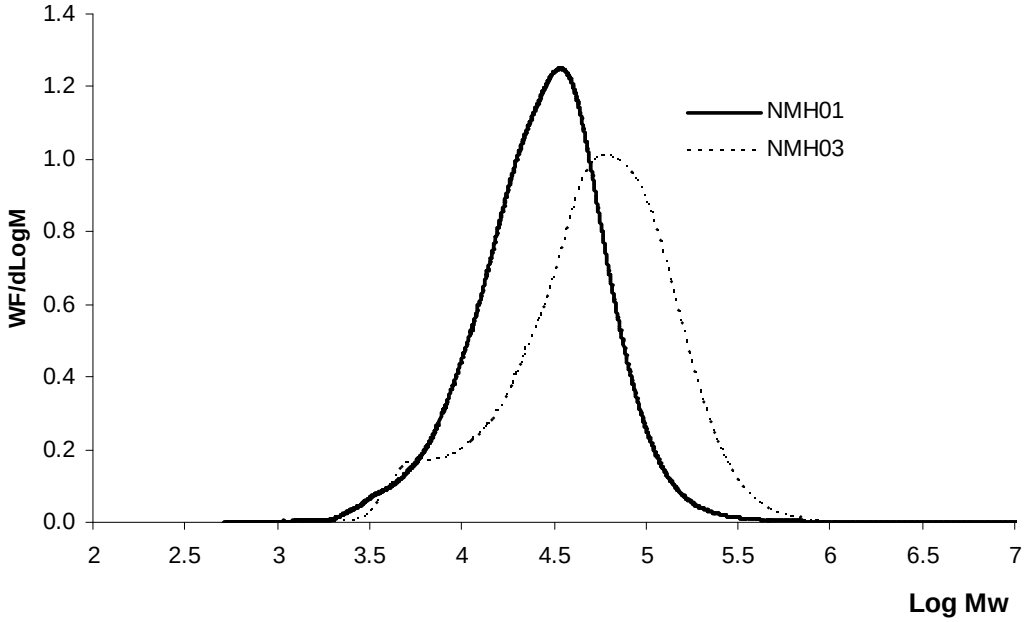

Figure 11 Comparison of the molar mass distributions of the samples prepared under high shear mixing conditions, reagent molar ratio THSB : TFPN : K_2CO_3 (1:1:3), DMF/Toluene as solvent, 150-155 °C, 8,13 minutes

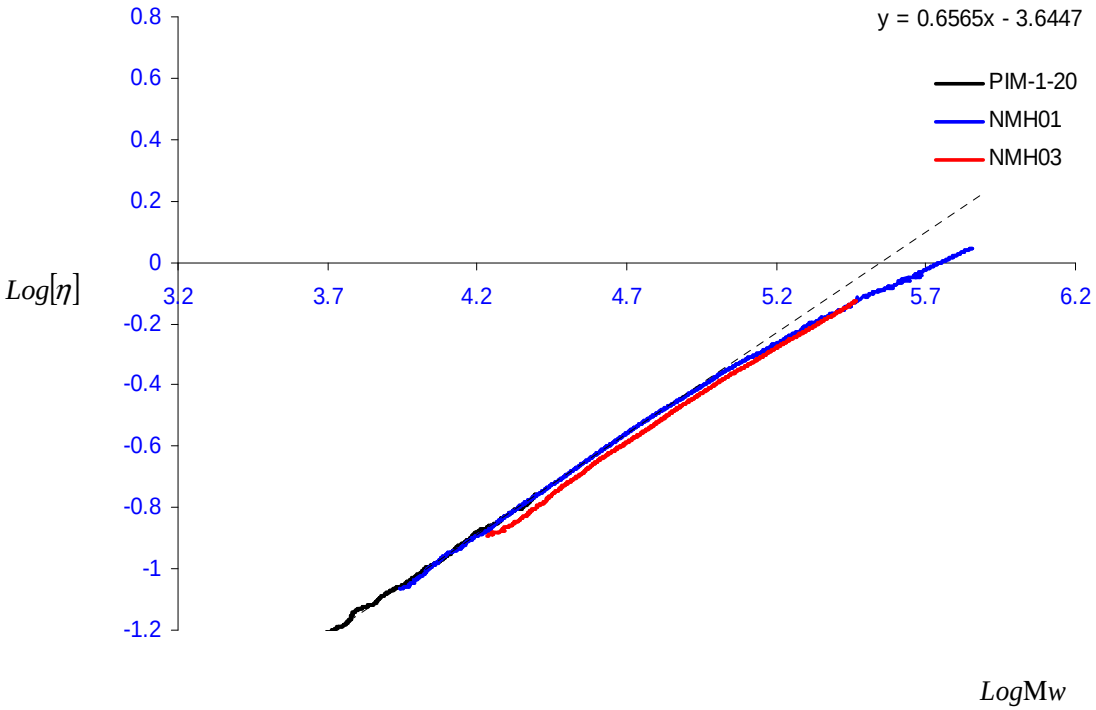

Figure 12 Mark-Houwink plots for the samples prepared under high shear mixing condition , reagent molar ratio THSB/ TFPN /K_2CO_3 (1:1:3), DMF/Toluene as solvent, 150-155 °C, 8,13 minutes

2.7 Conventional route

Under different reaction conditions, PIM-1 was synthesized using different setups. It was synthesized first in a round-bottomed flask, where mixing was achieved using a magnetic stirrer bar, and then using a LARA reactor, where mixing was achieved using a PTFE anchor stirrer. The idea was to improve the mixing efficiency, which would help to increase the solubility of the reaction mixture when a large quantity is applied.

In the conventional method, it was also observed that shortly after the reaction was started by addtion of K_2CO_3 to the monomer solution, the reaction mixture turned bright yellow, and the soluble material in the supernatant is much smaller than that of the precipitate. As the reaction time increases the amount of material present in the superntant decreases and the amount of precipitated material increases, suggesting that as the molecular weight increases precipitation occurs and polymerization continues in a concentated slurry of precipitated

oligomers or polymer solution due to the limited solubility of PIM-1 in DMF, which makes the precipitated phase to be the route to high molecular weight product.

2.7.1 Large scale preparation of PIM-1

Table 5 shows the average molecular weights of polymers synthesized on a large scale. A comparison of the molar mass distributions of the samples is shown in **Fig. 13** and **Fig.14** shows the Mark-Houwink plots. The results in **Table 6** show that the molecular weight of the JDS057 batch was low compared with previous batches. The difference in molecular weight could be due to many variables, such as a sudden change in the reaction conditions; presence of moisture, and the stoichiometry. For the JDS057 batch this was due to contamination of the N_2 gas supplied during the reaction time (It was later discovered the house of nitrogen had a high level of moisture at this time). This effect was investigated by Kevin Reynolds, who found that in the presence of O_2 the hydroxyl ended group in the THSB monomer can be oxidized to a 1,2-dione, which quenches the reaction, resulting in a low molecular weight product **(Fig. 15)**.[42]

Table 6 M_w, M_n and (M_w / M_n) results for PIM-1 samples prepared on a large scale

Batch	M_w	M_n	M_w / M_n
JDS056*	204000	77000	2.6
JDS057	56000	29000	1.9
CT-02-07 **	199000	65000	3.1

*samples prepared by J.D. Selbie

**sample prepared by K.J. Reynolds

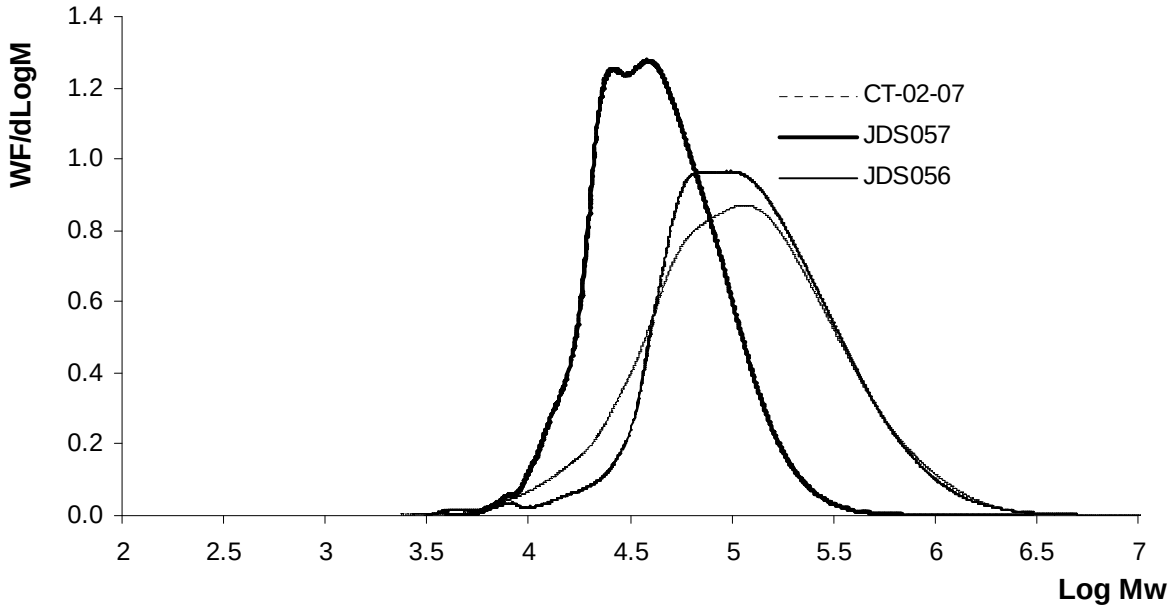

Figure 13 Comparison of the weight distributions of log (molar mass) for PIM-1 samples prepared on a large scale; reagent molar ratio THSB/ TFPN /K_2CO_3 (1:1:8), DMF as solvent, 65 °C, 72 hours

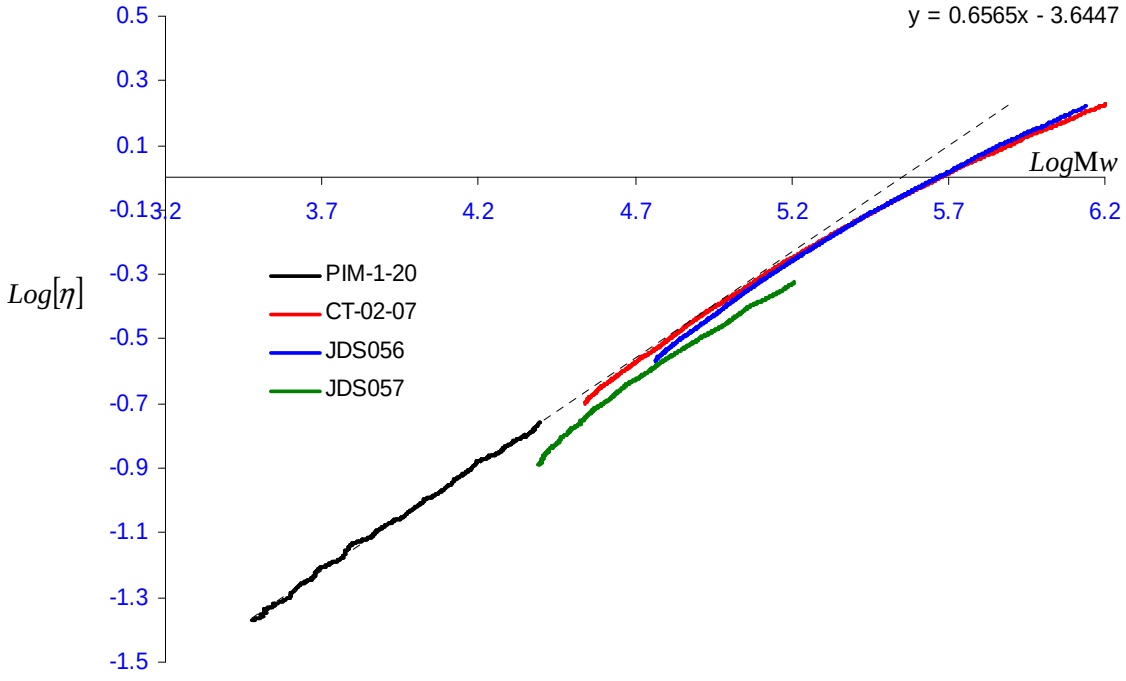

Figure 14 Mark-Houwink plots for PIM-1 samples prepared on a large scale reagent; molar ratio THSB/ TFPN /K_2CO_3 (1:1:8), DMF as solvent, 65 °C, 72 hours

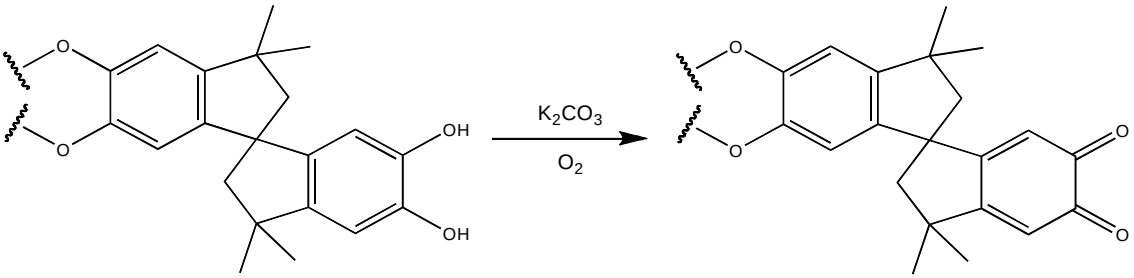

Figure 15 Oxidation of hydroxyl ended PIM-1

2.7.2 Small scale preparation of PIM-1

Table 7 shows the average molecular weights of the polymers synthesized on a small scale. A comparison of the molar mass distributions of the prepared samples is shown in **Fig. 16** and **Fig. 17** shows the Mark-Houwink plots.

Table 7 *M*w, *M*n, (*M*w / *M*n) results for PIM-1 samples prepared on a small scale

Sample ID	M_w	M_n	M_w / M_n
LMA02*	109000	23000	4.7
LMA03*	120000	41000	2.9
LMA04*	178000	51000	3.5

***** Samples were prepared by Louise Maynard-Atem

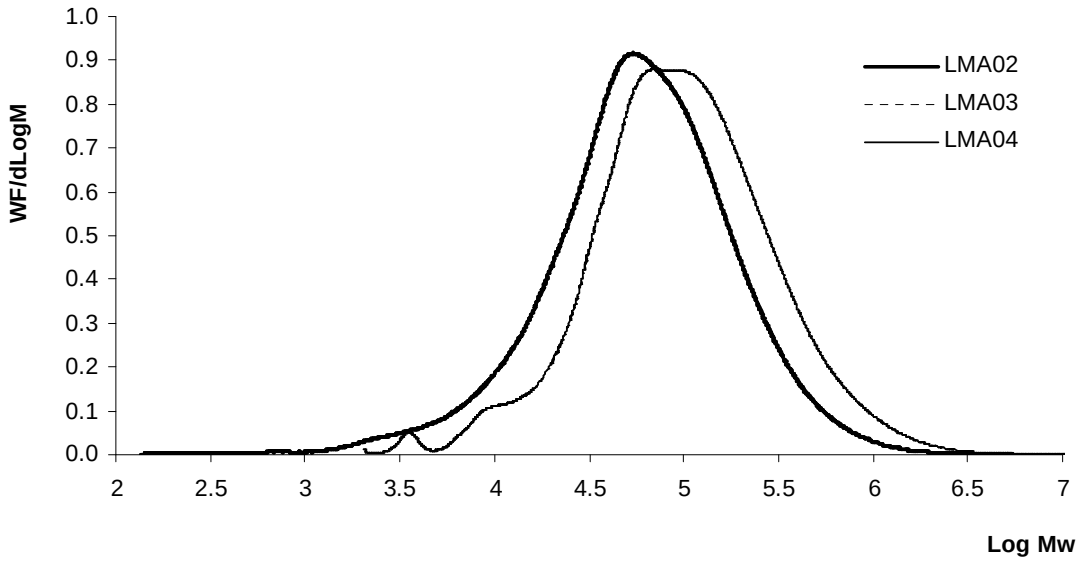

Figure 16 Comparison of the weight distributions of log(molar mass) for PIM-1 samples prepared on a small scale under conventional conditions; reagent molar ratio THSB/ TFPN /K_2CO_3 (1:1:2.5), DMF as solvent, 65 °C, 72 hours

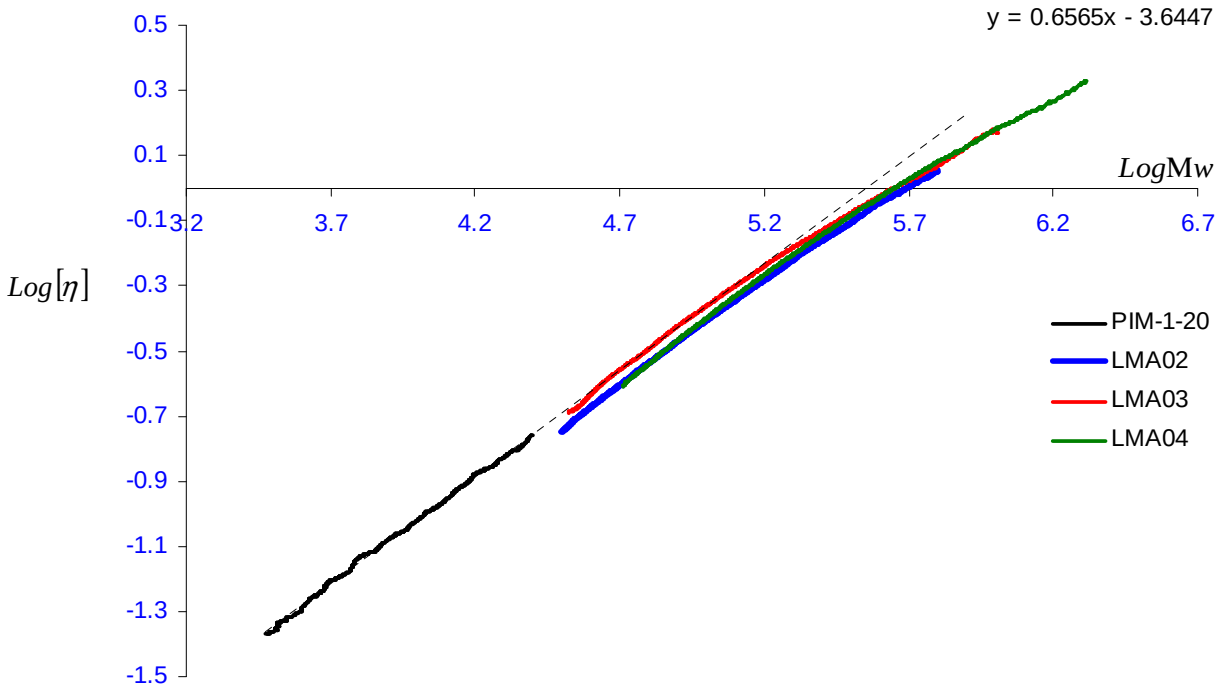

Figure 17 Mark-Houwink plots for PIM-1samples prepared on a small scale under tconventional conditions; reagent molar ratio THSB/ TFPN /K_2CO_3 (1:1:2.5), DMF as solvent, 65 °C, 72 hours

2.8 Low cost route

2.8.1 Synthesis procedure (method A)

In method A, the same procedure was followed as for the conventional synthesis, but in this instance the chloro-monomer was used, the reaction temperature was increased to 130 °C and the reaction time was decreased to 24 hours. **Table 8** shows the average molecular weights of the polymers synthesized. A comparison of the molar mass distributions of the prepared samples is shown in **Fig. 18** and **Fig. 19** shows the Mark-Houwink plots. The results confirm that a low-cost route for the preparation of PIM-1 was successfully established. High molecular weight PIM-1 was achieved using chloro-monomer. The possibility of making a film was investigated for all polymers and it was found to be possible.

Table 8 *M*w, *M*n, (*M*w / *M*n) results for PIM-1 samples prepared by the low cost route, method A.

Sample ID	M_w	M_n	M_w / M_n
LMA08*	107000	19000	5.6
LMA11*	150000	28000	5.3
LMA13*	103000	32000	3.2

***** Samples were prepared by Louise Maynard-Atem

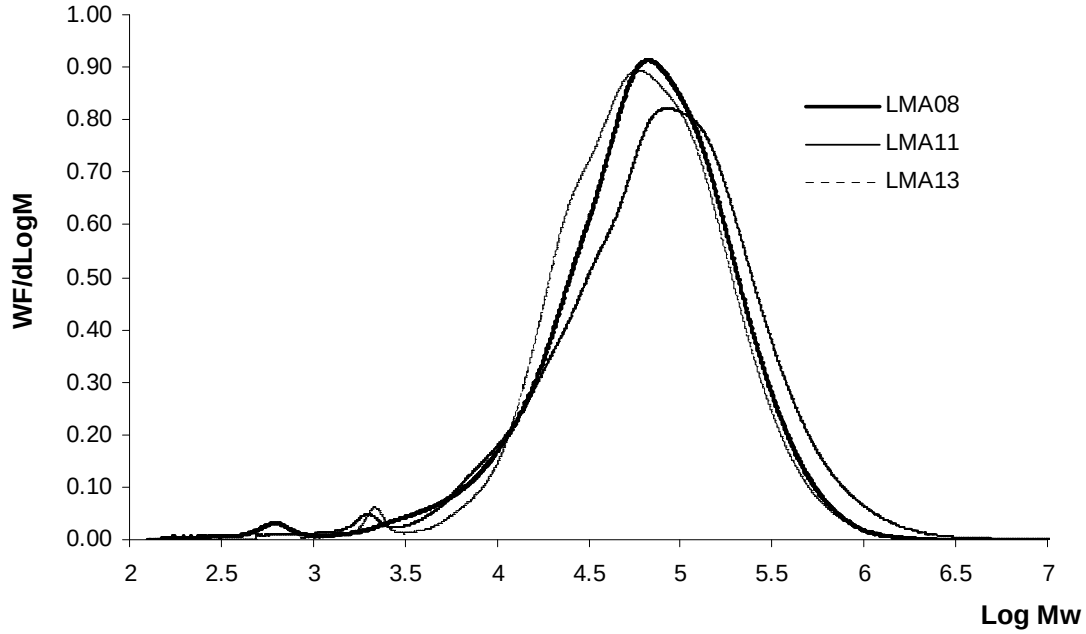

Figure 18 Comparison of the weight distribution of log(molar mass) for PIM-1 samples prepared using the low cost route, method A; reagent molar ratio THSB/ TCTPN /K_2CO_3 (1:1:2.5), DMF as solvent, 125-130 °C, 24 hours.

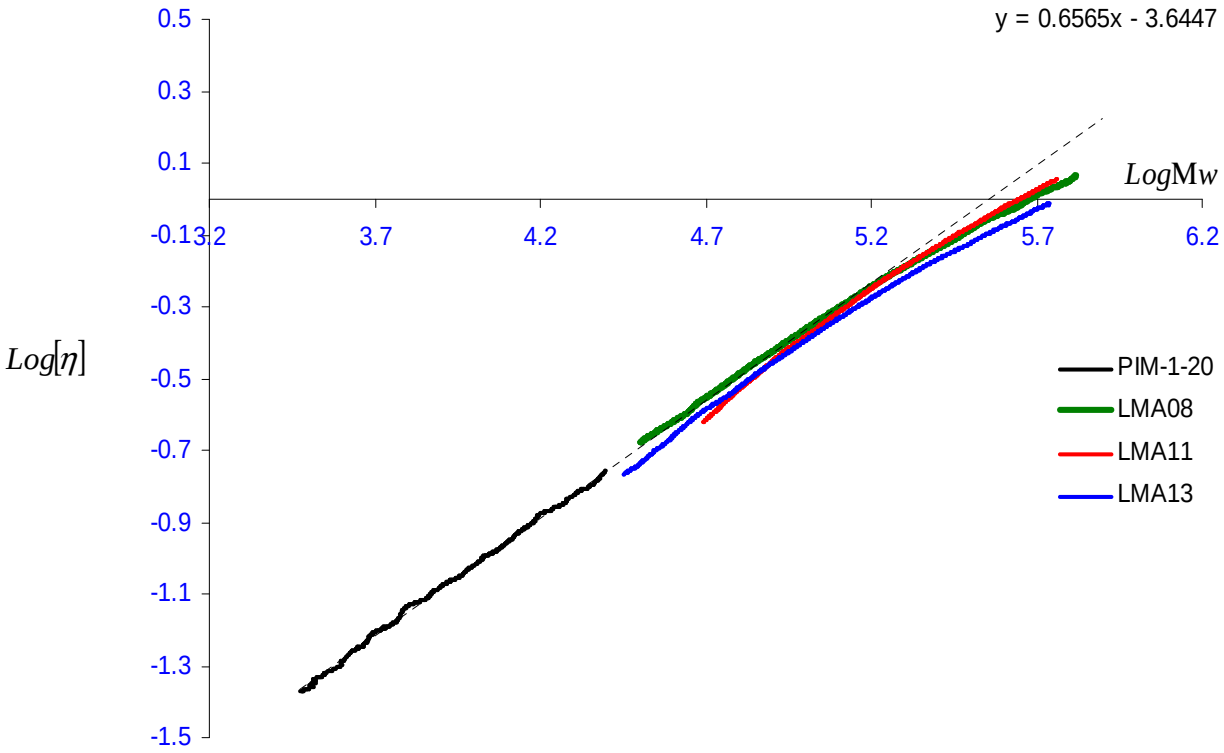

Figure 19 Mark-Houwink plots for PIM-1 samples prepared using the low cost route, method A; reagent molar ratio THSB/ TCTPN /K_2CO_3 (1:1:2.5), DMF as solvent, 125-130 °C, 24 hours

2.8.2 Synthesis procedure (method B and C)

In both methods B and C, it was observed that shortly after the reaction was started by addtion of K_2CO_3 to the monomer solution, the reaction mixture turned bright yellow. **Table 9** shows the molecular weights of the polymers synthesized, A comparison of the molar mass distributions of the prepared samples is shown in **Figs. 20-21** and **Figs. 22-23** show the Mark-Houwink plots.

Table 9 M_w, M_n, (M_w / M_n) results for PIM-1 samples prepared by alow cost route, methods B & C.

Sample ID	M_w	M_n	M_w / M_n
DNM46B**	129000	30000	4.3
DNM48B**	95000	45000	2.1
DNM32A**	61000	34000	1.8
NEW09*	89000	43000	2.1
PIM-1-10*	83000	26000	3.2

*****samples prepared under method B, reagent molar ratio THSB/ TCTPN /K_2CO_3 (1:1:3), DMF/Toluene solvent, 150-155 °C, 8 hours

******samples prepared under method C, reagent molar ratio THSB/ TCTPN /K_2CO_3 (1:1:6), DMAc/Toluene solvent, 155-160 °C, 17 hours, but DNM32A 8 hours.

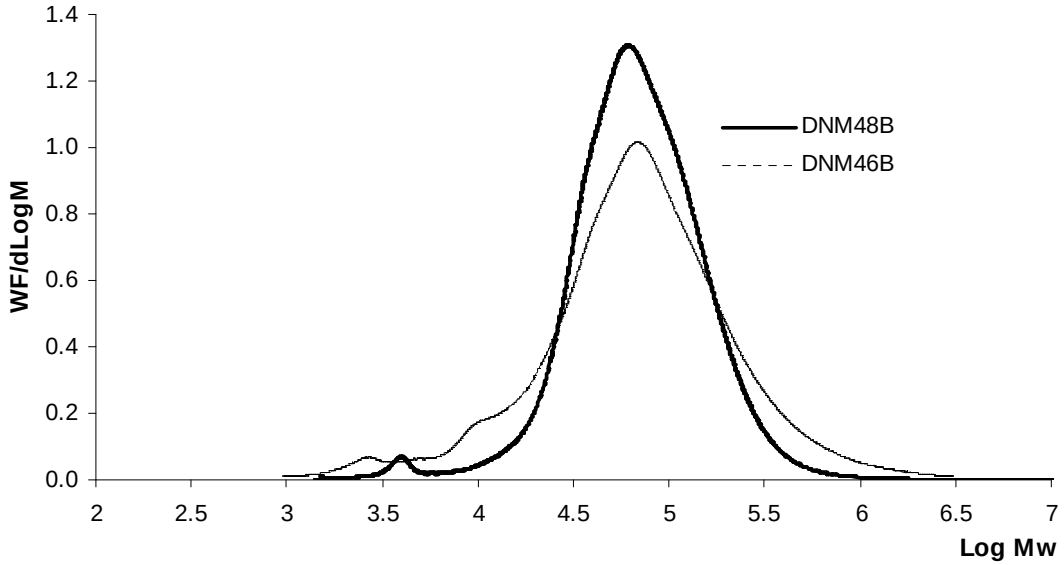

Figure 20 Comparison of the weight distribution of log (molar mass) for two PIM-1 samples prepared by the low cost route, method C; conditions, 155-160 °C, 17 hours, DMAc/Toluene as solvent

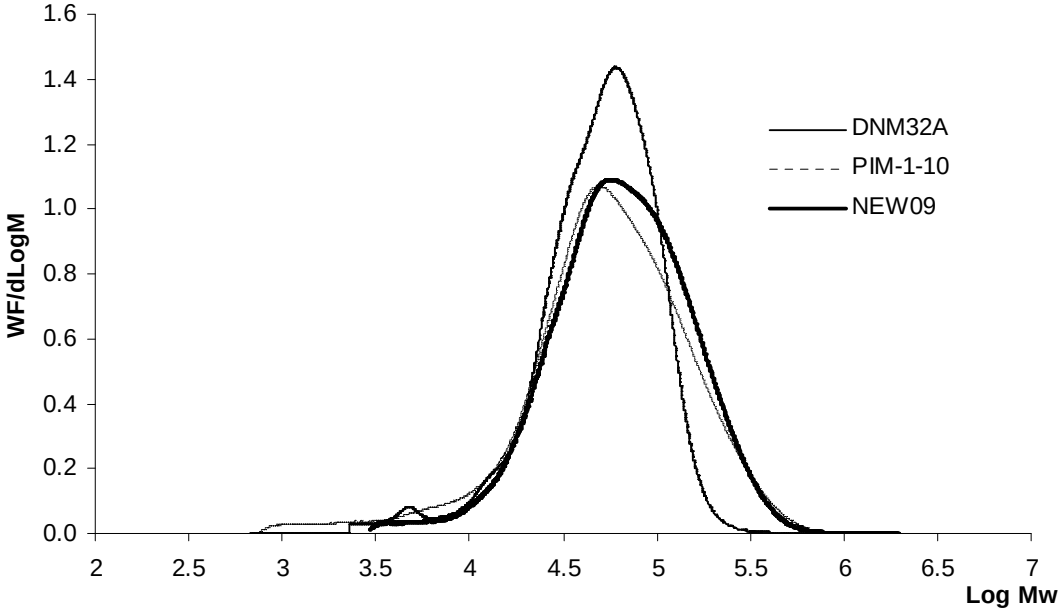

Figure 21 Comparison of the weight distribution of log(molar mass) for PIM-1 samples prepared by the low cost route, methods B and C): method B conditions, 150-155 °C, 8 hours, DMF as solvent; method C conditions, 155-160 °C, 8 hours, DMAc/ Toluene as solvent.

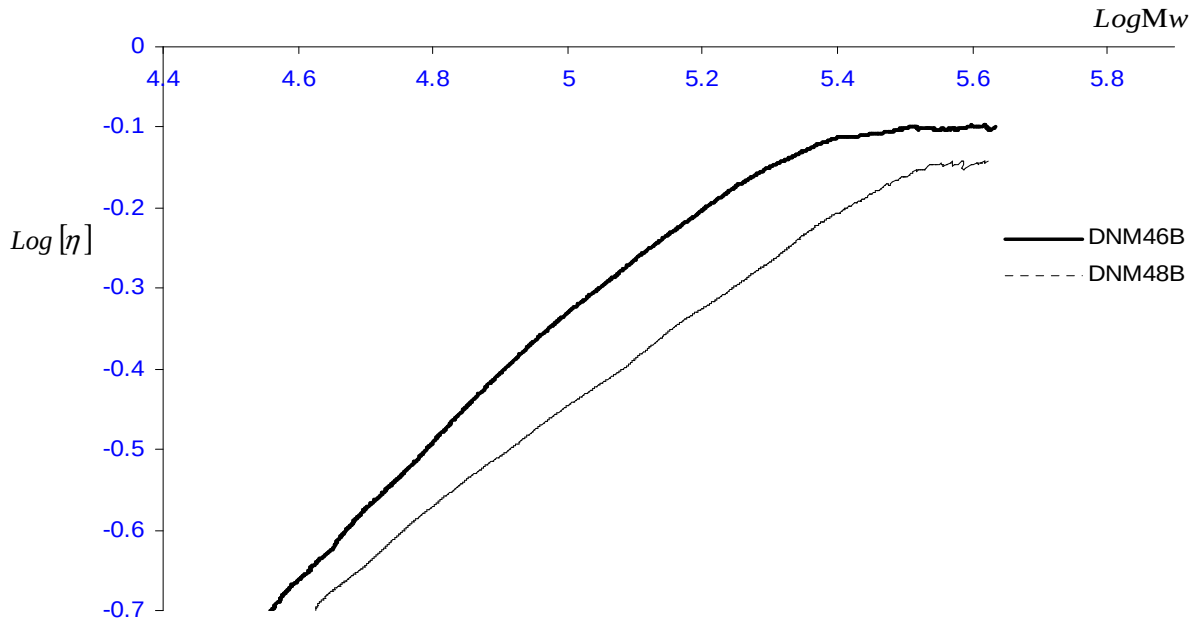

Figure 22 Mark-Houwink plots for two PIM-1 samples prepared by the low cost route, method C): method C conditions, 155-160 °C, 17 hours, DMAc/ Toluene as solvent

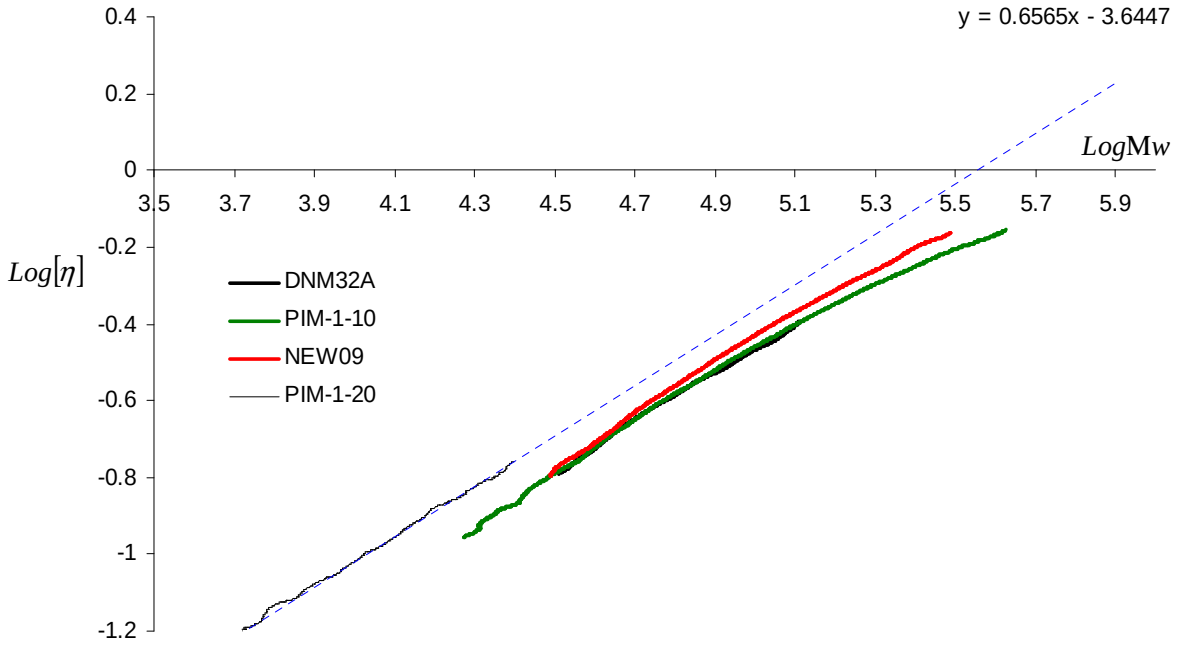

Figure 23 Mark-Houwink plots for PIM-1 samples prepared by the low cost route, methods B and C: method B conditions, 150-155 °C, 8 hours, DMF/Toluene as solvent, method C conditions, 155-160 °C, 8 hours, DMAc/ Toluene as solvent

Table 10 The correlation between the Mw and the polydspersity

Sample ID	M_w	M_n	M_w / M_n	Reaction time (minutes)
NMH01	38000	19000	2	8
NMH03	80000	29000	2.8	13
JDS056	204000	77000	2.6	4320
JDS057	56000	29000	1.9	3720
CT-02-07	199000	65000	3.1	4320
LMA02	109000	23000	4.7	4320
LMA03	120000	41000	2.9	4320
LMA04	178000	51000	3.5	4320
LMA08	107000	19000	5.6	1440
LMA11	150000	28000	5.3	1440
LMA13	103000	32000	3.2	1440
DNM46B	129000	30000	4.3	1020
DNM48B	95000	45000	2.1	1020
DNM32A	61000	34000	1.8	480
NEW09	89000	43000	2.1	480
PIM-1-10	83000	26000	3.2	480

2.9 Conclusion

In conclusion, PIM-1 was synthesized under different reaction conditions and a low-cost route for the preparation of PIM-1 was successfully established. A sample of PIM-1 with a molecular weight within the detection limit of MALDI ToF mass spectrometry and triple detector GPC was synthesized to help in getting information about its structure, which is needed to establish a GPC method for determining the differences in the structure for PIM-1 prepared under different reaction conditions. With reference to the results presented on **Table 10**, there is a correlation between low M_w and low polydispersity. However, a significant degree of scatter within sets of replicate polymerizations makes further generalized conclusion on polydispersity difficult. Further replicate synthesises are recommended to improve the statistical significance of the polydispersity data.

Chapter 3: Fractionation of PIM-1

3.1 Introduction

To describe the properties of a polymer, average molar masses and their ratios are insufficient, so information on molar mass distribution is required. This information can be obtained by fractionation which leads to obtain a number of fractions with narrow distribution of molar mass. Even in the presence of GPC, fractionation can be used often for the purpose of purification.

PIM-1 was fractionated into a number of fractions each of which has narrow distribution of molar mass to get more complete information on PIM-1 by determining the differences in the structure of each of the fractions using MALDI for the low molar mass end and GPC for the high molar mass end.

MALDI-ToF mass spectrometry has become a high-performance tool that can provide qualitative and quantitative analysis. It has advantages such as high sensitivity, minimal sample material required for the preparation step and rapid analysis, but it is limited for small mass range, for example molecules with 10,000 molecular weight. The idea behind using such a technique is to have information about the cyclic, short chain branching, and the linear product on fractionated PIM-1 samples at low molecular weight range.[82]

3.2 Theory of fractionation

The simplest procedure for polymer fractionation is liquid-liquid phase separation using a solvent-nonsolvent system. The polymer at low concentration is dissolved in a solvent and then a non-solvent is the added to the solution to precipitate the polymer. The highest molecular weight fraction precipitates first (when the quality of the solvent is made poorer) and then the next fraction, and so on.

In the phase separation

$$\mu_1' = \mu_1'' \qquad (3\text{-}1)$$

$$\mu_2' = \mu_2'' \qquad (3\text{-}2)$$

Where:

μ_1' is the chemical potential of the solvent in a dilute solution phase

μ_1'' is the chemical potential of the solvent in a concentrated solution phase

μ_2' is the chemical potential of the polymer in a dilute solution phase

μ_2'' is the chemical potential of the polymer in a concentrated solution phase

Equations (3-1) and (3-2) means that at equilibrium between two existing phases, the chemical potential is the same in both phases. The chemical potentials can be calculated in terms of the Flory-Huggins lattice theory, which leads to the following relations

For the solvent

$$\mu_1 - \mu_1^\circ = R\mathrm{T}\left[\ln\phi_1 + \left(1 - \frac{1}{x}\right)\phi_2 + \chi\phi_2^2\right]$$

And per polymer chain segment

$$\mu_s - \mu_s^\circ = R\mathrm{T}\left[\ln\phi_2 / x - \left(1 - \frac{1}{x}\right)\phi_1 + \chi\phi_2^2\right]$$

ϕ_1 is volume fraction of solvent

ϕ_2 is volume fraction of polymer

μ_1° is the chemical potential of the solvent in a standard state

μ_s° is the chemical potential of each polymer species in its standard state

x is the number of segments in each of the polymer molecules

χ is a parameter which characterises the energy of interaction between polymer and solvent.

If the polymer density is independent of x, then the ratio of molar mass fractions f''_{2x} and f'_{2x} of *x*-mers is given by

$$f''_{2x} / f'_{2x} = \mathrm{Re}^{\sigma x}$$

Where $\mathrm{R}=V''/V'$

V'' and V' are the volumes of the concentrated and dilute co-existing phases respectively. The condition for efficient fractionation is σ <<1 and R<<1. To ensure that $V'>V''$ it is necessary to begin with very dilute homogeneous solutions. The concentrated phase mostly contains higher molar mass species, whereas the volume fraction ratio ϕ''_{2x}/ϕ'_{2x} is close to unity for low molar mass species present in the dilute phase. Therefore, the polymer present in the concentrated phase has a relatively narrow molar mass distribution, typically $\mathrm{M}_w/\mathrm{M}_n$ in range of 1.1-1.3.[47]

3.3 Fractionation of polystyrene standard sample

3.3.1 Introduction

The purpose of using a standard material is to investigate the possibility of using the Radleys LARA™ reactor system for fractionating polymers, and PIM-1, which is the polymer of interest. The idea was to use an automated system instead of using a water-bath, in which temperature control is neither easy nor accurate. Before starting the fractionation process, determination of the cloud point was important to select a suitable solvent-nonsolvent system for the fractionation method. This step was taken into account and it was found that the most suitable solvent-nonsolvent system at room temperature for the PS sample was toluene and methanol respectively.[47, 83, 84]

3.3.2 Fractionation procedure

For the fractionation study, a polystyrene sample with weight average molecular weight M_w = 296000 g mol^{-1}, and polydispersity (M_w/M_n) = 2.1 was used. The polystyrene solution was first prepared by dissolving a 0.4991 g sample in 300 ml toluene at 25 °C. Then methanol (non-solvent) was added with rapid stirring until a cloudy solution was observed. The solution was heated to 40 °C to obtain a clear solution and then the solution was cooled to 25 °C (cooling rate was 10 °C per hour) with slow stirring to obtain equilibrium phase separation. When a clear separation of the two liquid phases was observed, the concentrated phase, which was the lower layer containing the polymer, was removed and then recovered by evaporating the solvent using nitrogen gas. This procedure was repeated to collect all fractions.

3.4 Fractionation of 0.5 g of PIM-1 sample JDS056

The purpose of this work was to fractionate the PIM-1 sample in order to study each fraction individually. The procedure used to fractionate the PIM-1 sample was analogous to that used for the polystyrene sample, except the last step, in which the polymer was removed and then recovered using an oven at 100 °C. Solubility and the cloud point of PIM-1 in several solvents were investigated for the selection of suitable solvent-nonsolvent systems for the fractionation method.

3.4.1 Solubility study

For solubility measurement of PIM-1, different solvents were used, including acetone, toluene, chloroform, n-hexane, water, tetrahydrofuran, methanol and dichloromethane. It was found that the PIM-1 sample was soluble in tetrahydrofuran, chloroform and

dichloromethane. It was insoluble in n-hexane, water, methanol and acetone but partially soluble in toluene.

3.4.2 Cloud point measurement

To measure the cloud point of PIM-1, two solvent-nonsolvent systems were investigated at room temperature. The first used chloroform and methanol respectively, while the second used tetrahydrofuran-acetone. It was found that the most suitable solvent-nonsolvent system at room temperature for the PIM-1 sample was chloroform-methanol, because in the second system the acetone solvent suspended the PIM-1 sample.

3.4.3 Fractionation procedure

For the fractionation study, a PIM-1 sample (JDS056) with weight average molecular weight M_w = 204 000 g mol^{-1} and polydispersity (M_w/M_n) = 2.6 was used. The PIM-1 solution was first prepared by dissolving a 0.5011 g sample in 300 ml chloroform at room temperature. Then at 25 °C, methanol (non-solvent) was added with rapid stirring until a cloudy solution was observed. The solution was heated to 45 °C to obtain a clear solution and this was cooled to 25 °C (cooling rate was 10 °C per hour) with slow stirring to obtain equilibrium phase separation. Then the precipitated polymer was collected and dried using an oven at 100 °C. This procedure was repeated to collect all fractions. The last fraction (the residue) was obtained by evaporating the solvent using a rotary evaporator.

3.5 Fractionation of 2.0 g of PIM-1 sample (JDS056)

The reason behind fractionating a large quantity of PIM-1 is to have suitable amounts of fractionated samples for further analysis and also to prove the validity of the solvent-non solvent system used.

3.5.1 Fractionation procedure

For the fractionation study, a PIM-1 sample with weight average molecular weight M_w = 204000 g mol^{-1}, and polydispersity (M_w/M_n) = 2.6 was used. The PIM-1 solution was first prepared by dissolving 1.8766 g sample in 1200 ml Chloroform at room temperature. Then at 25 °C, methanol (non-solvent) was added with rapid stirring until a cloudy solution was observed. The solution was heated to 45 °C to obtain a clear solution and this was cooled to 25 °C (cooling rate was 10 °C per hour) with slow stirring to obtain equilibrium phase separation. The precipitated polymer was collected and then dried using an oven at 100 °C. This procedure was repeated to collect all fractions. The residue was obtained by evaporating the solvent using a rotary evaporator.

3.6 Characterization results

3.6.1 Fractionation of polystyrene standard sample

Polymer fractionation is achieved when the quality of the solvent is made poorer by using solvent-nonsolvent systems in which the highest molecular weight fraction precipitates firstly and then the next fraction, and so on. The original PS sample and the fractionated samples were analysed using the conventional GPC system associated with two mixed-bed columns with a single 500 Å column in series to determine their molecular weight averages and dispersites. The GPC system was calibrated with narrow molar mass distribution polystyrene

standards and dodecane was used as a flow rate marker. In each case, the mobile phase was THF at a flow rate of 1 ml/min, while sample solution concentrations were 1 mg/ml and 100 µl injected. The sample solution was filtered before each run using a 0.45 µ filter. The GPC results for the fractionated samples are shown in **Fig. 24**.

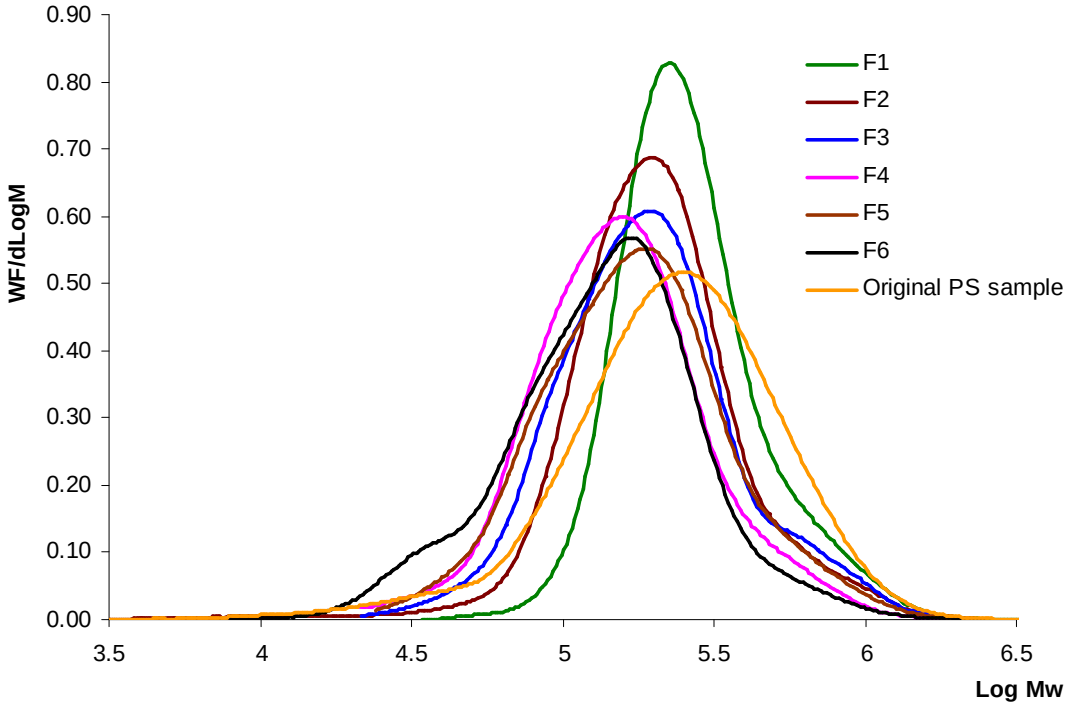

Figure 24 Weight distribution of log (molar mass) for the original polystyrene sample and its fractions

The results in **Table 11** show that the molecular weight decreased for fractions one to six. The dispersity value for the first two fractions decreased from 2.1 to 1.3, 1.4 respectively. The weight average molecular weight was found to decrease from 296000 to 172000 g mol^{-1}. In conclusion, the results for those fractions illustrate the possibility of using a Radleys LARA™ reactor for fractionating polymers.

Table 11 M_w and (M_w / M_n) from GPC for the original and fractionated polystyrene samples

Fraction No.	M_w	M_w / M_n
1	450000	1.3
2	301000	1.4
3	241000	1.7
4	234000	1.5
5	216000	1.7
The residue	172000	1.7
Original	296000	2.1

3.6.2 Fractionation of 0.5 g of PIM-1 sample JDS056

3.6.2.1 Solubility measurement

It was found that the PIM-1 sample is soluble in tetrahydrofuran, chloroform and o-dichlorobenzene. It is insoluble in n-hexane, water, methanol, and acetone, but it is partially soluble in toluene.

3.6.2.2 Multiple-detector GPC results

The original PIM-1 sample JDS056 and the fractionated samples were analysed using a Viscotek triple-detector GPC system**.** The GPC results for the fractionated samples of 0.5 g of PIM-1 are shown in **Fig. 25.**

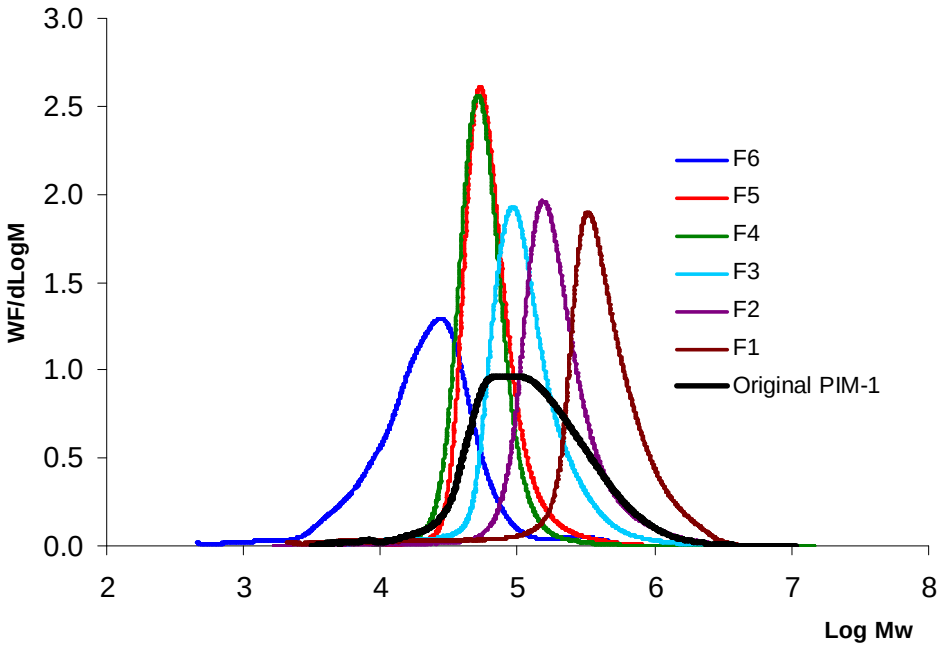

Figure 25 Weight distribution of log (molar mass) for fractionated and original PIM-1 sample JDS056.

The results presented in **Table 12** shows that the molecular weight decreases on going from fraction one to fraction 6 (the residue). The weight average molecular weight is found to decrease from 204000 to 34000 g mol^{-1}. In conclusion, the presented results in **Fig. 25** prove the validity of the employed procedure for fractionation of PIM-1 sample.

Table 12 *M*w, *M*n, (*M*w / *M*n), fraction weight (g), and recovery % result for the original and fractionated PIM-1 sample JDS056

Fraction No.	weight (g)	M_w	M_w / M_n	(wt/wt)%
1	0.0623	508000	3.5	12.43
2	0.1957	247000	1.9	39.05
3	0.0993	148000	1.7	19.82
4	0.0117	72000	1.2	2.33
5	0.0180	59000	1.2	3.59
The residue	0.0692	34000	2.6	13.81
Original		204000	2.6	

3.6.3 Fractionation of 2.0 gm of PIM-1 sample (JDS056)

3.6.3.1 Multiple-detector GPC result

The GPC results for the fractionated samples of 2.0 g of PIM-1 are shown in **Fig. 26**.

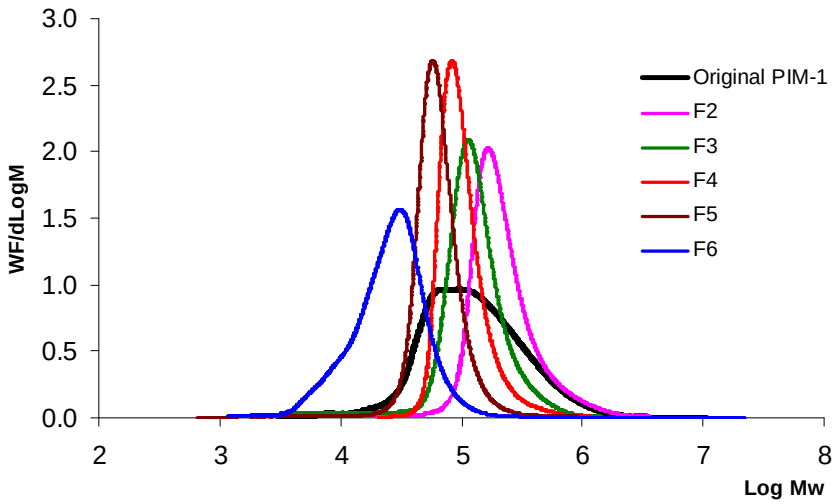

Figure 26 Weight distribution of log (molar mass) for fractionated and original PIM-1 sample JDS056

The results presented in **Table 13** shows that the molecular weight decreases from fraction one to fraction 6 (the residue). In conclusion, the above presented results in **Fig. 26** prove the validity of the employed procedure for fractionation of PIM-1 sample on a large scale.

Table 13 M_w, M_n, (M_w / M_n), fraction weight (g), and recovery % result for the original and fractionated PIM-1 sample (JDS056)

Fraction No.	weight (g)	M_w	M_w / M_n	(wt/wt)%
1[a]	0.1117	…..	…….	5.95
2	0.4618	270000	2.4	24.61
3	0.363	150000	1.8	19.34
4	0.1261	116000	1.2	6.72
5	0.2461	72000	1.4	13.11
The residue	0.3098	32000	1.7	16.56
Original		204000	2.6	

a all the recovered amount has been used when THF was used as a mobile phase

Fig.s 27-36 illustrates the Mark-Houwink plot and overlay plot: $Log([\eta]*\mathrm{M})$ versus $Log\mathrm{M}$ results for all the fractionated samples of JDS056 PIM-1 sample which will be discussed in more details in chapter 5.

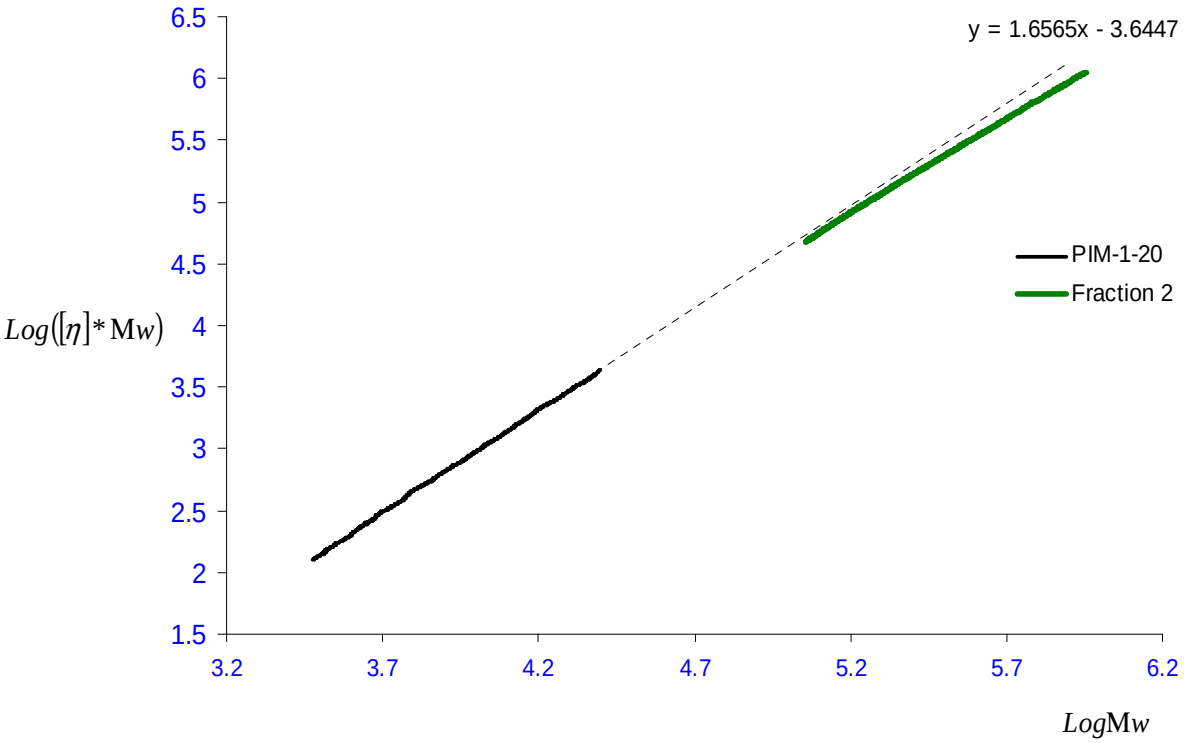

Figure 27 Overlay plot: $Log\ ([\eta]*\mathrm{M})$ versus $Log\mathrm{M}$ for fraction 2 of JDS056 sample and PIM-1-20 (Linear PIM-1 sample)

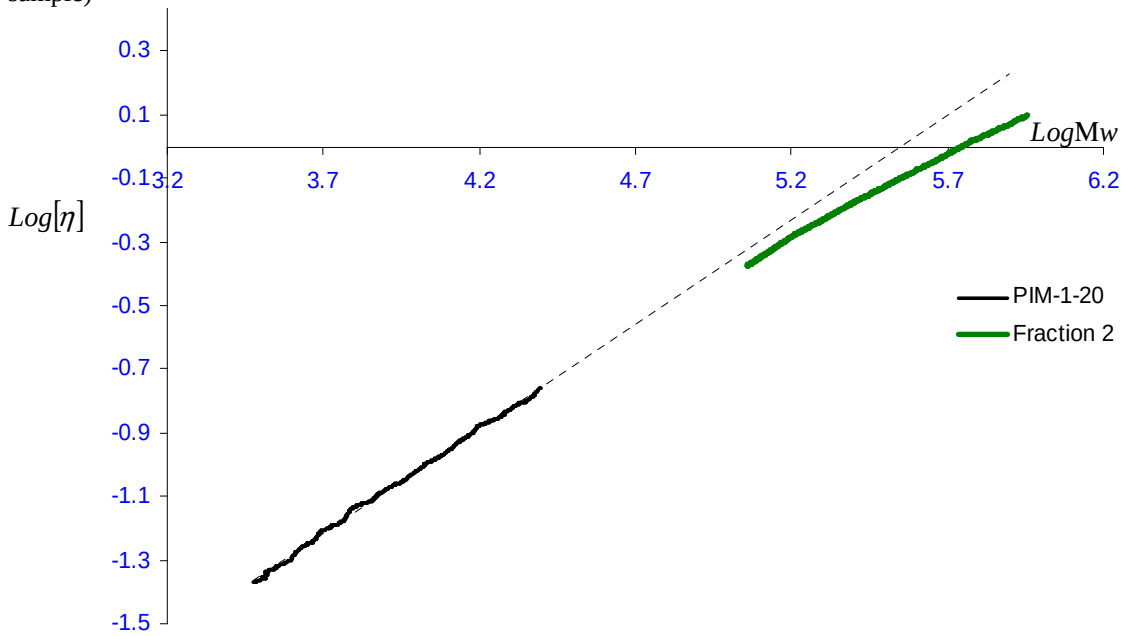

Figure 28 Mark-Houwink plot for fraction 2 of JDS056 sample and PIM-1-20 (Linear PIM-1 sample)

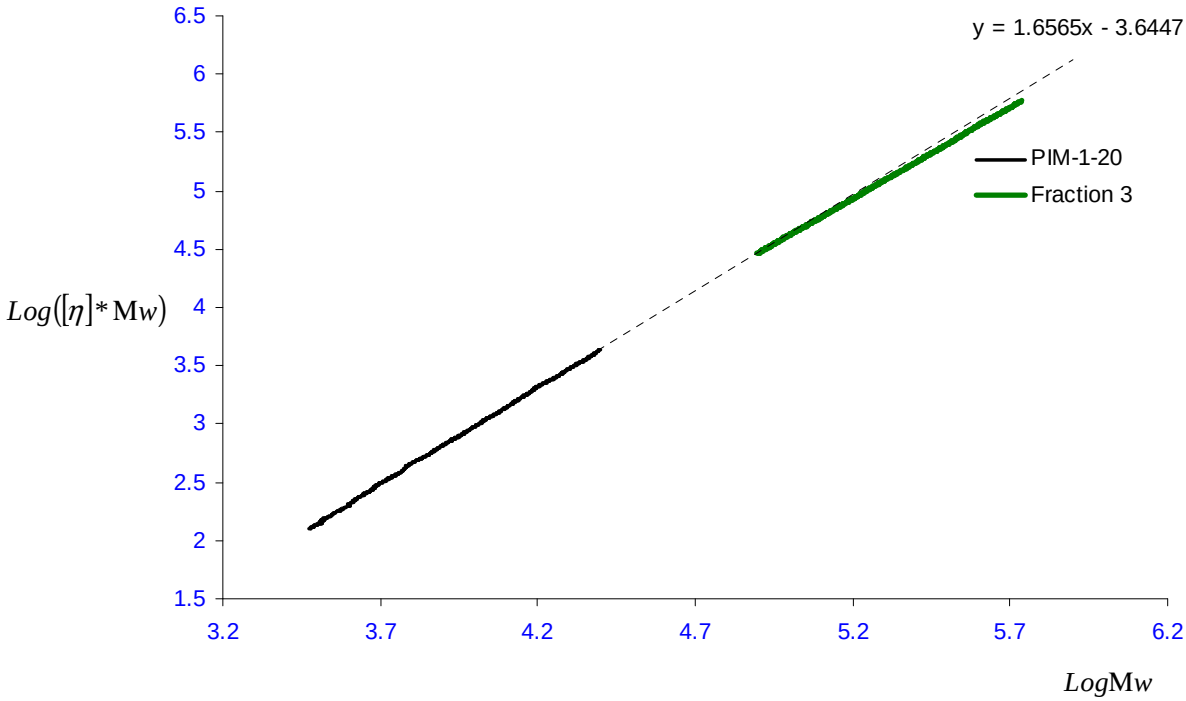

Figure 29 Overlay plot: $Log\ ([\eta]* \mathrm{M})$ versus $Log\mathrm{M}$ for fraction 3 of JDS056 sample and PIM-1-20 (Linear PIM-1 sample)

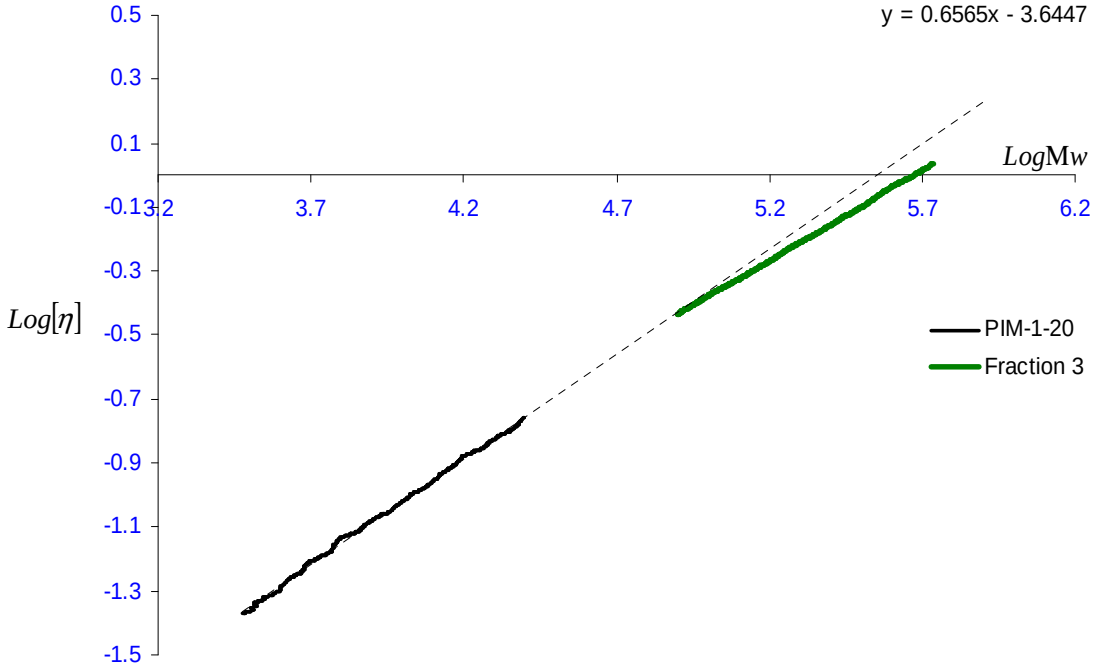

Figure 30 Mark-Houwink plot for fraction 3 of JDS056 sample and PIM-1-20 (Linear PIM-1 sample)

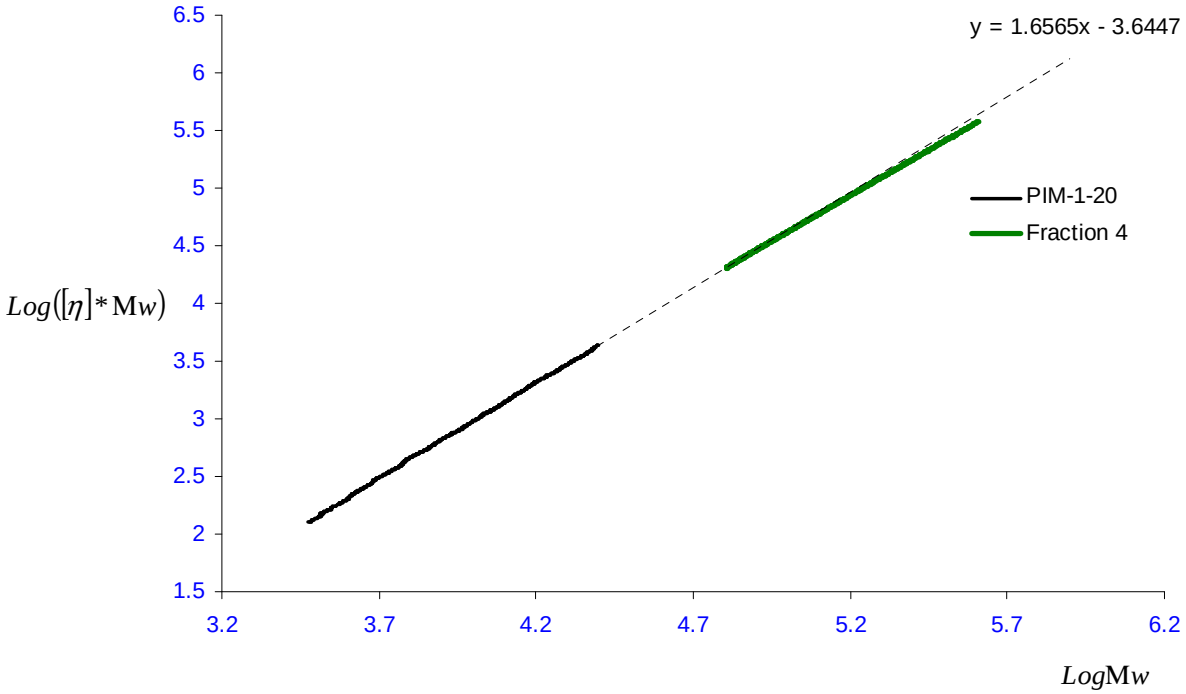

Figure 31 Overlay plot: $Log\ ([\eta]*\mathrm{M})$ versus $Log\mathrm{M}$ for fraction 4 of JDS056 sample and PIM-1-20 (Linear PIM-1 sample)

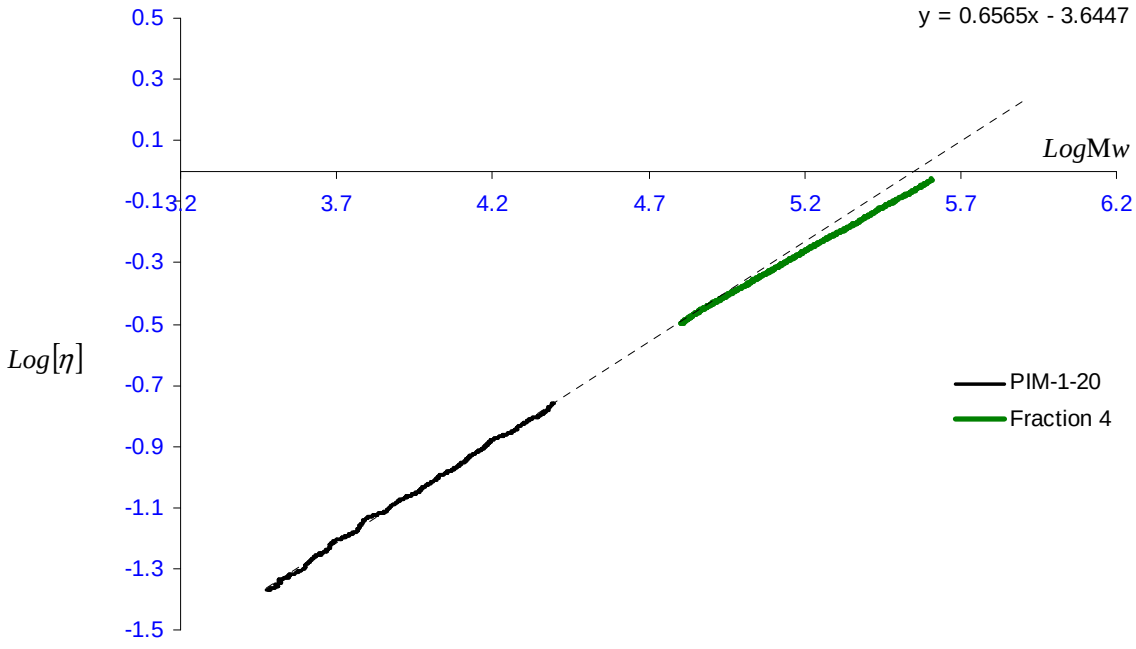

Figure 32 Mark-Houwink plot for fraction 4 of JDS056 sample and PIM-1-20 (Linear PIM-1 sample)

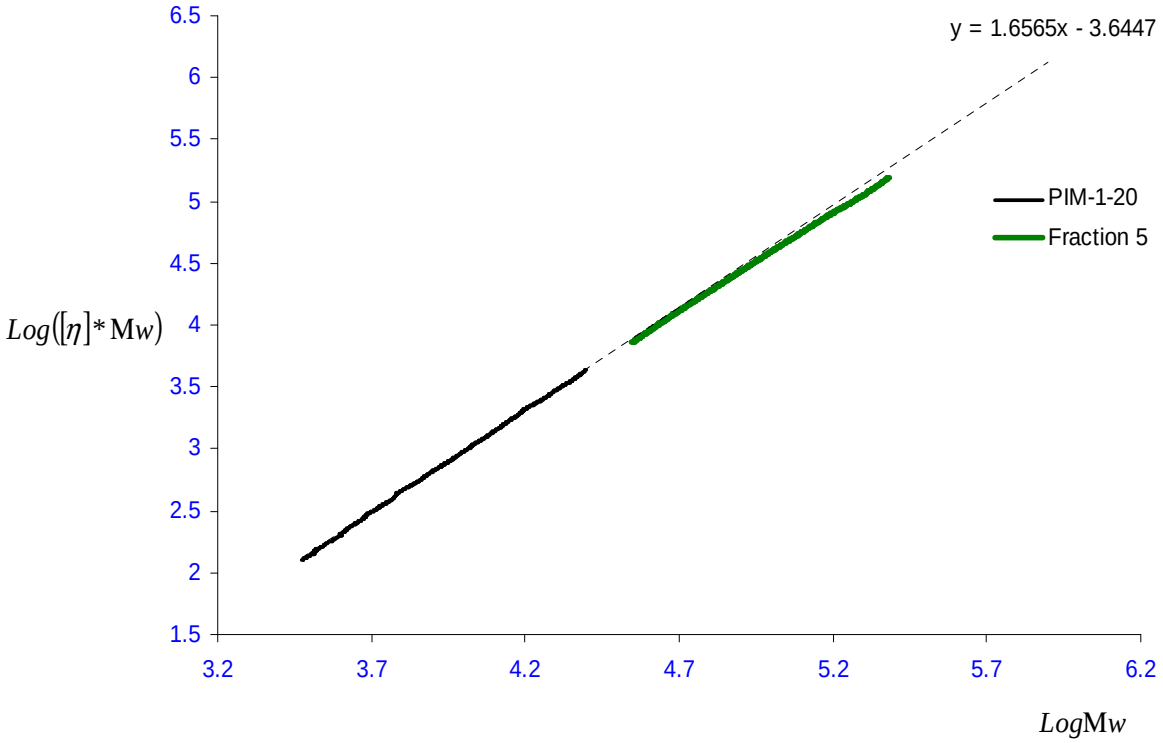

Figure 33 Overlay plot: $Log\ ([\eta]* \mathrm{M})$ versus $Log\mathrm{M}$ for fraction 5 of JDS056 sample and PIM-1-20 (Linear PIM-1 sample)

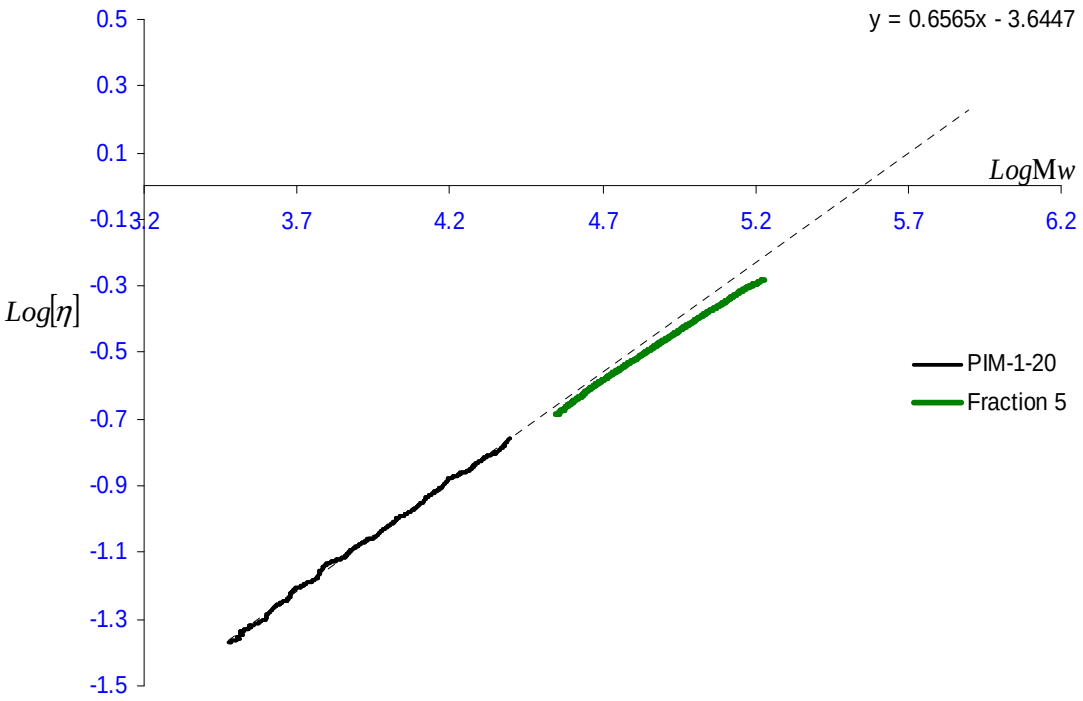

Figure 34 Mark-Houwink plot for fraction 5 of JDS056 sample and PIM-1-20 (Linear PIM-1 sample)

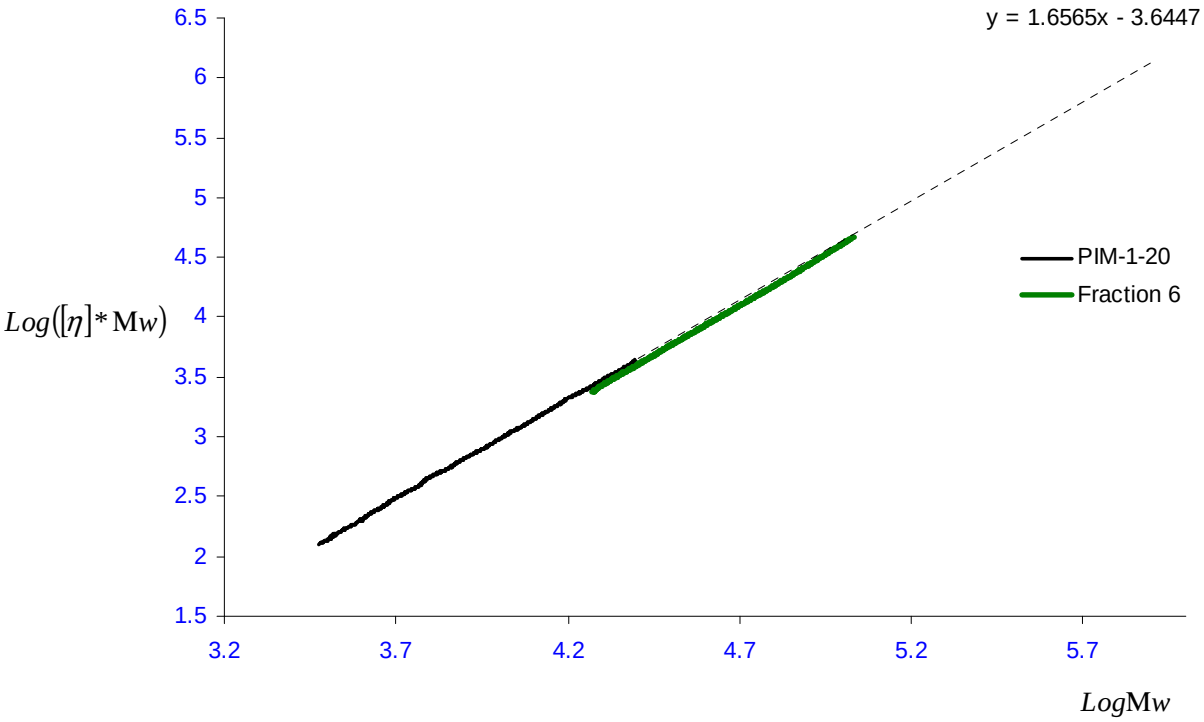

Figure 35 Overlay plot: $Log\ ([\eta]*\mathrm{M})$ versus $Log\mathrm{M}$ for fraction 6 (the residue) of JDS056 sample and PIM-1-20 (Linear PIM-1 sample)

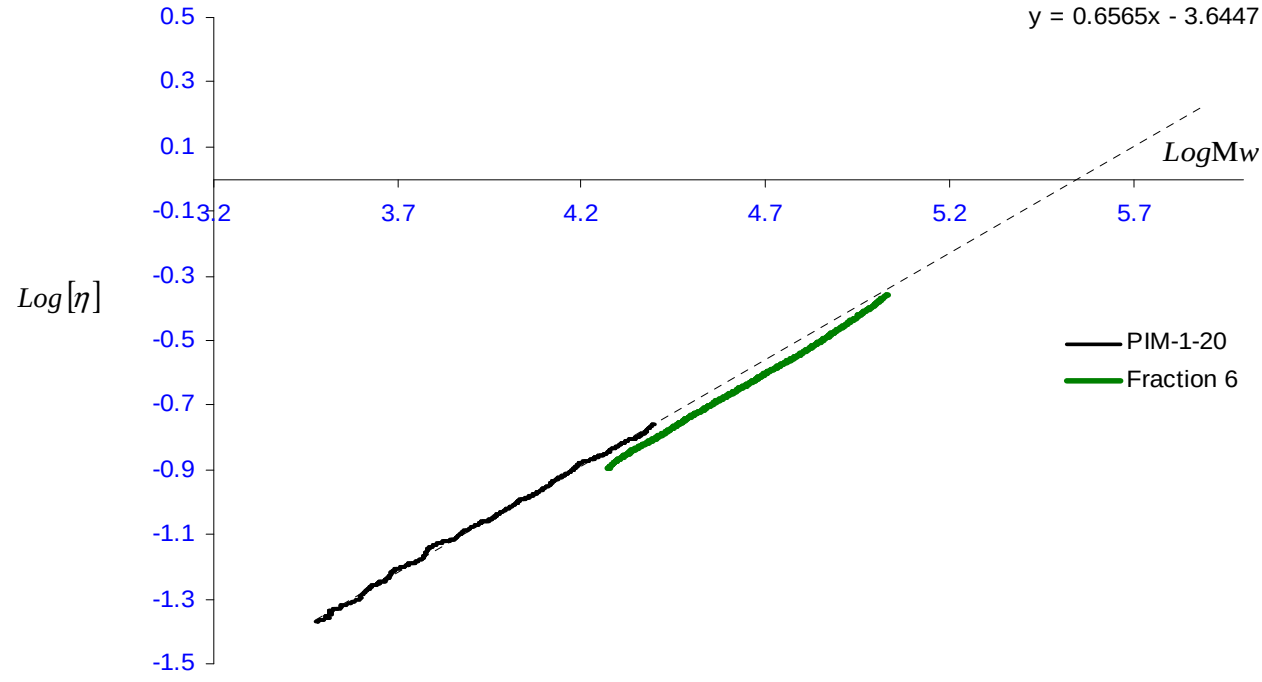

Figure 36 Mark-Houwink plot for fraction 6 (the residue) of JDS056 sample and PIM-1-20 (Linear PIM-1 sample

3.6.3.2 MALDI-ToF mass spectrometry results

The MALDI-ToF mass spectra for the fractions obtained from 2.0 g PIM-1 sample (JDS056) show the presence of both linear and branched species in fractions **1, 2,** and **3.** In fraction 6, which is the recovered residue, only cyclic species were observed. **Figs. 37** and **38** show the MALDI-ToF mass spectra of fraction No.3 and No.6, which are presented as representative results. The spectrum for fraction No.3 shows a series of peaks which may be attributed to branched PIM-1 (**Schemes 2-5**) (**Table 14**) and a series of peaks for fluorine, hydroxyl, and mixed fluorine-hydroxyl ended linear fractions (**Fig. 10**). In contrast, only a series of peaks for cyclic species (Cn) (**Scheme 6**) were observed in fraction No.6, as seen in **Fig. 38**. The most prominent distribution Cn contains molecular ions of n (460) + 23, which corresponds to cyclic structures with sodium cations (**Table 15**).

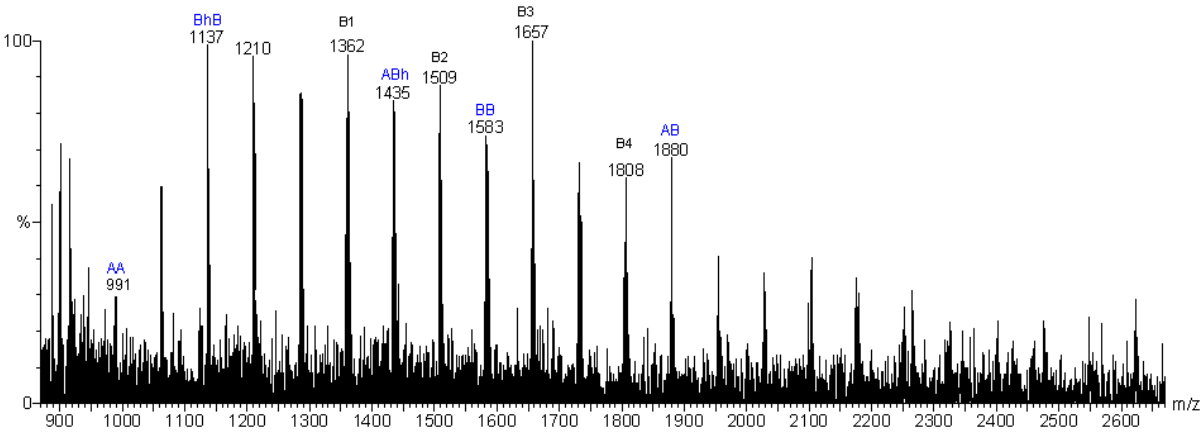

Figure 37 MALDI-ToF mass spectrum of fraction No.3 obtained on fractionation of 2 g PIM-1 sample (JDS056)

Table 14 The calculated and the observed mass for the dominant distributions

Endgroup Type	Endgroup formula	Repeat unit	n	Cation	Overall formula	Mass (calc.)	Mass (obs.)
AB	H_2, F_2	$C_{29}H_{20}O_4N_2$	4	H^+	$(C_{29}H_{20}O_4N_2)_4H_3F_2^+$	1881	1880
ABh	H_2, $(OH)_2$	$C_{29}H_{20}O_4N_2$	3	Na+	$(C_{29}H_{20}O_4N_2)_7H_3(OH)_2^+$	1439	1435
BhB	F_2, $C_8N_2(OH)_2$	$C_{29}H_{20}O_4N_2$	2	Na+	$(C_{29}H_{20}O_4N_2)_7\ C_8N_2(OH)_2\ F_2^+$	1141	1137
BB	F_2, $C_8N_2F_2$	$C_{29}H_{20}O_4N_2$	3	H^+	$(C_{29}H_{20}O_4N_2)_7\ C_8N_2F_2\ F_2^+$	1581	1583
AA	H_2, $C_{20}O_2H_{18}$	$C_{29}H_{20}O_4N_2$	1	Na+	$(C_{29}H_{20}O_4N_2)_1C_{20}O_2H_{18}H^+$	985	991
B1	F, $C_{29}H_{21}O_4N_2F_2$, 2 $C_8F_3N_2$	$C_{29}H_{20}O_4N_2$	1	K^+	$C_{74}H_{41}\ F_8N_8\ O_8\ K^+$	1360	1362
B2	2 $C_8F_3N_2$, $2(C_{21}H_{23}O_4)$	$C_{29}H_{20}O_4N_2$ – CH_4	1	Na^+	$C_{87}H_{66}\ F_6N_6O_{12}Na^+$	1508	1509
B3	2 $C_8F_3N_2$, $C_{21}H_{23}O_4$, $C_{29}H_{21}O_4N_2F_2$	$C_{29}H_{20}O_4N_2$	1	H^+	$C_{95}H_{64}\ F_8N_8O_{12}H^+$	1661	1657
B4	2 $C_8F_3N_2$, $2(C_{21}H_{23}O_4)$	$C_{29}H_{20}O_4N_2$ – CH_4	1	Na^+	$C_{101}H_{58}\ F_8N_{10}O_{14}Na^+$	1809	1808

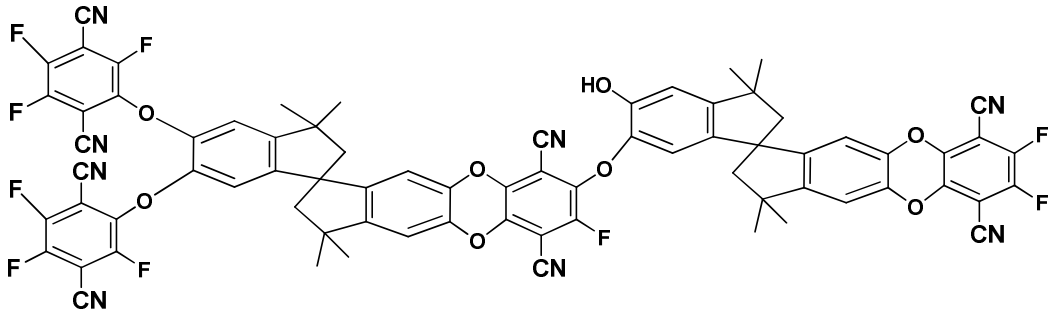

B1

Scheme 2 Molecular structure of branched PIM-1(1360m/z)

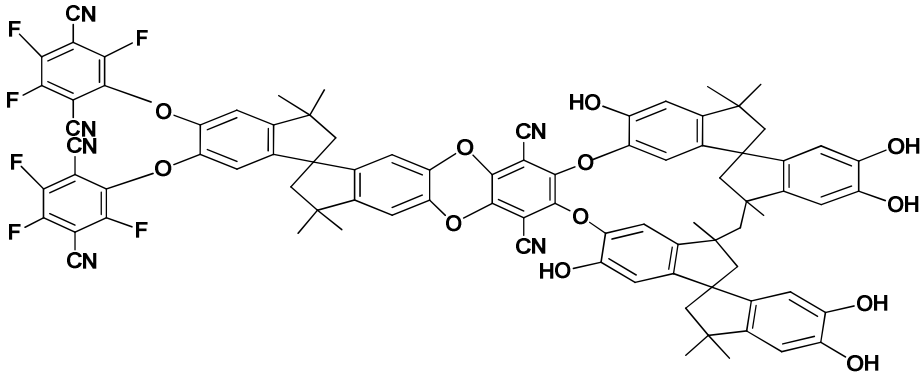

B2

Scheme 3 Molecular structure of branched PIM-1 (1508m/z)

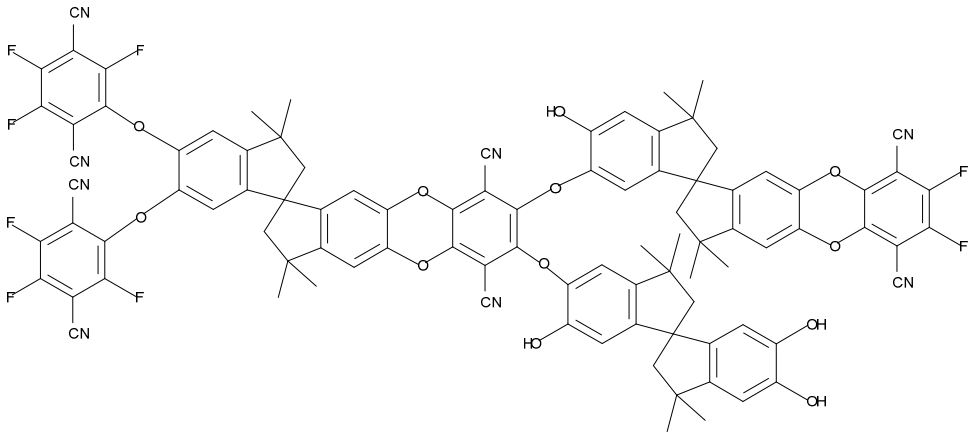

B3

Scheme 4 Molecular structure of branched PIM-1 (1661m/z)

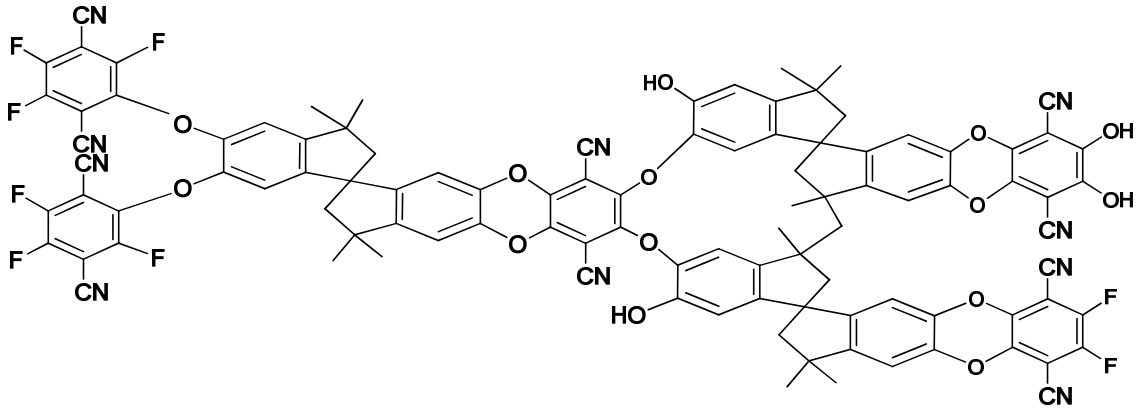

B4

Scheme 5 Molecular structure of branched PIM-1 (1809m/z)

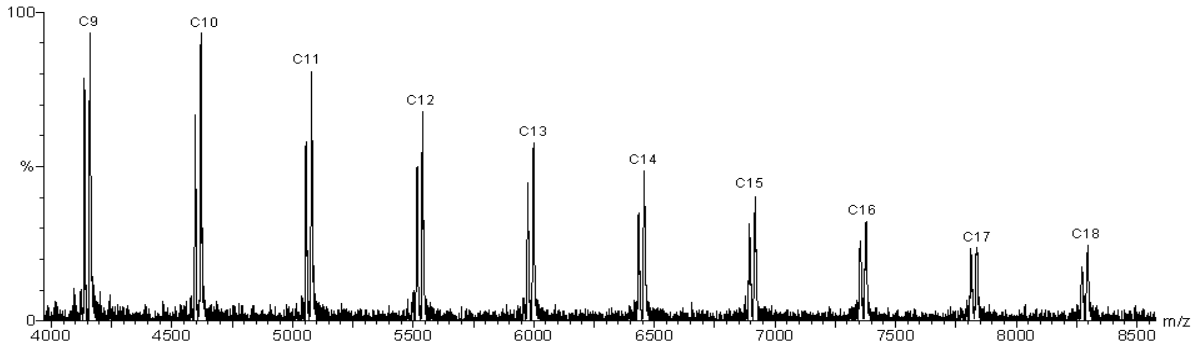

Figure 38 MALDI-ToF mass spectrum of fraction No.6 (the residue) obtained on fractionation of 2 g PIM-1 sample (JDS056)
Cn = n (460) + 23

Table 15 The calculated and the observed mass for the dominant distributions

Repeat unit	n	Cation	Overall formula	Mass (calc.)	Mass (obs.)
$C_{29}H_{20}O_4N_2$	9	Na^+	$(C_{29}H_{20}O_4N_2)_9\ Na^+$	4163	4160
$C_{29}H_{20}O_4N_2$	10	Na^+	$(C_{29}H_{20}O_4N_2)_{10}\ Na^+$	4623	4621
$C_{29}H_{20}O_4N_2$	11	Na^+	$(C_{29}H_{20}O_4N_2)_{11}\ Na^+$	5083	5078
$C_{29}H_{20}O_4N_2$	12	Na^+	$(C_{29}H_{20}O_4N_2)_{12}\ Na^+$	5543	5538
$C_{29}H_{20}O_4N_2$	13	Na^+	$(C_{29}H_{20}O_4N_2)_{13}\ Na^+$	6003	5999
$C_{29}H_{20}O_4N_2$	14	Na^+	$(C_{29}H_{20}O_4N_2)_{14}\ Na^+$	6463	6458
$C_{29}H_{20}O_4N_2$	15	Na^+	$(C_{29}H_{20}O_4N_2)_{15}\ Na^+$	6923	6918
$C_{29}H_{20}O_4N_2$	16	Na^+	$(C_{29}H_{20}O_4N_2)_{16}\ Na^+$	7383	7377
$C_{29}H_{20}O_4N_2$	17	Na^+	$(C_{29}H_{20}O_4N_2)_{17}\ Na^+$	7843	7836
$C_{29}H_{20}O_4N_2$	18	Na^+	$(C_{29}H_{20}O_4N_2)_{18}\ Na^+$	8303	8296

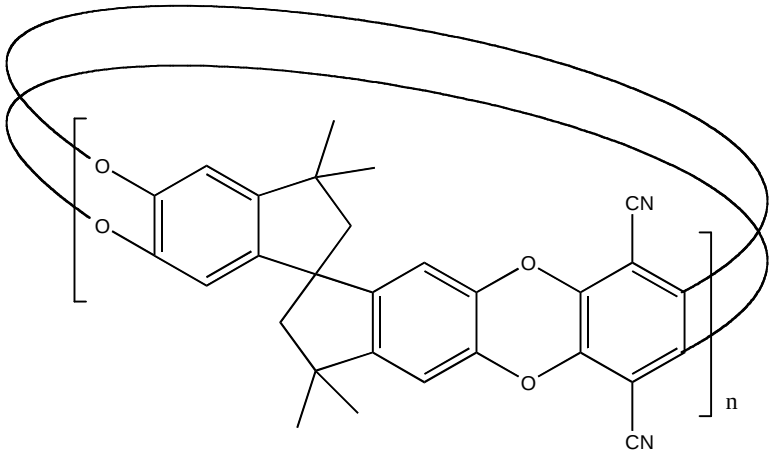

Scheme 6 Molecular structure of cyclic PIM-1 sample (JDS056)

3.7 Conclusion

In conclusion, the procedure to fractionate PIM-1 was successfully established and its repeatability was proved. The fractionated samples will help in giving more complete information on the structure of JDS056 sample made by the conventional method on a large scale.

Chapter 4: Validation of multi detector GPC methodology

4.1 Multi-detector GPC

4.1.1 Introduction

To ensure that the instrument is operating correctly, and to validate the system to demonstrate that it is suitable for the intended purpose, and the method was tested to ensure a good reproducibility and repeatability. There was a need to do the analysis for the same samples on two separate laboratories to ensure good reproducibility of the results and to give a more accurate indication of precision. The same sample was prepared eight times, with fresh solutions being prepared each time to see how close they are to each other under the same analytical conditions.

4.1.2 Operating procedure

Before starting analysis, the column oven temperature was set to 35 °C ensuring high SEC efficiency, stable baseline, and consistent results.[85] The inlet pressure (IP) of the viscometer detector was set to zero with flow off. Then the flow was turned on and a check for air bubbles (a non-stable baseline) was then conducted. Any bubbles were removed by running the 'purge' function at a pump flow of 1 ml/minute and performing a needle wash. Next, the GPC system was equilibrated at the desired flow conditions and the baseline and backpressure were monitored until a stable baseline and column backpressure were obtained (which typically took 1 hour). If the pressure was found to be excessive, the temperature was raised to five degrees below the boiling point of the mobile phase at a pump flow of 1 ml/minute. The purging step and needle wash were also repeated. When the system was ready a standard PS sample (M_w = 96000 g mol^{-1}) was run to compare and correct the inter-detector delay volumes among the three detectors, to obtain the calibration factor or constants for the three detectors, and to effectively rectify the band broadening effect due to serial connections

of the three detectors.[85] This was repeated from time to time make sure that the calibration remained true.

4.1.3 Sample preparation

The samples were dried in a vacuum oven for at least 24 hours, allowing them to be weighed accurately using an analytical balance with 0.0001 g readability, then the required amount of the filtered solvent was added using a chromatography syringe to obtain an accurate concentration measurement. Once the sample was completely dissolved, sufficient filtrate (1.5 ml) was collected using a 0.45 µm filter with PTFE membrane. Each sample was filtered using a new filter to avoid any contamination from earlier use.

4.2 Determination of $\frac{dn}{dc}$ value for PIM-1

The determination of the $\frac{dn}{dc}$ value, which depends on the chemical structure of the sample and the refractive index of the solvent, was carried out in chloroform at 35 °C for a wavelength of 670 nm. As the detectors were calibrated using a standard polystyrene sample, the calibration constant for the RI detector could be calculated by analyzing a standard polystyrene sample of known $\frac{dn}{dc}$ and known concentration; consequently, the $\frac{dn}{dc}$ value for the polymer of interest could be determined.

The measurement of the $\frac{dn}{dc}$ value was performed for PIM-1 sample PIM-1-20 by plotting the RI detector peak area versus sample concentration (**Table 16, Fig. 39**) at a constant injection volume (0.1 ml) for a variety of concentrations of sample solution and applying equation 4-1.

$$RI_i = \left(\frac{RI_{cal} C_i}{n_0} \right) \bullet \left(\frac{dn}{dc} \right) \quad (4\text{-}1)$$

Where RI_{cal} is the calibration constant for the RI detector (2573000), established by analyzing samples of known $\left(\frac{dn}{dc} \right)$ and known concentration; RI_i is the measured response from the detector; C_i is the sample concentration; and n_0 is the refractive index of the solvent (1.443).

Determination of the $\frac{dn}{dc}$ value was carried out for sample PIM-1-20 and found to be 0.2 ml/g at 35 °C in chloroform for a wavelength of 670 nm.

Table 16 Sample concentration and area of RI peak for PIM-1-20

PIM-1-20	
Concentration (g/ml)	RI.Area (mvml)
0.00058	20.52
0.00086	30.52
0.00118	41.93
0.00184	64.51

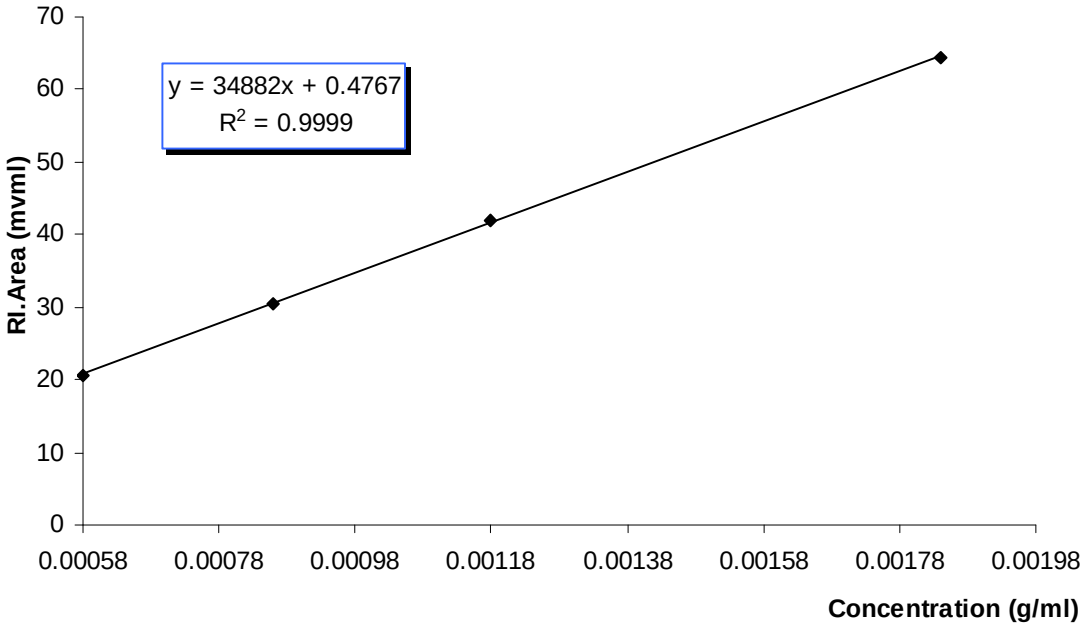

Figure 39 Change in the peak area (mvml) measured by the RI detector versus sample concentration; from which the d*n*/d*c* can be calculated from the measured slope.

4.3 Evaluation of the analysis procedure

The reliability of the analysis procedure was assured through a collaborative GPC study by the University of Manchester and the GKSS Research Centre Geestacht GmbH, Germany, to compare the molar mass results of three PIM-polyimide samples (**Fig. 40**), PIM-PI-1, PIM-PI-3, and PIM-PI-8 using triple detector GPC with low angle (University of Manchester) and multiple angle (GKSS) light scattering detectors.[86]

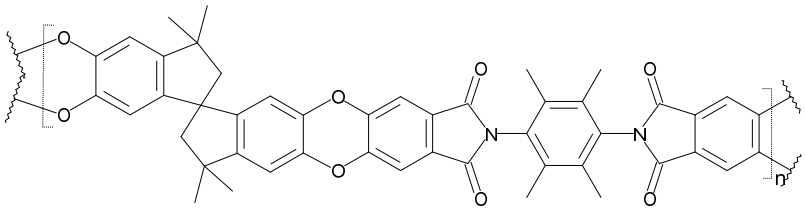

PIM-PI-1

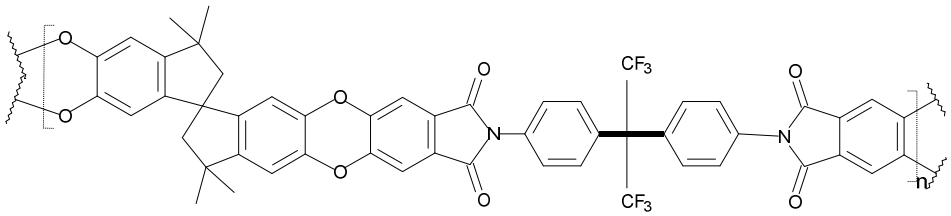

PIM-PI-3

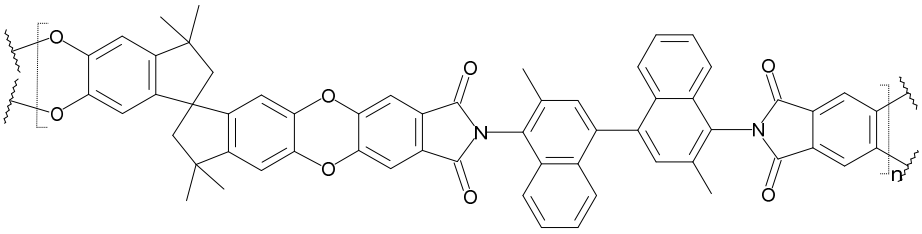

PIM-PI-8

Figure 40 Molecular structures of PIM-PI-1, PIM-PI-3, and PIM-PI-8

Good agreement was achieved, as shown in **Tables 17-19**.

Table 17 Comparison of GPC results from the University of Manchester and GKSS for PIM-P1-1

	Molar mass		
Sample ID	M_n	M_w	*Mp*
PIM-PI-1 (UoM)	23718	40397	35780
PIM-PI-1 (GKSS)	22200	48940	45930
RSD %	5	14	18

Table 18 Comparison of GPC results from the University of Manchester and GKSS for PIM-P1-3

	Molar mass		
Sample ID	M_n	M_w	*Mp*
PIM-PI-3 (UoM)	28686	54508	45138
PIM-PI-3 (GKSS)	21870	44810	46190
RSD %	19	14	2

Table 19 Comparison of GPC results from the University of Manchester and GKSS for PIM-P1-8

	Molar mass		
Sample ID	M_n	M_w	*Mp*
PIM-PI-8 (UoM)	19360	41065	29330
PIM-PI-8 (GKSS)	18370	41080	32370
RSD %	4	0.03	7

Repeatability was assured by running a single PIM-1 sample (NMH02) eight times, with fresh solutions being prepared each time **(Figs. 41-43)**. The agreement within the results seems very reasonable. Average values for M_w and M_n are shown in **Table 20** and the relative standard deviation were 2% and 4% respectively, which can be considered as the experimental uncertainty for the procedure.

Table 20 Repeatability of average molar masses from multi-detector GPC for PIM-1 sample NMH02

NMH02	M_w *g mol*$^{-1}$	M_n *g mol*$^{-1}$
Replicate 1	27,801	11,289
Replicate 2	27,442	11,209
Replicate 3	27,378	12,188
Replicate 4	26,820	11,689
Replicate 5	26,216	10,966
Replicate 6	26,568	11,171
Replicate 7	26,720	11,613
Replicate 8	26,878	11,895
Mean	26,978	11,503
STDEV	521	414
RSD %	2	4

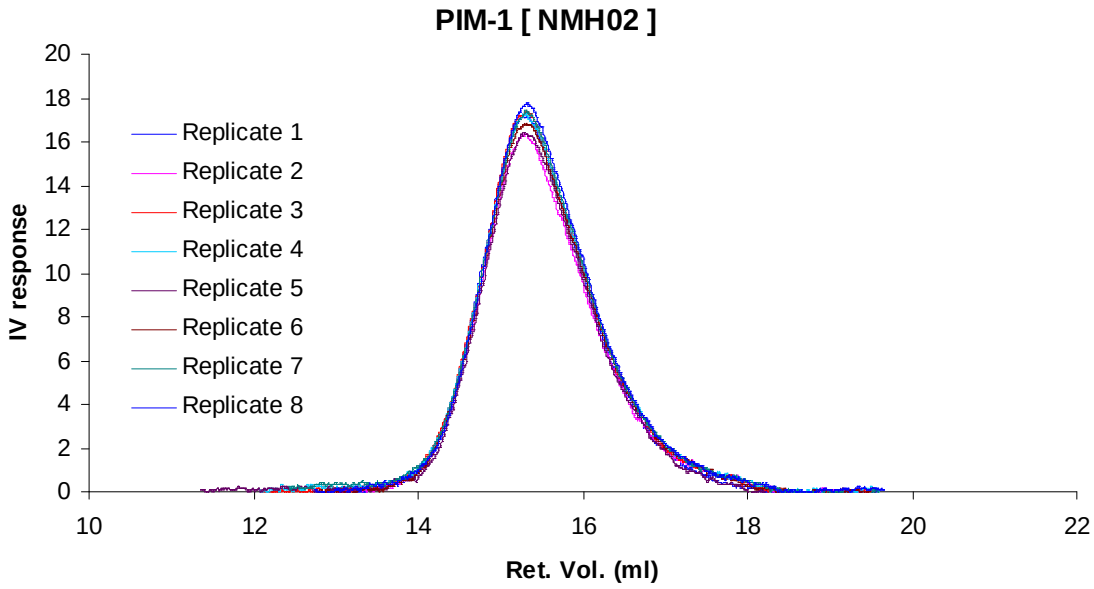

Figure 41 Viscometer response versus elution volume for PIM-1 sample NMH02

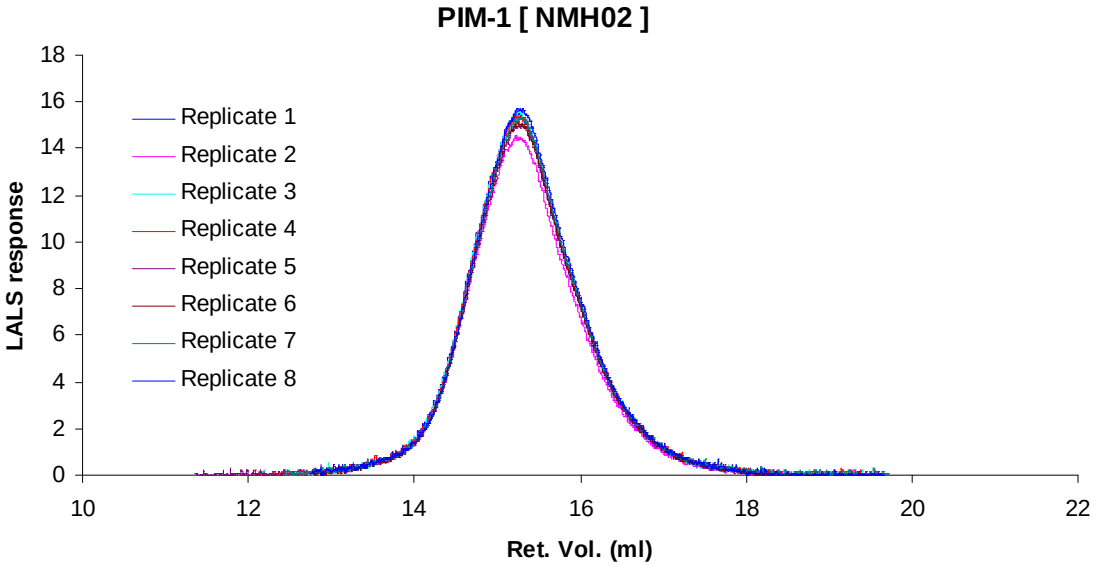

Figure 42 Low angle light scattering response versus elution volume for PIM-1 sample NMH02

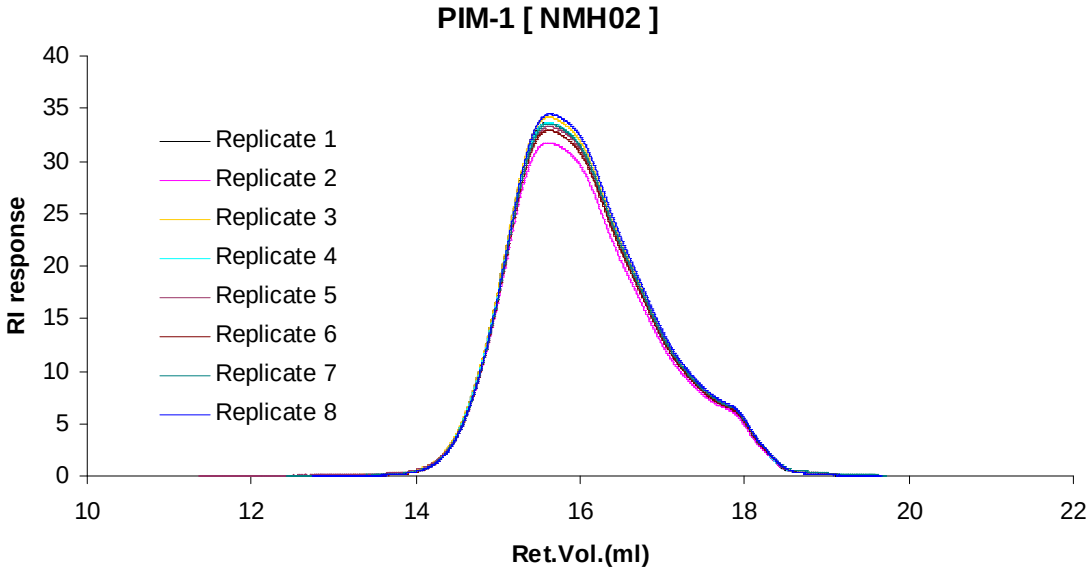

Figure 43 Differential refractive index detector response versus elution volume for PIM-1 sample NMH02

4.4 Conclusions

In conclusion, a reliable GPC method using multiple-detector GPC was successfully established and it was validated by assuring its repeatability and reproducibility.

Chapter 5: Structural analysis

5.1 Introduction

The aim of the work described in this chapter was to develop methods for analyzing structural differences between PIM-1 samples, employing both multi-detector GPC and, at the low molar mass end, MALDI-ToF mass spectrometry. PIM-1 may include linear, cyclic and branched structures, as discussed below. Different structural types of the same molar mass, *M*, may be expected to have different values of intrinsic viscosity, [η]. Intrinsic viscosity is proportional to an effective specific volume of the polymer in solution (*i.e.*, a higher effective density, as for a branched polymer, will result in a lower [η] for the same *M*). Different structural types of the same molar mass will also have different hydrodynamic volumes, as expressed by the hydrodynamic volume parameter [η]*M*. Thus, plots of either log[η] versus log*M* (Mark-Houwink plot) or of log[η]*M* versus log*M*, may be used to compare samples. For a given change in the Mark-Houwink parameters *K* and *a*, where $[\eta]=KM^a$, a greater visual difference is seen in a Mark-Houwink plot than in a plot of log[η]*M*. However, hydrodynamic volume is of interest as it directly controls separation in GPC.

Kricheldorf *et al.*[41] found that cyclization competes with chain growth at all stages of polycondensations, even at high conversions. Cyclic molecules form because, as the concentration of the unreacted functional groups decreases as the polymerization continues, cyclization will be then favoured.[41] Kricheldorf *et al.*[40] compared a PIM-1 sample prepared under seemingly similar reaction conditions as those reported by Budd *et al*.[40] with one which was provided by Budd and he concluded that the majority of the reaction product was cyclic, which is consistent and in good agreement with the theory of polycondensations published by Kricheldorf and Schwarz,[40] and agrees with the experimental results obtained from numerous syntheses of aromatic polyethers.[40]

More recently, a Canadian research group optimized the reaction conditions reported by Budd and co-workers, using a high-speed homogenizer at about 155 °C to provide a high molecular weight PIM-1 ladder polymer in high yield within a few minutes which is almost free of crosslinked and cyclic species.[33]

It was also found that high temperature or high concentration conditions results in a decrease in cyclic oligomers because at high concentration there is increased chance of intermolecular reaction or defected chain growth, by the reduced amount of oligomeric and increased amount of high molecular weight material, possibly caused by branching or cross-linking.[42]

The presence of branched material was investigated and reported by Kevin Reynolds,[42] who found that the presence of the activating nitrile groups and the high temperature conditions could result in opening the dibenzodioxane ring by nucleophilic cleavage. The proposed mechanism is shown in **Fig. 44**. The nucleophile attacks the C-O bond in the dibenzodioxane ring, opens it and leaves the oxygen electronegative, making it a nucleophilic reagent. This attack creates a branch point, but further nucleophilic attack might result in a low molecular weight oligomeric product, as shown in **Fig. 44.** An example where this may have occurred is sample DNM48B (**Fig. 22**), which show a low molecular weight.[42]

Branching could also be a result of some phenol groups being oxidized into a benzoquinone-type structure (**Scheme 7**). The residual F reacts with phenolate chain ends of another PIM-1 chain, resulting in branched or crosslinked structures.[107]

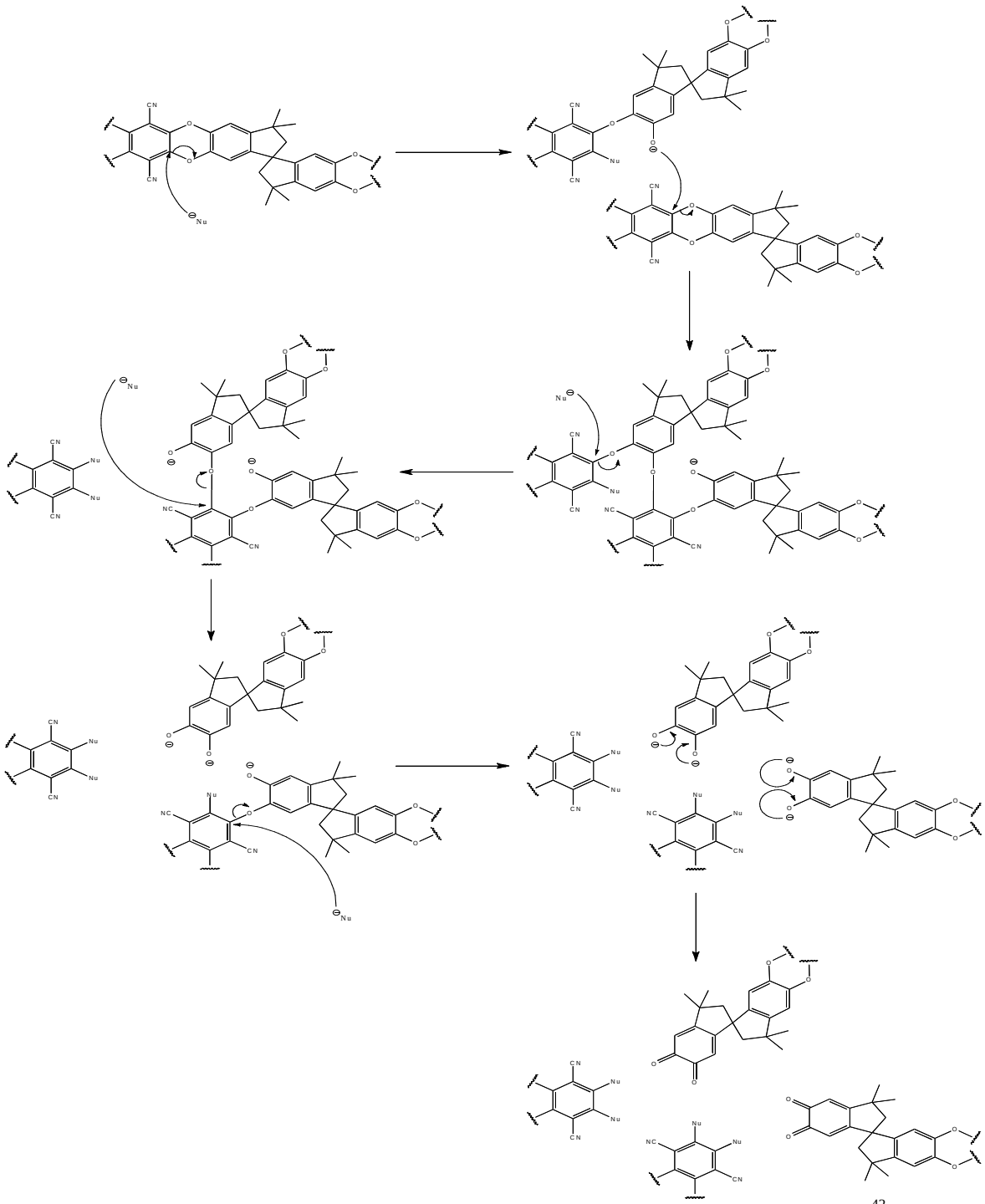

Figure 44 Proposed mechanism for the branching and degradation of PIM-1 at high temperature [42]

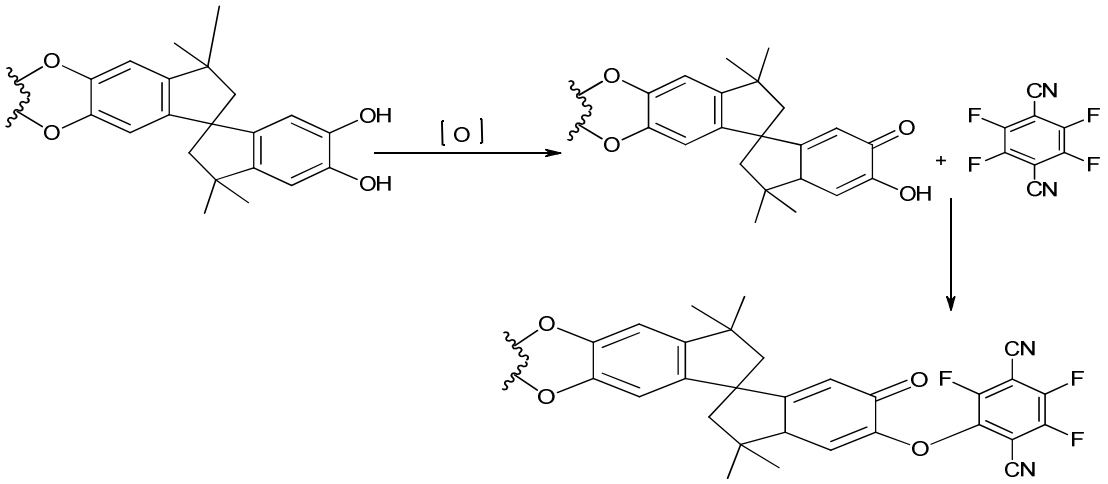

Scheme 7 Proposed mechanism for branching of PIM-1 as the result of the oxidation of a phenol group.[107]

5.2 Linear PIM-1

In **Chapter 2** it was shown that the MALDI-ToF mass spectrum for the low molar mass sample PIM-1-20 (**Fig. 9**) contained only peaks consistent with linear species. The hydrodynamic properties of this sample may therefore be taken as representative of linear PIM-1, at least at low molar mass. PIM-1 sample NMH01, like PIM-1-20, was prepared by the high shear method developed by a group in Canada. PIM-1-20 was prepared with a lower molar ratio of base compared to NMH01 to form a polymer within the detection limit of MALDI and GPC.

Fig. 45 shows double logarithmic plots of the hydrodynamic volume parameter $[\eta]M$ versus M for samples PIM-1-20 and NMH01. It can be seen in **Fig. 45** that the data for both NMH01 and PIM-1-20 overlay more or less completely up to around 100,000 g mol^{-1}. This shows that NMH01 has the same hydrodynamic volume as the linear analogues (PIM-1-20) having identical molar masses, and hence suggests it also has a largely linear structure. A change in hydrodynamic volume appears around $Log\mathrm{M}w$ = 5.03 or molecular weight ≈ 107,000 g mol^{-1}. This is clearly illustrated in the Mark-Houwink plots (**Fig. 46**) which is the preferred method of structural comparison; note the greater change in slope around $Log\mathrm{M}w$

= 5.03. The lower intrinsic viscosity value indicates higher density. Therefore it could be proposed that this change is due to a change in the structure (branched species). These results are consistent with the results (within the range of the MALDI-ToF) reported by Naiying Du. *et al.*[33] in which the present reaction conditions were reported to provide linear ladder polymers of PIM-1 which are almost free of crosslinked and cyclic species.

The data presented here suggest that for linear PIM-1 the Mark-Houwink parameters are K = 2.27×10^{-4} cm^3 g^{-1} and a = 0.66 (T= 35 °C, Chloroform was used as a solvent), at least up to a molar mass in the region of 50,000 g mol^{-1}. This will be used as a basis for comparison with other PIM-1 samples, as discussed below.

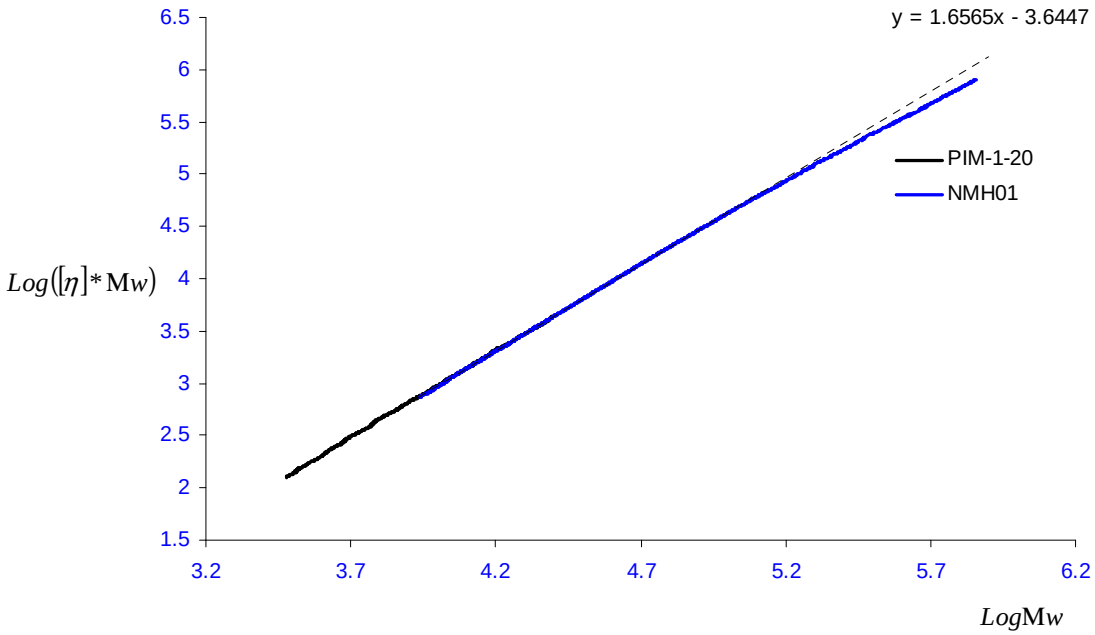

Figure 45 $Log\ ([\eta]*\mathrm{M})$ versus $Log\mathrm{M}$ for PIM-1 samples PIM-1-20 and NMH01. Sample NMH01 was prepared under high mixing condition, reagent molar ratio THSB/ TFPN /K_2CO_3 (1:1:3), DMAc/Toluene as solvent, 150-155 °C, 8 minutes

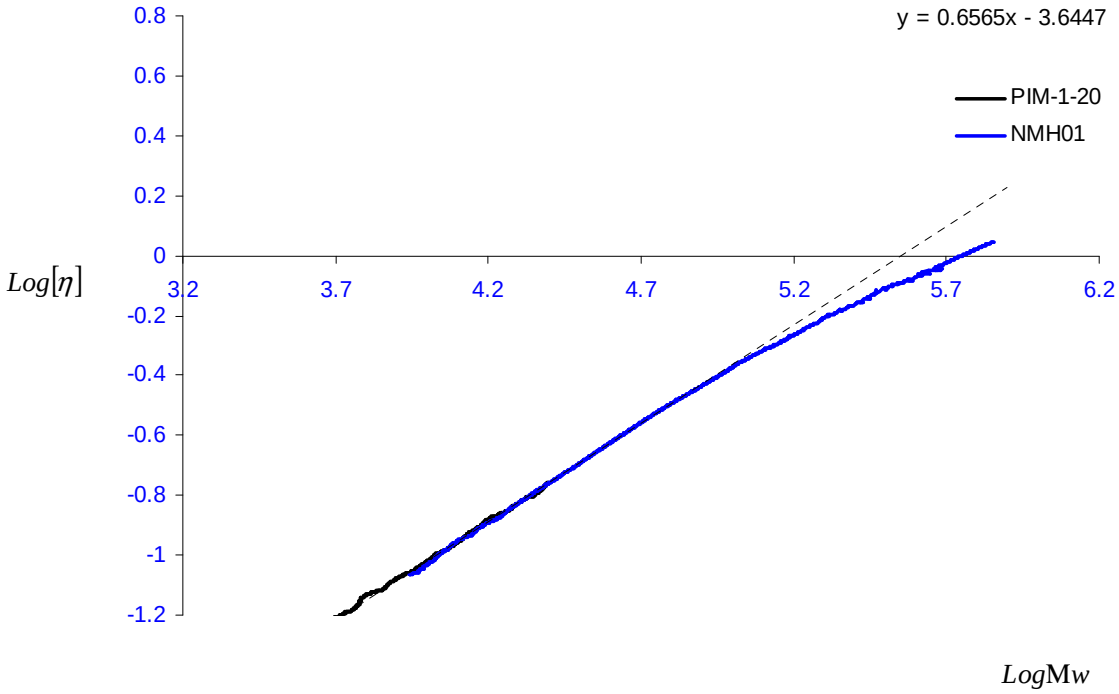

Figure 46 Mark-Houwink plots for PIM-1 samples PIM-1-20 and NMH01, Sample NMH01 was prepared under high mixing condition ,reagent molar ratio THSB/ TFPN /K_2CO_3 (1:1:3), DMAc/Toluene as solvent, 150-155 °C, 8 minutes

5.3 Cyclic PIM-1

Liquid chromatography is the commonest technique used for the characterization of cyclic and linear polymers.[87-97] To investigate the possibility of measuring structural differences between cyclic and linear fractions using the GPC technique, two samples (PIM-1-20 and LMA24) having a molecular weight within the detection limits of both techniques GPC and MALDI, prepared in-house, were analyzed. The MALDI-ToF mass spectrum for PIM-1-20 (**Fig. 9**) shows the presence of only linear species, indicating that the sample is linear at least in this mass range. The MALDI-ToF mass spectrum for LMA24 (**Fig. 47**) shows the presence of only cyclic species (**Table 21**). As in the GPC technique it is often supposed that GPC utilizes a non-interactive mode of separation, molecules will be separated according to their size,[98] and consequently, the hydrodynamic volume as a function of a molecular weight was

applied to reflect structural changes in the polymer. The results displayed in **Fig. 48**, for PIM-1-20 (linear PIM-1) and LMA24 (cyclic PIM-1), indicates that the mostly cyclic polymer (LMA24) has lower hydrodynamic volume than the linear analogues (PIM-1-20) having identical molar masses. This result is consistent with the results presented by Li Guo,[99] P. V. Wright,[100] and J. A. Semlyen[101] in which similar behavior is observed for cyclic polymers. In conclusion, although the linear and cyclic distributions overlap in molecular weight range and cannot be completely separated by GPC,[102] it seems that it is possible to determine and differentiate between cyclic and linear species at least in this mass range.

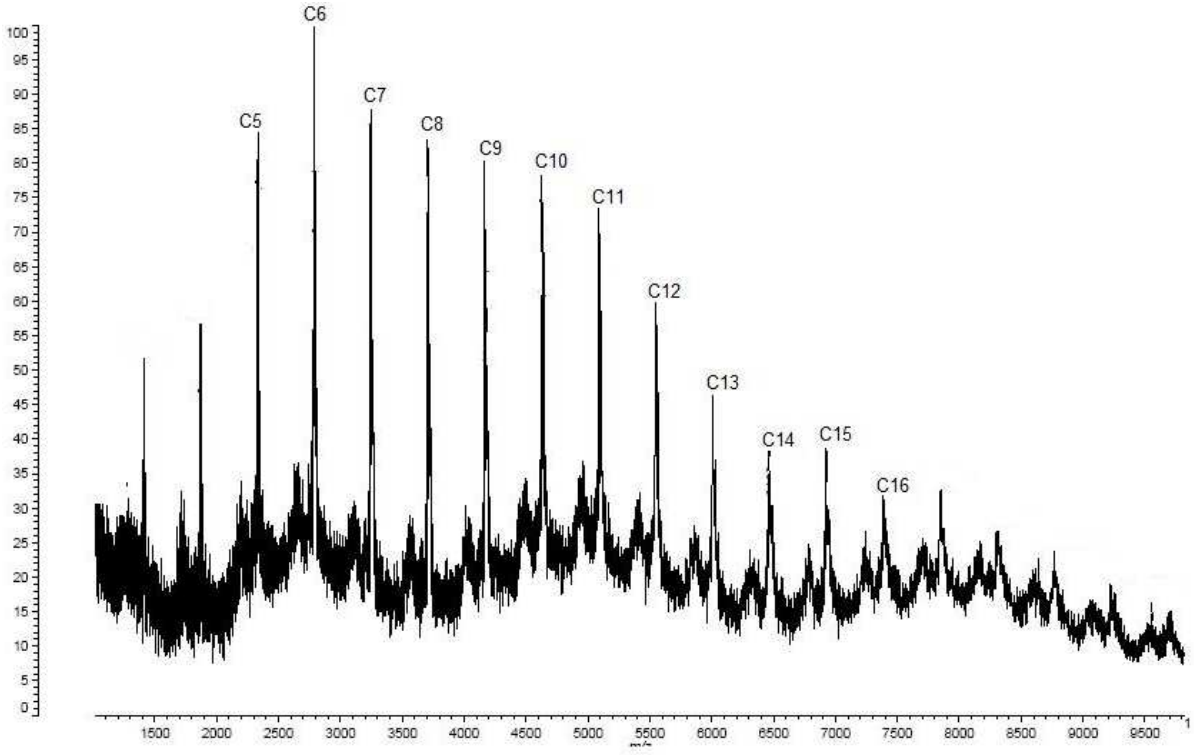

Figure 47 MALDI-ToF mass spectrum of LMA24 (cyclic PIM-1 sample) prepared on a small scale under the conventional condition, reagent molar ratio THSB/ TFPN /K_2CO_3 (1:1:2.5), DMF as solvent, 125-130 °C, 24 hours. Sample was collected from the supernatant phase after 16 hours. The x-axis is m/z and plotted on the y-axis a %.

Table 21 The calculated and the observed mass for the dominant distributions

Repeat unit	n	Cation	Overall formula	Mass (calc.)	Mass (obs.)
$C_{29}H_{20}O_4N_2$	5	Na^+	$(C_{29}H_{20}O_4N_2)_{11}\ Na^+$	2323	2324
$C_{29}H_{20}O_4N_2$	6	Na^+	$(C_{29}H_{20}O_4N_2)_{12}\ Na^+$	2783	2785
$C_{29}H_{20}O_4N_2$	7	Na^+	$(C_{29}H_{20}O_4N_2)_{13}\ Na^+$	3243	3246
$C_{29}H_{20}O_4N_2$	8	Na^+	$(C_{29}H_{20}O_4N_2)_{14}\ Na^+$	3703	3706
$C_{29}H_{20}O_4N_2$	9	Na^+	$(C_{29}H_{20}O_4N_2)_{15}\ Na^+$	4163	4167
$C_{29}H_{20}O_4N_2$	10	Na^+	$(C_{29}H_{20}O_4N_2)_{16}\ Na^+$	4623	4628
$C_{29}H_{20}O_4N_2$	11	Na^+	$(C_{29}H_{20}O_4N_2)_{17}\ Na^+$	5083	5088
$C_{29}H_{20}O_4N_2$	12	Na^+	$(C_{29}H_{20}O_4N_2)_{18}\ Na^+$	5543	5547
$C_{29}H_{20}O_4N_2$	13	Na^+	$(C_{29}H_{20}O_4N_2)_{13}\ Na^+$	6003	6010
$C_{29}H_{20}O_4N_2$	14	Na^+	$(C_{29}H_{20}O_4N_2)_{14}\ Na^+$	6463	6468
$C_{29}H_{20}O_4N_2$	15	Na^+	$(C_{29}H_{20}O_4N_2)_{15}\ Na^+$	6923	6923
$C_{29}H_{20}O_4N_2$	16	Na^+	$(C_{29}H_{20}O_4N_2)_{16}\ Na^+$	7383	7886

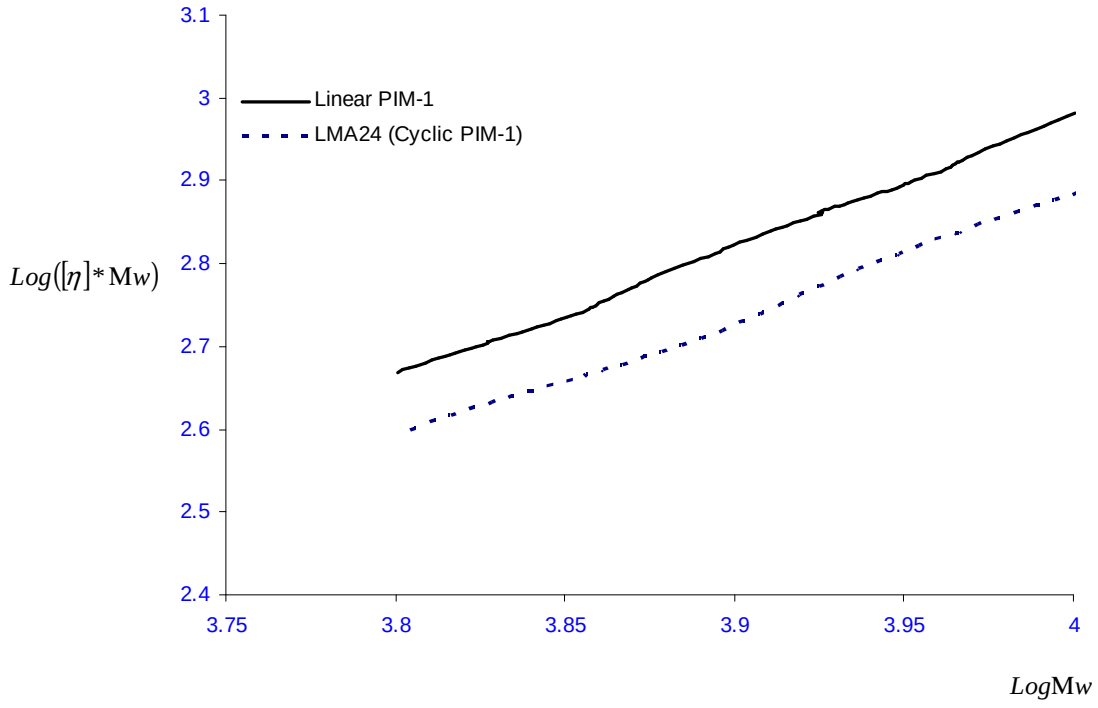

Figure 48 $Log\ ([\eta]^*\ \mathrm{M})$ versus $Log\mathrm{M}$ for Linear PIM-1 sample (PIM-1-20) and cyclic PIM-1 sample (LMA24).

.

5.4 Branched PIM-1

A polymer chain could be linear or branched in terms of its physical structure. Branching causes a decrease in molecular size and hence the hydrodynamic volume, as compared to linear analogues having identical molar masses,[103] making GPC a rapid method for determining not only molecular weight distribution but also the branching distribution.[104, 105]

5.4.1 PIM-1 sample JDS056 and its fractions

For PIM-1 sample JDS056 (see chapter 2), **Figs. 49 and 50** show the variation with molar mass of hydrodynamic volume and intrinsic viscosity, respectively. The hydrodynamic volume is close to that expected for a linear PIM-1 sample up to log M = 5.3 (M = 200,000 g mol^{-1}). At higher molar masses, slopes of both plots decrease with increasing polymer molecular weight. Since intrinsic viscosity is inversely proportional to molecular density, it could be concluded that it is an indication of the presence of branched species at this mass range. However, for further investigation, the JDS056 sample was fractionated into small fractions.

Results for Fractions 2, 3, and the original PIM-1 sample (JDS056) are shown in **Fig. 51**. It shows that fraction 3 has the same density to molecular weight relationship as sample JDS056, indicating they are all similar in composition while Fraction 2 is richer in more dense species than the original PIM-1 sample. This is consistent with expectations, as an increase in branching would lead to a decrease in the intrinsic viscosity.

The MALDI-ToF mass spectra (see chapter 3) for these two samples show the presence of only linear and branched species, giving an indication that both samples contain branched species and consequently JDS056 contained branched species.

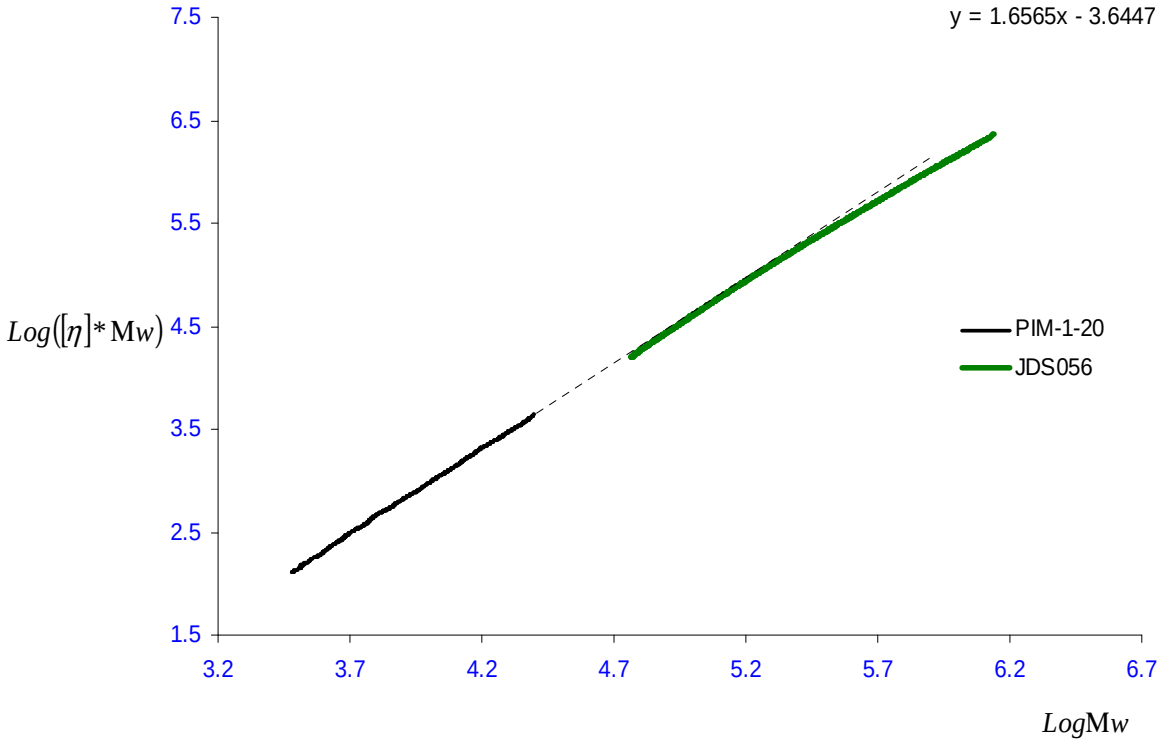

Figure 49 Overlay plot: $Log\ ([\eta]^* \mathrm{M})$ versus $Log\mathrm{M}$ for JDS056 sample prepared on a large scale reagent molar ratio THSB/ TFPN /K_2CO_3 (1:1:8), DMF as solvent, 65 °C, 72 hours

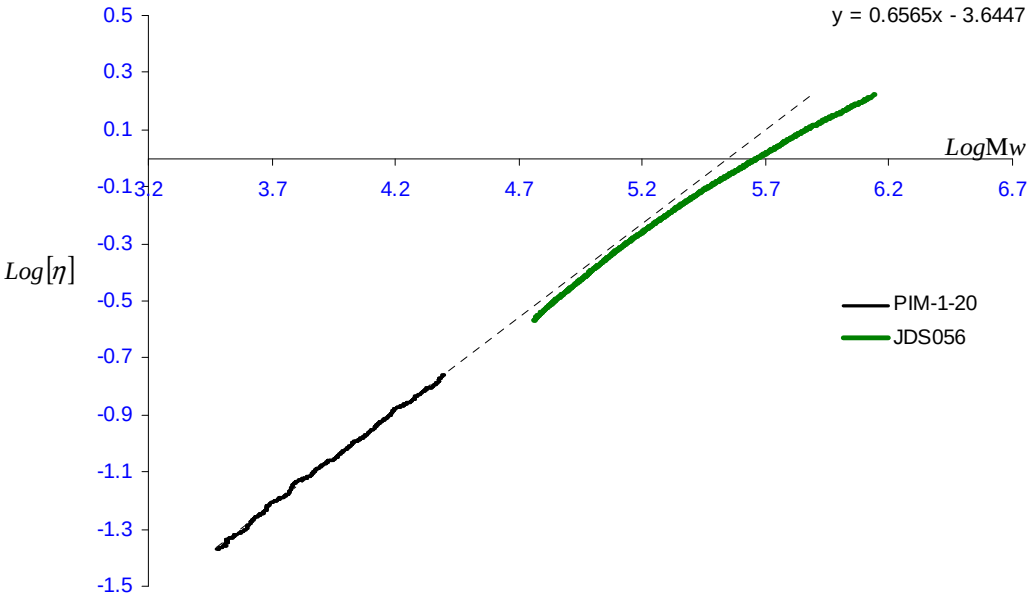

Figure 50 The Mark-Houwink plot for JDS056 sample prepared on a large scale reagent molar ratio THSB/ TFPN /K_2CO_3 (1:1:8), DMF as solvent, 65 °C, 72 hours

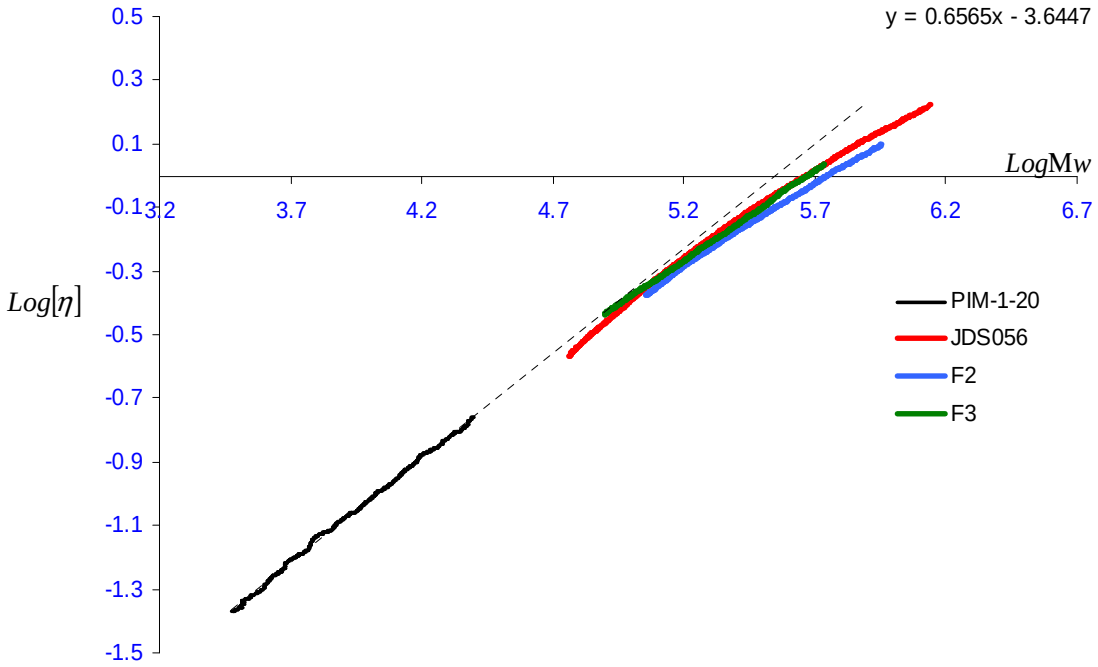

Figure 51 The Mark-Houwink plot for fractions 2 and 3 of JDS056 sample, and the linear PIM-1 sample (PIM-1-20)

5.4.2 PIM-1 samples containing microgel (DNM48B and DNM46B)

Figs. 52 and **53** show the hydrodynamic volume plot as a function of a molecular weight for samples DNM48B, and DNM46B. It was observed that these two samples did not give a clear transparent solution but a solution with insoluble product (microgel), which is possibly a result of branching or cross linking. The common feature between these two samples is that both samples were prepared at high temperature under a high molar ratio of base and the reaction was continued for 17 hours. **Fig. 52** illustrates that DNM48B has lower hydrodynamic volume than the linear analogues (PIM-1-20) having identical molar masses, which may be attributed to there being significant amounts of branched or cyclic polymer over the whole molar mass range. For DNM46 (**Fig. 53**), it has the same hydrodynamic volume as the linear analogues (PIM-1-20) having identical molar masses, and hence most probably a predominately linear structure, but a change in hydrodynamic volume appears

around $Log\mathrm{M}w$ = 5.4. This change is possibly due to branching. These results are consistent with the results reported by Schwarz *et al.*[107] for a similar reaction (polycondensations of silylated TTBSI with DCTB) in which temperatures above 100 °C were reported to increase the molecular weights by side reactions, which resulted in reduced solubility and broader molecular weight distribution, and consequently, it could be concluded that the change in structure was a result of the reaction conditions.

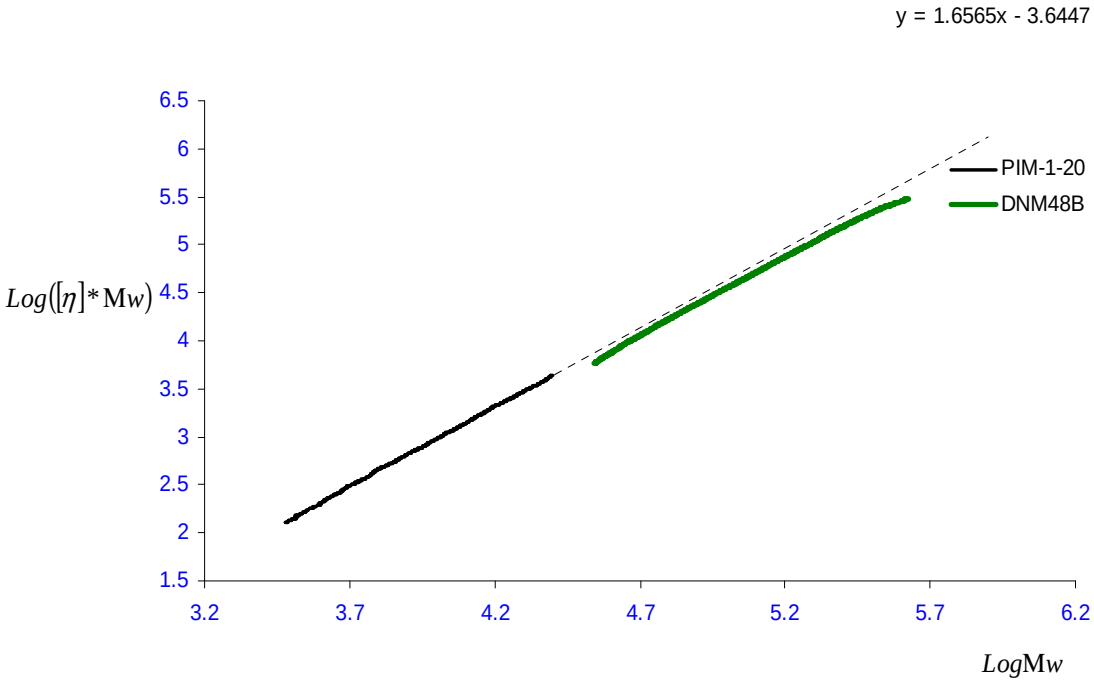

Figure 52 Overlay plot: $Log\ ([\eta]*\mathrm{M})$ versus $Log\mathrm{M}$ for DNM48B sample prepared on an alternative method (low cost route, method C): method C conditions, 155-160 °C, 17 hours, DMAc/Toluene as solvent

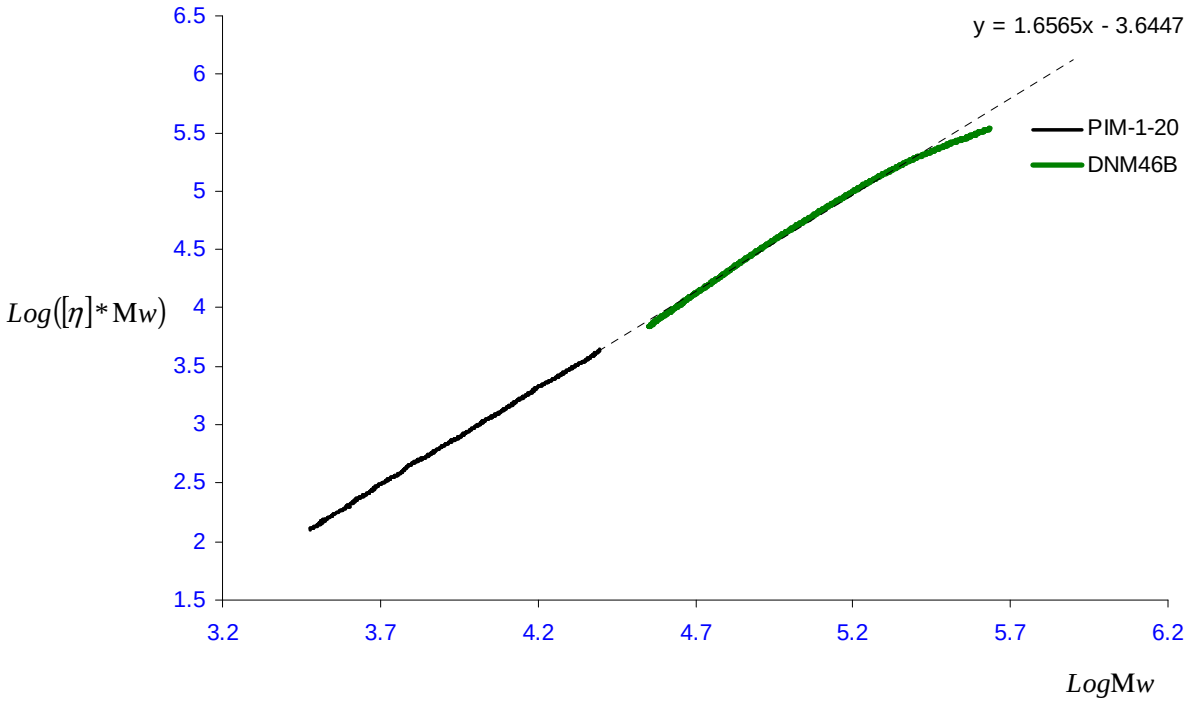

Figure 53 Overlay plot: $Log\ ([\eta]* \mathrm{M})$ versus $Log\mathrm{M}$ for DNM46B sample prepared on an alternative method (low cost route, method C): method C conditions, 155-160 °C, 17 hours, DMAc/Toluene as solvent

5.4.3 PIM-1 samples exhibiting low hydrodynamic volume (DNM48B, DNM32A, PIM-1-10, and NEW09)

As previously discussed (**Section 5.4.2**), sample DNM48B (**Fig. 52**) has lower hydrodynamic volume than expected for linear PIM-1, across the whole distribution. The same is observed for DNM32A, NEW09 and PIM-1-10, as can be seen in **Figs. 54**, **55, and 56**, respectively. The common feature between these samples is that they were prepared at high temperature under a high molar ratio of base. This observation is consistent with expectations, as an increase in temperature and high concentration would result in yielding a branched or crosslinked product and subsequent decrease in hydrodynamic volume.[33, 39, 106]

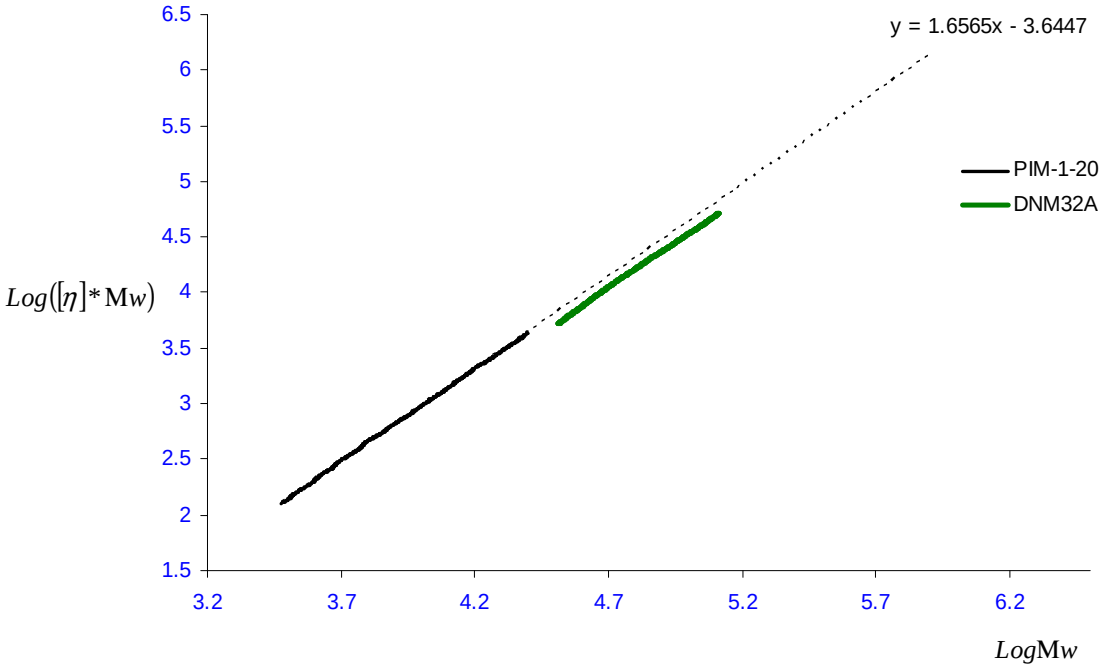

Figure 54 Overlay plot: $Log\ ([\eta]* \mathrm{M})$ versus $Log\mathrm{M}$ for DNM32A sample prepared on an alternative method (low cost route, method C): method C conditions, 155-160 °C, 17 hours, DMAc/Toluene as solvent

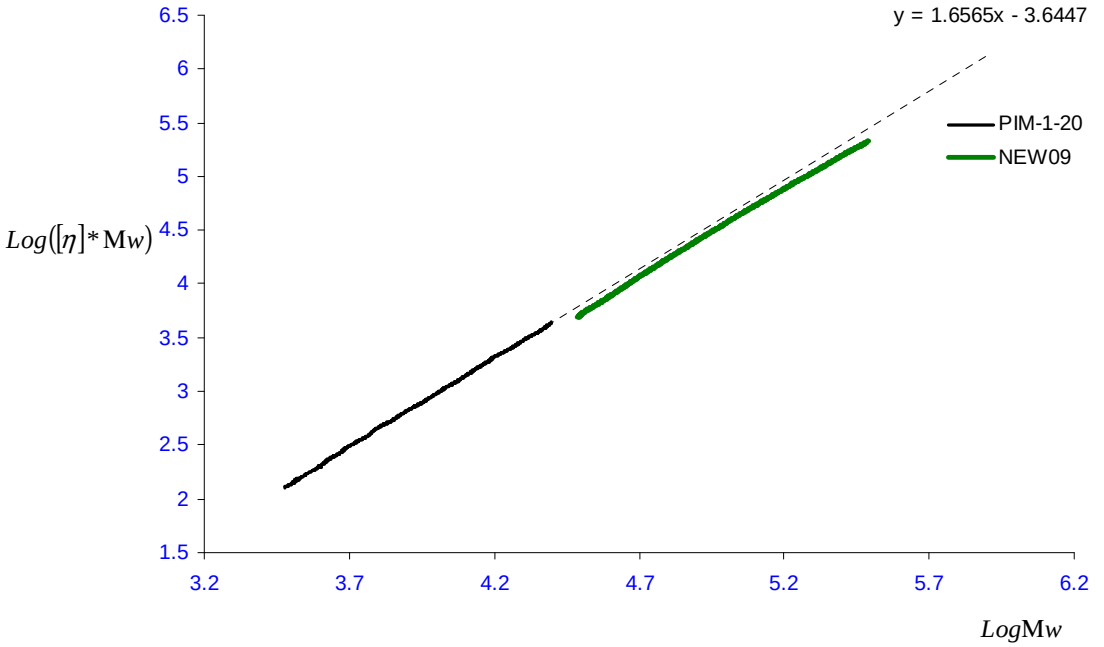

Figure 55 Overlay plot: $Log\ ([\eta]* \mathrm{M})$ versus $Log\mathrm{M}$ NEW09 sample prepared on an alternative method (low cost route, method B): method B conditions, 150-155 °C, 8 hours, DMF/Toluene as solvent

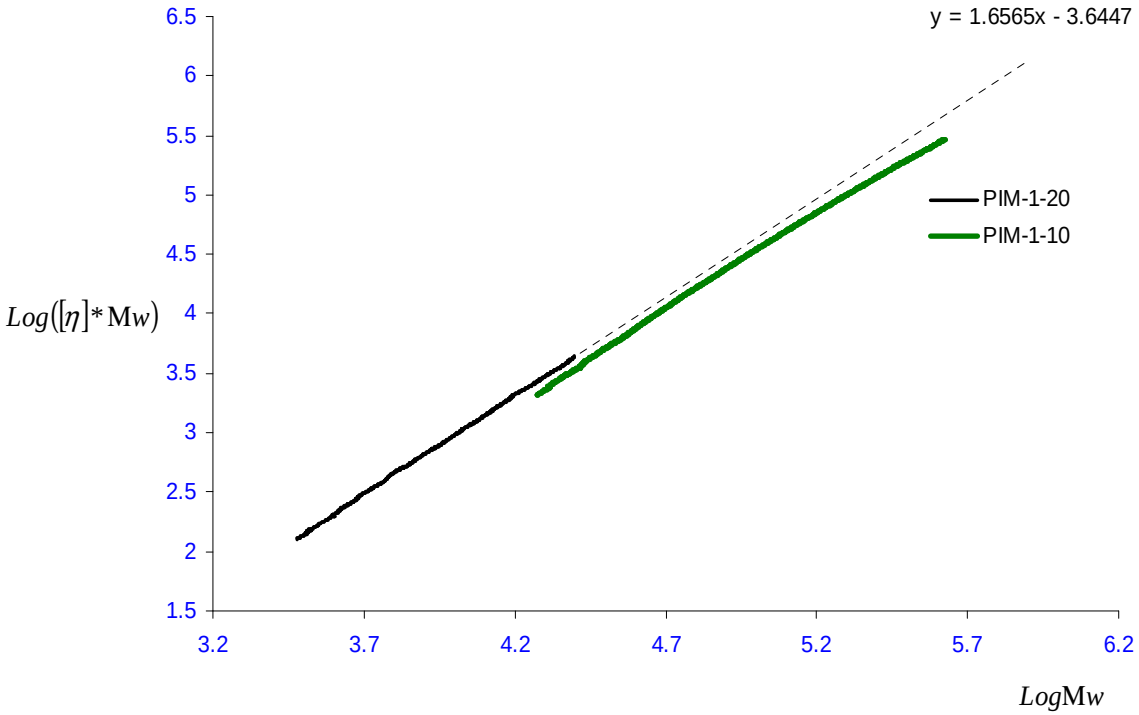

Figure 56 Overlay plot: $Log\ ([\eta]*\mathrm{M})$ versus $Log\mathrm{M}$ PIM-1-10 sample prepared on an alternative method (low cost route, method B): method B conditions, 150-155 °C, 8 hours, DMF/Toluene as solvent

5.4.4 PIM-1 samples prepared by the conventional method from fluoro- or chloro-monomer (CT-02-07, LMA03, LMA02, LMA04, LMA08, LMA11, LMA13 and NMH03)

In PIM-1 samples made of Cl-monomer or F-monomer by the conventional method (**Figs. 57-64**), at around log$M$ = 5.3 a slight downward curvature in the plot of hydrodynamic volume can be seen. This could be due to the chemistry of how the high molecular weights were achieved, possibly as a result of side reactions, suggesting that branching or cross-linking had occurred.

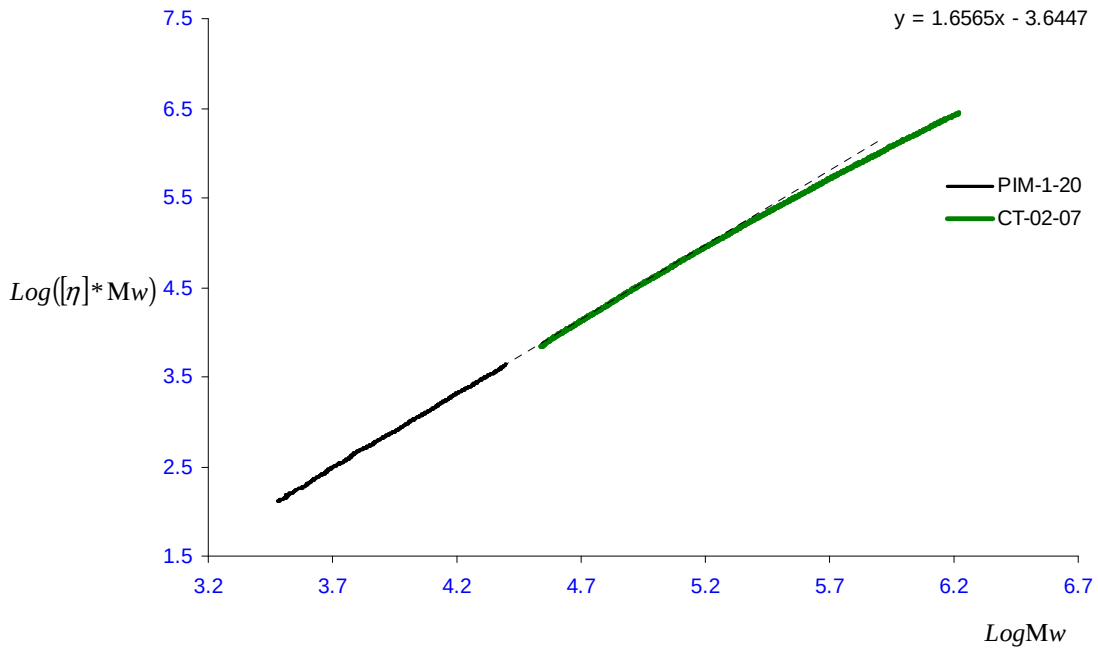

Figure 57 Overlay plot: $Log\ ([\eta]*\mathrm{M})$ versus $Log\mathrm{M}$ for CT-02-07 sample prepared on a large scale reagent molar ratio THSB/ TFNP /K_2CO_3 (1:1:8), DMF as solvent, 65 °C, 72 hours

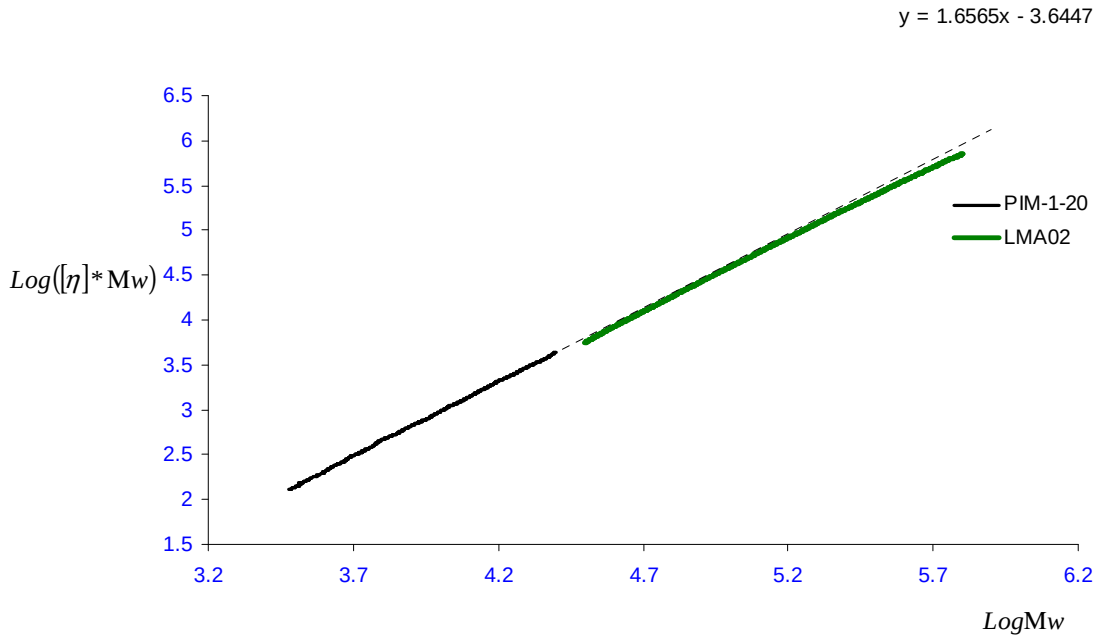

Figure 58 Overlay plot: $Log\ ([\eta]*\mathrm{M})$ versus $Log\mathrm{M}$ for LMA02 sample prepared on a small scale under the conventional condition, reagent molar ratio THSB/ TFPN /K_2CO_3 (1:1:2.5), DMF as solvent, 65 °C, 72 hours

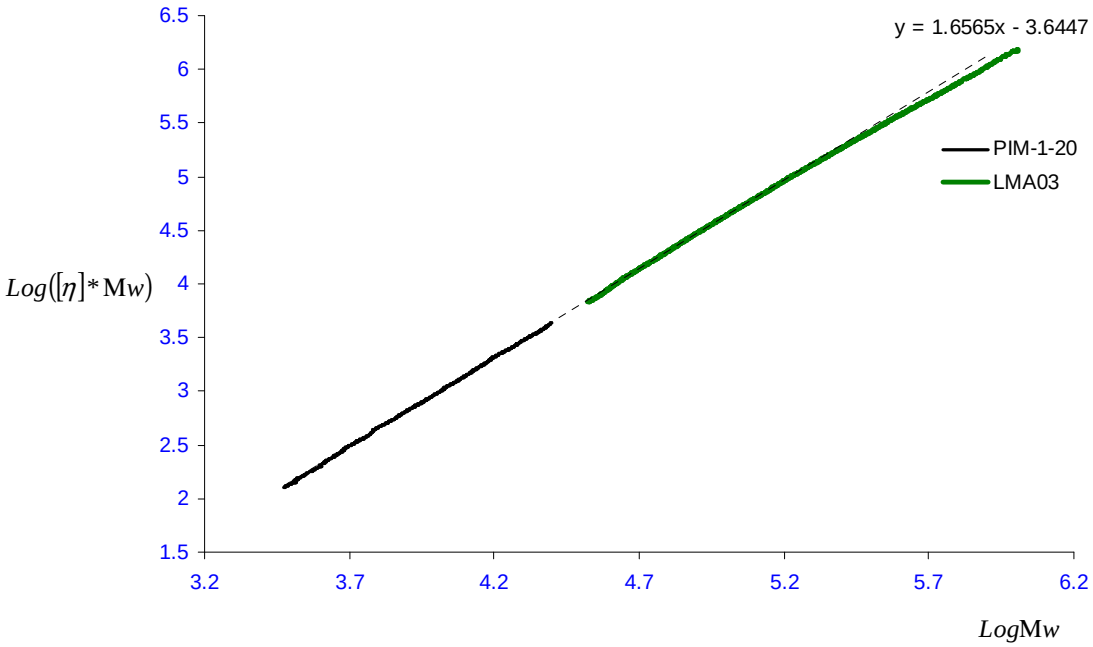

Figure 59 Overlay plot: $Log\ ([\eta]*\mathrm{M})$ versus $Log\mathrm{M}$ for LMA03 sample prepared on a small scale under the conventional condition, reagent molar ratio THSB/ TFNP /K_2CO_3 (1:1:2.5), DMF as solvent, 65 °C, 72 hours

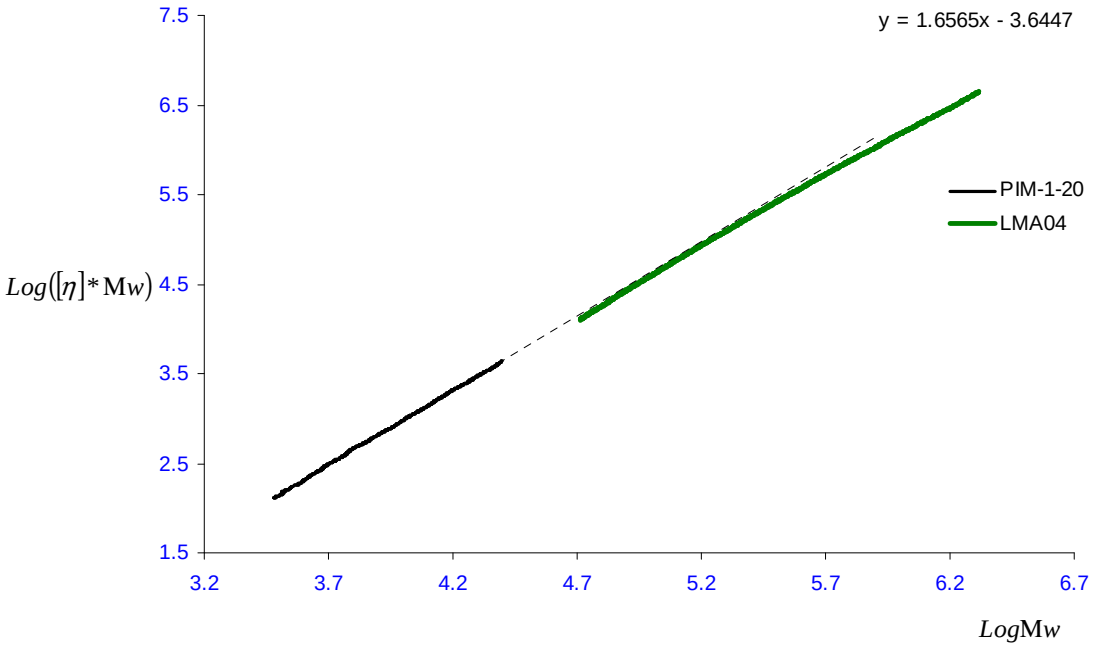

Figure 60 Overlay plot: $Log\ ([\eta]*\mathrm{M})$ versus $Log\mathrm{M}$ for LMA04 sample prepared on a small scale under the conventional condition, reagent molar ratio THSB/ TFNP /K_2CO_3 (1:1:2.5), DMF as solvent, 65 °C, 72 hours

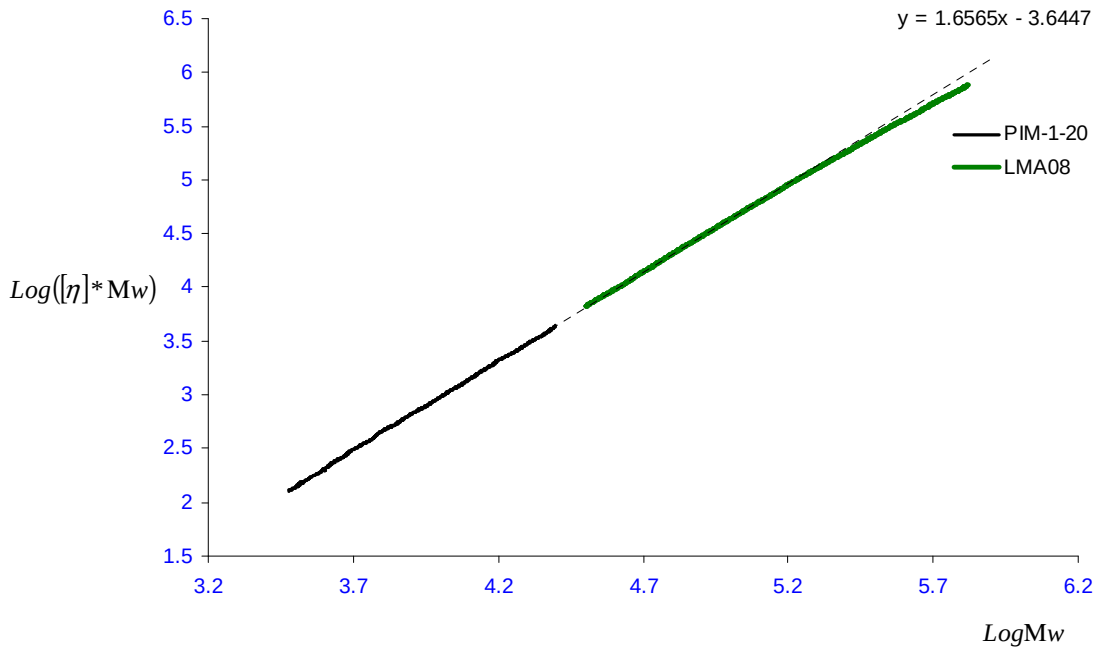

Figure 61 Overlay plot: $Log\ ([\eta]*\mathrm{M})$ versus $Log\mathrm{M}$ for LMA08 sample prepared on an alternative conventional method (low cost route, method A): reagent molar ratio THSB/ TCTNP /K_2CO_3 (1:1:2.5), DMF as solvent, 125-130 °C, 24 hours

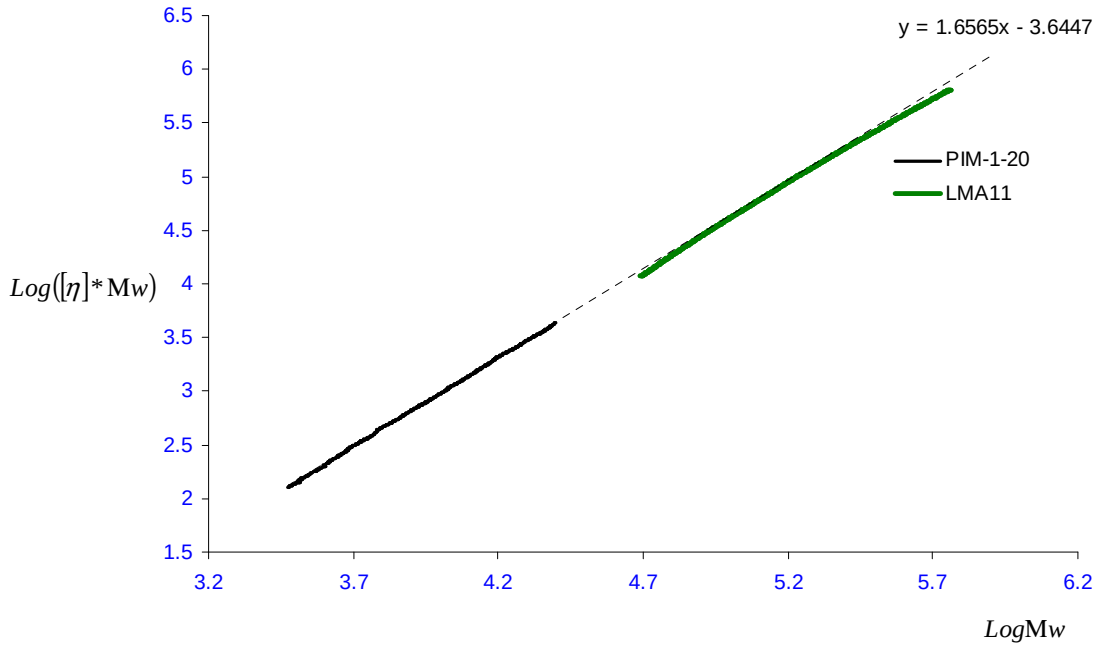

Figure 62 Overlay plot: $Log\ ([\eta]*\mathrm{M})$ versus $Log\mathrm{M}$ for LMA11 sample prepared on an alternative conventional method (low cost route, method A): reagent molar ratio THSB/ TCTNP /K_2CO_3 (1:1:2.5), DMF as solvent, 125-130 °C, 24 hours

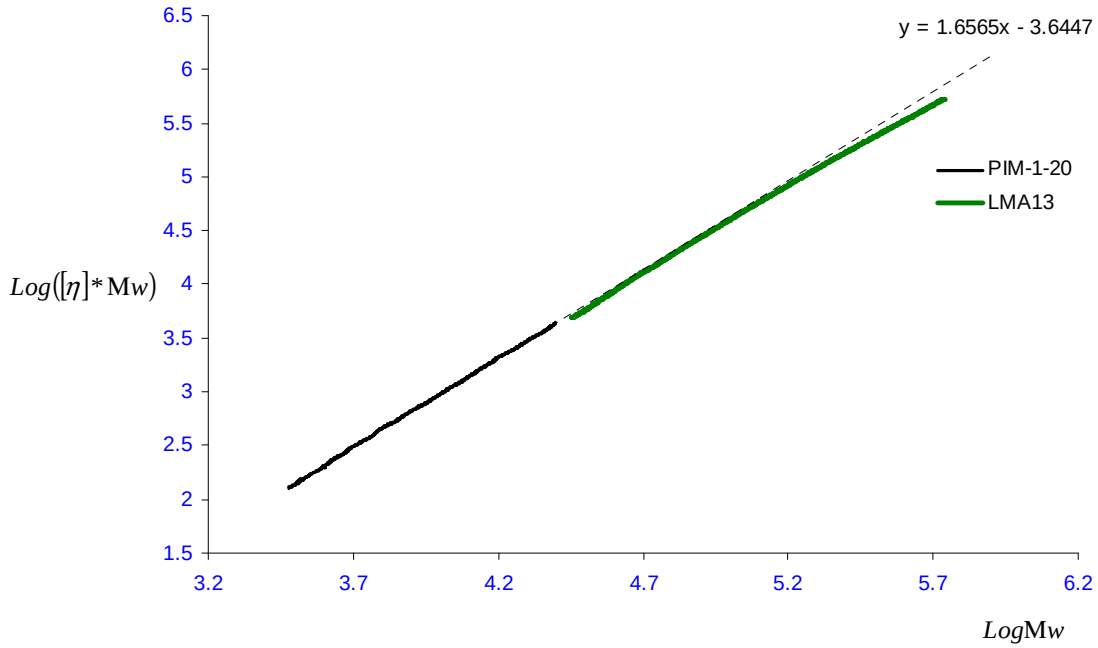

Figure 63 Overlay plot: $Log\ ([\eta]*\mathrm{M})$ versus $Log\mathrm{M}$ for LMA13 sample prepared on an alternative conventional method (low cost route, method A): reagent molar ratio THSB/ TCTNP/K_2CO_3 (1:1:2.5), DMF as solvent, 125-130 °C, 24 hours

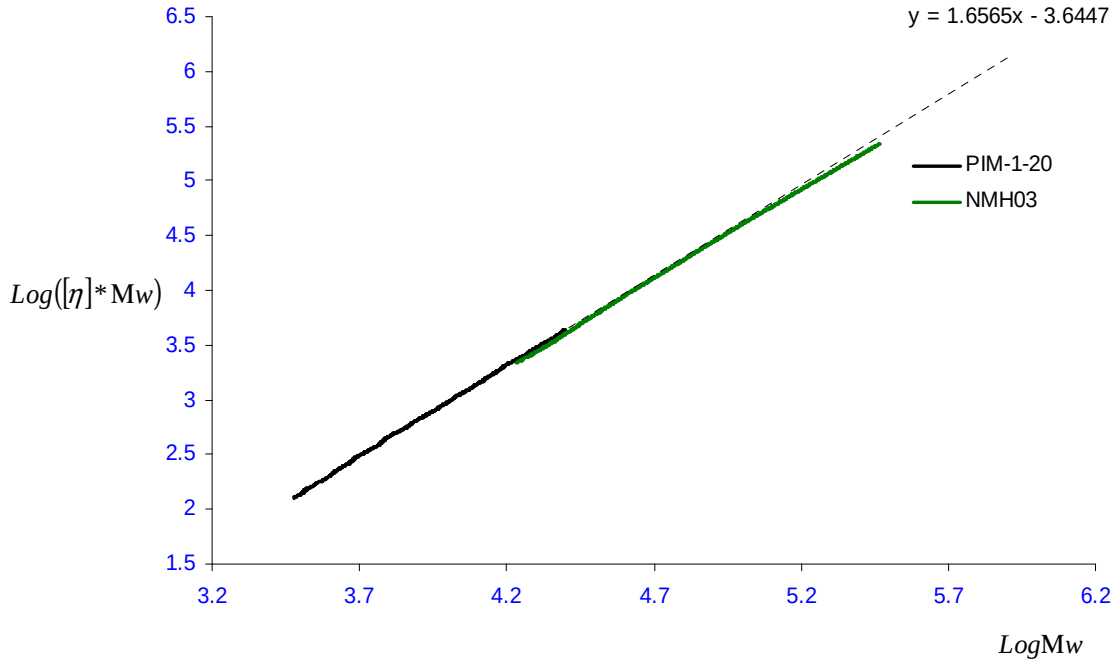

Figure 64 Overlay plot: $Log\ ([\eta]*\mathrm{M})$ versus $Log\mathrm{M}$ for NMH03 prepared under high mixing condition, reagent molar ratio THSB/ TFNP /K_2CO_3 (1:1:3), DMF/Toluene as solvent, 150-155 °C, 13 minutes

5.4.5 PIM-1 sample JDS057

Fig. 65 shows that JDS057 is different from other samples (JDS056 and CT-02-07) which have been prepared under the same reaction conditions. It was found that the N_2 gas supplied into the JDS057 reaction mixture was contaminated (It was later discovered that the house nitrogen had a high level of moisture at this time). This effect was investigated by Kevin Reynolds, who found that in the presence of O_2 the hydroxyl end groups in the THSB monomer can be oxidized to a 1, 2-dione, which quenches the reaction, resulting in a low molecular weight product[42] or could be results in branched or crosslinked structures as a result of that some phenol groups oxidized into a benzoquinone-type structure **Scheme 8** then the residual F reacts with phenolate chain ends of another PIM-1 chain.[107] This explains why JDS057 sample was different form the other samples made by the same method under the same reaction conditions.

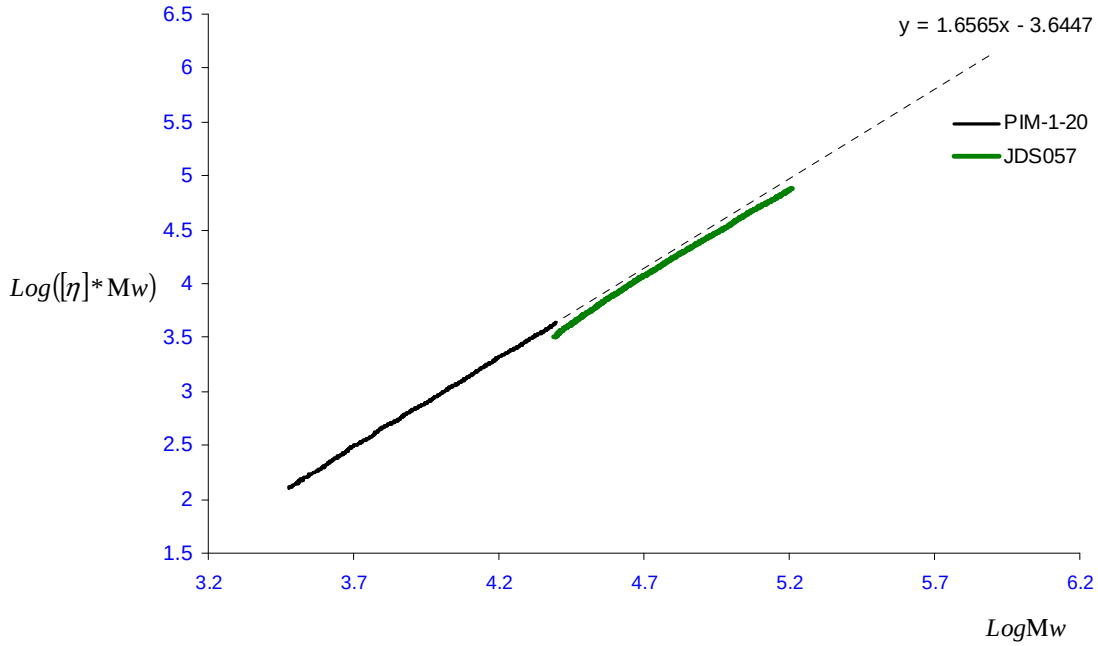

Figure 65 Overlay plot: $Log\ ([\eta]* M)$ versus $Log M$ for JDS057 sample prepared on a large scale reagent molar ratio THSB/ TFNP /K_2CO_3 (1:1:8), DMF as solvent, 65 °C, 72 hours

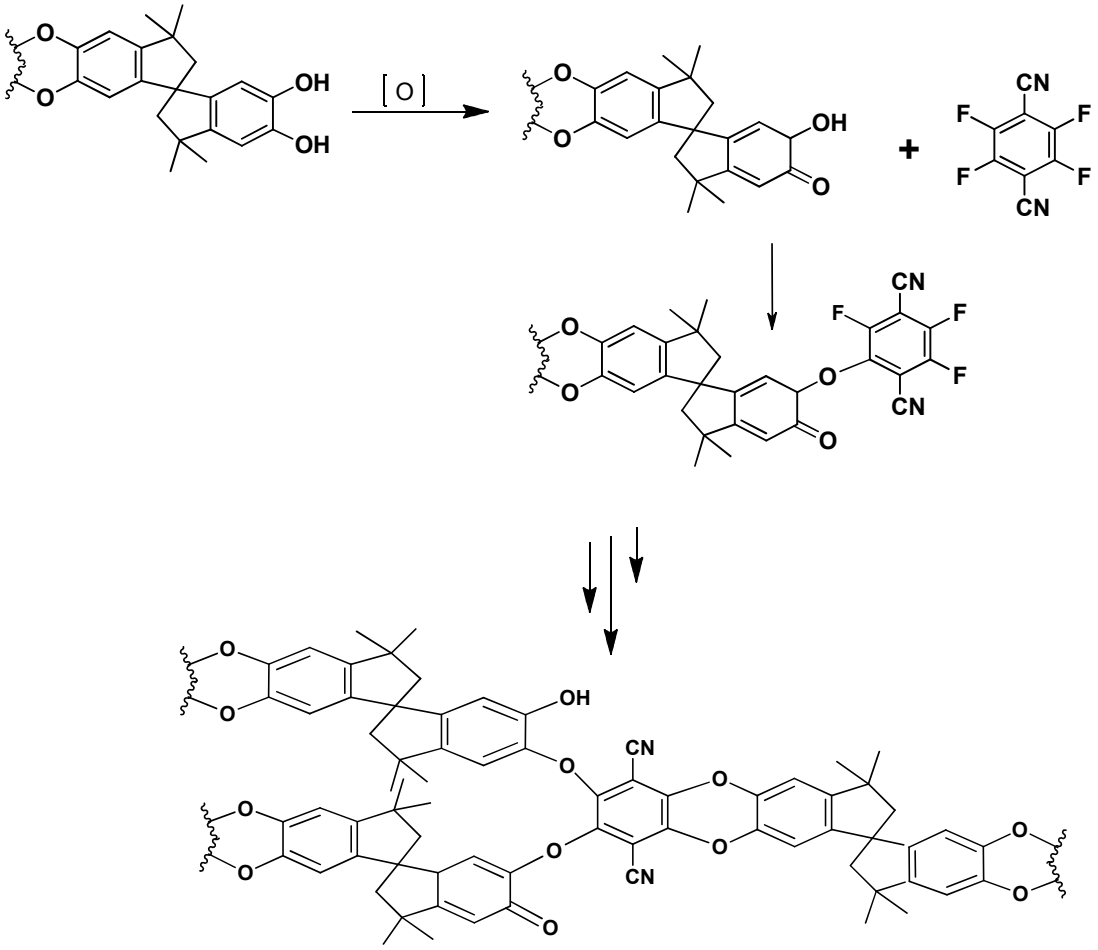

Scheme 8 The proposed mechanism for the branching of PIM-1 as the results of an oxidization of some phenol group.[107]

5.5 Conclusion

In conclusion, it is clear that a convenient and reliable way to differentiate clearly between linear PIM-1, cyclic PIM-1, and its branched structure is established utilizing advanced Triple Detection GPC technique. Low molecular weight linear PIM-1 sample was shown to give very linear Mark-Houwink behaviour, and higher molecular weight PIM-1 samples showed deviation from linearity at *M*w = 200000 g mol^{-1}, which is possibly as a result of side reactions, suggesting that branching or cross-linking had occurred. A high molecular weight-

branching correlation is suspected, consistent with the observation of microgelation at high molecular weight and identification of branched species in low molecular weight samples by MS. A correlation between longer reaction times and broader polydispersity is suggested, though further work is needed to confirm these trends. However, the use of advanced triple-detection GPC technique would help in achieving tight control over molecular structure and molar mass by optimizing the polymerization reaction conditions and applying the technique to see the differences in the resultant products.

Chapter 6: Film Forming Application

6.1 Introduction

In this chapter we are aiming to investigate the effects of both molecular weight and molecular structure on the film forming ability of PIM-1. PIM-1 films were prepared by solvent casting using circular, flat-bottomed, glass Petri dishes as moulds. Slow evaporation of the solvent under a gentle flow of nitrogen, followed by drying under vacuum at 100 °C for 24 hours yielded homogeneous, free standing and mechanically stable films (**Fig. 66**).

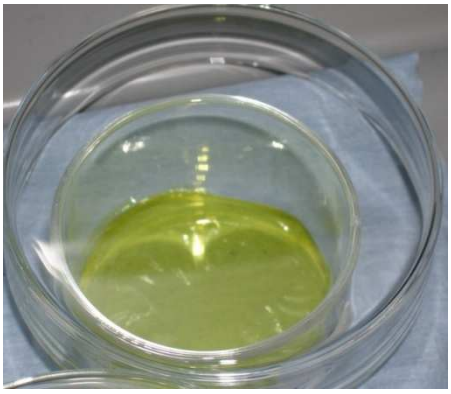

Figure 66 PIM-1 solvent cast film

6.2 Preparation procedure

The PIM-1 membranes for all PIM-1 samples were prepared using a solvent casting method. The PIM-1 solution was first prepared by dissolving 0.05 gm sample in 2.5 ml distilled chloroform at room temperature. The solution was then left for about 1 hour with rapid stirring until a clear solution was observed. When completely dissolved, the solution was poured into a flat based Petri dish of 3.3 cm diameter and placed in the fume hood to enable slow evaporation of the solvent under a gentle flow of nitrogen, followed by drying under vacuum at 100 °C for 24 hours yielded homogeneous, free standing stable films.[42]

6.3 Results and discussion

As shown on **Tables 22** and **23**, it was found during membrane forming studies for PIM-1 samples that some samples form a very flexible free standing membrane (4a), some samples form a very flexible free standing membrane but have microgel present in solution before casting (4b), some samples form a free standing membrane which is very brittle and snaps on bending (3), while in some samples the membrane cracks upon evaporation of residual solvent (the membrane is intact after evaporation of bulk solvent but cracks as residual solvent evaporates from the membrane over the next 3-4 days) (2), and in some samples the membrane cracks upon evaporation of bulk solvent after 1 day (1) (**Fig. 69**). It was clear that the molecular weight has an effect **(Fig. 70)**, increasing the molecular weight helps in getting homogeneous films that were suitable for use as membranes. In **Fig. 70** it can be seen that a critical weight-average molar mass of about 83,000 g mol^{-1} is necessary for film formation.

Those samples that have microgel present in solution before casting probably have highly branched species at the high molar mass end of the distribution for soluble species. As shown in **Fig. 71**; the two samples labelled 4b have a very low Mark-Houwink *a*-value compared to the other samples at molar masses in the range 280,000 to 350,000 g mol^{-1}. This indicates that for these samples there are some very dense species present in solution, For other membrane-forming samples, much higher molar mass species are present in solution, with higher *a*-values suggesting less dense structures.

Figure 68 4a (clear transparent solution

Figure 67 4b (insoluble material present)

1 – Splits upon evaporation of bulk solvent

2– Splits upon evaporation of residual solvent

3 and 4 – form free standing membranes

3 – brittle

4 - flexible

Figure 69 Physical characteristics of each membrane classification

Table 22 Reaction Conditions, GPC results

sample	T, °C	Time, hours	*M*w g mol^{-1}	Monomers	reagent ratio,[a]
PIM-1-20	150-155	8 minutes	8000	TFPN + THSB[b]	1:1:1
LMA02*	65	72	137000	TFPN + THSB[c]	1:1:2.5
LMA03*	65	72	120000	TFPN + THSB[c]	1:1:2.5
LMA04*	65	72	178000	TFPN + THSB[c]	1:1:2.5
LMA07*	65	72	166000	TFPN + THSB[c]	1:1:2.5
LMA18*	65	72	122000	TFPN + THSB[c]	1:1:2.5
LMA19*	65	72	173000	TFPN + THSB[c]	1:1:2.5
LMA08*	125-130	24	107000	TCTPN + THSB[c]	1:1:2.5
LMA11*	125-130	24	150000	TCTPN + THSB[d]	1:1:2.5
LMA13*	125-130	24	103000	TCTPN + THSB[d]	1:1:2.5
LMA14*	125-130	24	123000	TCTPN + THSB[d]	1:1:2.5
DNM18**	155-160	8	29000	TCTPN + THSB[d]	1:1:6
DNM20**	155-160	8	42000	TCTPN + THSB[d]	1:1:6
DNM32A**	155-160	8	61000	TCTPN + THSB[d]	1:1:6
DNM34A**	155-160	8	43000	TCTPN + THSB[d]	1:1:6
DNM34B**	155-160	8	48000	TCTPN + THSB[d]	1:1:6
DNM47B**	155-160	8	62000	TCTPN + THSB[d]	1:1:6
DNM50**	155-160	8	59000	TCTPN + THSB[d]	1:1:6
DNMBR1**	155-160	8	53000	TCTPN + THSB[d]	1:1:6
DNMBR2**	155-160	8	41000	TCTPN + THSB[d]	1:1:6
DNM16R3**	155-160	8h	86000	TCTPN + THSB[d]	1:1:6
DNM46B**	155-160	17	129000	TCTPN + THSB[d]	1:1:6
DNM48B**	155-160	17	95000	TCTPN + THSB[d]	1:1:6
DNM48A**	155-160	17	49000	TCTPN + THSB[d]	1:1:6
NEW09	150-155	8	89000	TCTPN + THSB[J]	1:1:3
PIM-1-10	150-155	8	83000	TCTPN + THSB[J]	1:1:3
NMH01	150-155	8 minutes	38000	TFPN + THSB[b]	1:1:3

a Reagent molar ratio THSB/TFPN/K_2CO_3 or THSB/TCTPN/K_2CO_3

b High Mixing Condition using DMAc as solvent

c Conventional Condition using DMF as solvent

d High temperature Condition using DMAc as solvent

J High Mixing Condition using DMF as solvent

*samples prepared by Louise Maynard-Atem

**samples prepared by Christopher Mason

Table 23 Membrane-forming classification of PIM-1 samples of various molecular weights

sample	*M*w g mol^{-1}	Membrane forming category
PIM-1-20	8000	1
LMA02	137000	4a
LMA03	120000	4a
LMA04	178000	4a
LMA07	166000	4a
LMA18	122000	4a
LMA19	173000	4a
LMA08	107000	4a
LMA11	150000	4a
LMA13	103000	4a
LMA14	123000	4a
DNM18	29000	1
DNM20	42000	1
DNM32A	61000	3
DNM34A	43000	1
DNM34B	48000	1
DNM47B	62000	3
DNM50	59000	3
DNMBR1	53000	3
DNMBR2	41000	1
DNM16R3	86000	4a
DNM46B	129000	4b
DNM48B	95000	4b
DNM48A	49000	2
NEW09	89000	4a
PIM-1-10	83000	4a
NMH01	38000	1

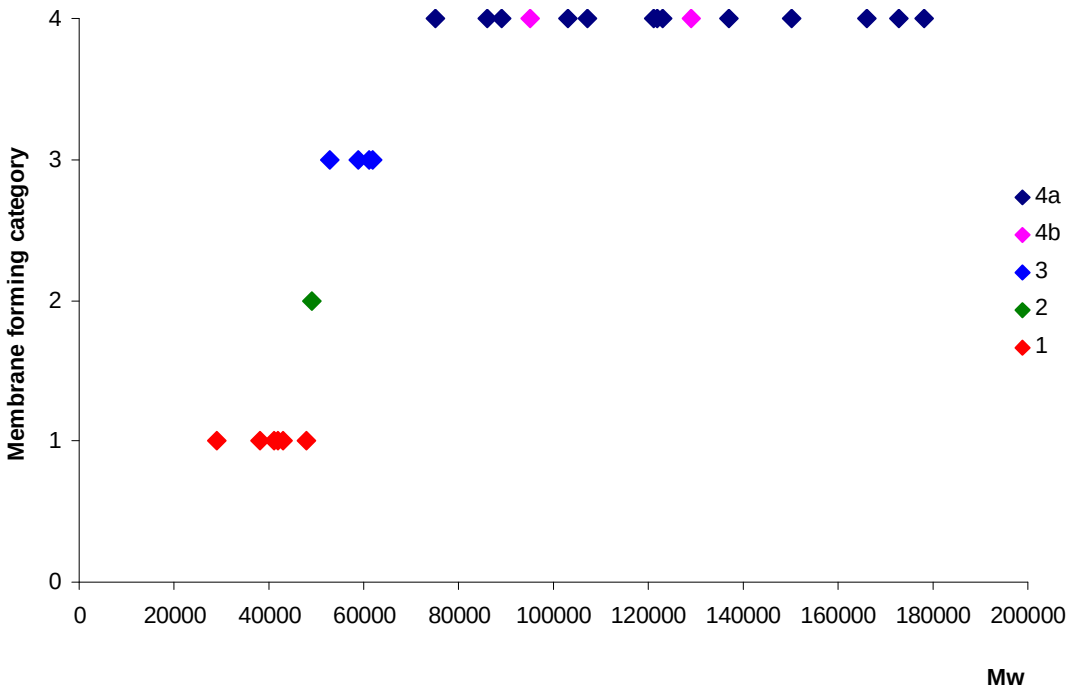

Figure 70 category type based on membrane forming ability versus weight-aveage molar mass for 26 samples of PIM-1 investigated experimentally in house

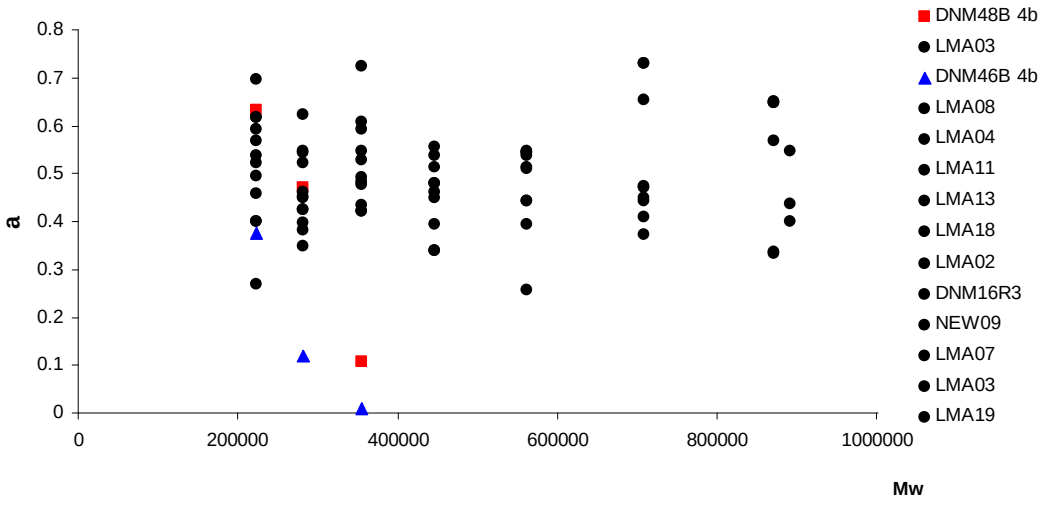

Figure 71 Mark-Houwink *a*-value versus molecular weight for 14 samples of PIM-1 that form a very flexible free standing membrane

6.4 Conclusion

In conclusion, a high molecular weight sample of PIM-1 (83000 g mol^{-1} and more) is needed to form suitable membranes.

Chapter 7: Additives extraction

7.1 Additives in polymers

Unprotected (without additives) polypropylene and some polyethylene resins can degrade when exposed, to either oxygen and/or light; such degradation may take the form of the breaking of the polymer chains resulting in a loss of physical properties. The degradation of polyolefin resins maybe a consequence of either its thermal histories during product processing and/or the production of free radicals brought about by heat or light, or the presence of reactive metals such as catalyst residues, causing a hydrogen atom to be removed from the polymer chain to give a polymer radical [R] and a free hydrogen.[108]

The generated free radicals are extremely reactive leading to a number of degradation pathways. Once they are formed, they react not only with other polymer molecules, but also with molecules of oxygen present in the system, leading to the formation of peroxy radicals [ROO], which may in turn react with the polymer, removing another hydrogen atom from the chain generating either unstable hydroperoxides [ROOH], alcohols [ROH] or new hydrocarbon free radicals. These hydrocarbon free radicals feed back into cycle 1**(Fig. 72)**.[108]

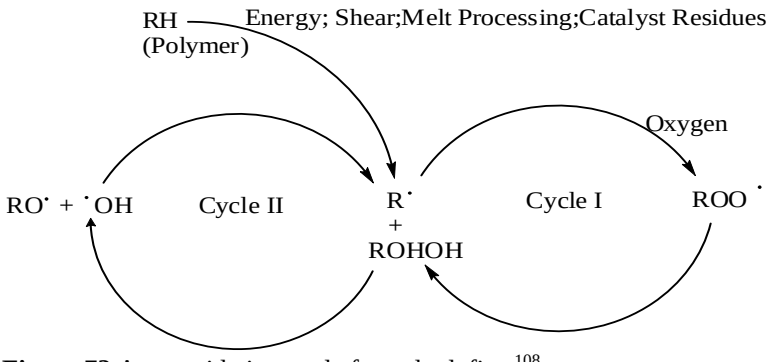

Figure 72 Auto-oxidation cycle for polyolefins [108]

The oxygen-centred radicals can react with other polymer molecules, leading to the formation of more hydrocarbon free radicals which also feed back into cycle 1, resulting, for example, in unwelcome effects such as changes in molecular weight and molar mass distribution that can alter the physical properties of the finished product. In order to avoid such undesirable consequences, there is a need to eliminate the types of reaction described above a range of stabilising additives have been developed.[108]

Stabilising additives can be placed in the following main classes: primary and secondary stabilizers, anti-acids, UV stabilizers, anti-statics, anti-gas, nucleating agents, slip agents, flame retardants, surfactants, mineral fillers and pigments.[17]

This thesis considers one of the major categories of additives, antioxidants, which are employed to retard the degradation of polymers by oxidation and which may be termed either primary or secondary. Primary antioxidants intercept and stabilize free radicals by donating an active hydrogen atom, earning them the alternative name of 'radical scavengers'. They are added to protect the finished product during storage and transportation by stopping the propagation of free radicals resulting from thermal or photo-degradation. The important point here is that primary antioxidants function well in the absence of other additives. The two main classes of primary antioxidants are hindered phenols and hindered aromatic amines. A few examples of commercially available products of these types are listed in **Table 24**. There is a wide selection of hindered phenols commercially available, for example Irganox 1010 and Irganox 1076. **Scheme 9** illustrates their structures.[16]

Table 24 Examples of commercially available hindered phenols and hindered aromatic amines used as primary antioxidants

Trade Name	M_w (g mol^{-1})	Type
BHT	220	Hindered Phenols
Irganox 1076	531	Hindered Phenols
Irganox 1010	1178	Hindered Phenols
Irganox 3114	784	Hindered Phenols
Tinuvin 770	481	Hindered Amines

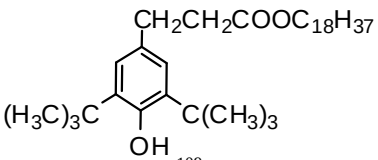

IRG 1076 [109]

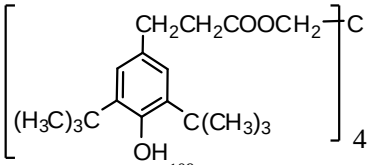

IRG 1010[109]

Scheme 9 Chemical structure of the selected antioxidants

Secondary antioxidants (hydroperoxide decomposers) are organic molecules consisting of phosphates and lower molecular weight hindered phenols; they inhibit colour formation and stabilize the polymer during processing, but not during storage or use at normal temperature.[108]

With reference to **Fig. 73**, the way in which these antioxidants terminate the autoxidation process is that the phenolic antioxidant (primary antioxidant) is added to react with oxygen-centred free radicals, such as alkoxy, hydroxyl and peroxy type species, by donating an active hydrogen atom, while further formation of free radicals is prevented by secondary antioxidants (organic phosphite processing stabilizers) through the decomposition of unstable hydroperoxides prior to yielding inactive products (ROH). Thus, the unstable hydroperoxide forms a stable product, earning the name peroxide decomposers for these antioxidants. Another function of secondary antioxidants is that they may also regenerate a primary antioxidant. Phosphites and thioesters are the two main types of secondary antioxidant and they both function in the same manner. **Table 25** lists two examples of commercially available phosphates; their structures are shown in **Scheme 10**.[108]

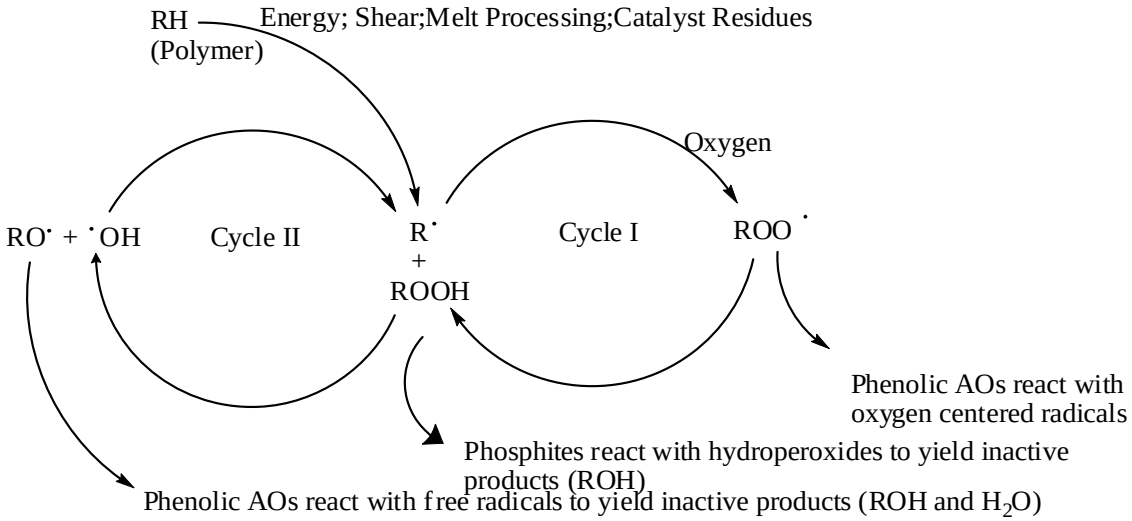

Figure 73 Traditional inhibited auto-oxidation Cycle for polyolefins

Table 25 Examples of commercially available phosphites used as secondary antioxidants

Trade Name	M_w (g mol^{-1})
Weston 399	688
Irgafos 168	647

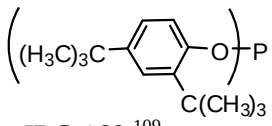

IRG 168 [109]

Scheme 10 Chemical structure of the selected antioxidants

In practice both primary and secondary antioxidants are used in combination to provide a improved polyolefin stabilisation. It is worth noting that all or nearly all types of primary antioxidant can be incorporated with any type of secondary antioxidant. Indeed, secondary antioxidants function well with the correct combination of primary antioxidant. The most commonly used type of secondary antioxidant is deemed to be the phosphates.[16]

Other types of additive which are also incorporated within polymers are acid scavengers, which are required to counter the effects of catalyst residues. The quantity of acid residues is

normally lower, but as a precaution, their neutralization is necessary to prevent the corrosion of processing equipment. Acid scavengers include calcium stearate and dihydrotalcite.[16]

Additives may be used in a single polymer resin in various types and categories. For example, both primary and secondary antioxidants, as well as some other additives, may all be added to a high-density polyethylene resin.[16]

7.2 Analysis of Additives

The use of polyolefins in food and medical packaging has resulted in improved end-use performance but necessitated rapid resolution of analytical problems in terms of swiftness of response, more understanding of degradation and/or interactions between additives present in the same polymeric matrix.[17] Extraction, subsequent separation and quantification of chemical additives used in various polymers present challenging problems for analytical chemists. Such additives are usually included in the polymers at low concentrations (ppm) which makes analysis difficult. There is a large range of extraction techniques available and a wide range of equipments on the market from the simplest and cheapest one to the more complicated and expensive one.[14-20, 110-118]

Wheeler and Crompton[18] reviewed analytical procedures used in the determination of polymer additives and the problems associated with such analysis. They found that the difficulties in identifying and determining antioxidants arise from three factors: their high reactivity and low stability, the low concentrations at which they are present, and relatively insoluble polymer matrices. They suggested that the second and third factors generally require a separation of the additives from the polymer, while the first and second require careful handling of the extracts if quantitative results are to be obtained. In addition, the wide variety of commercially available antioxidants further complicates the interpretation of data.[18]

Different techniques, such as ultraviolet or infrared spectrometry, which have to be directly applied to the polymer, can be utilized in the analytical evaluation of additives. However, such techniques are not expressly applicable to matrices containing fillers or strong pigments. Moreover, such techniques become uninformative when many additives are contained in the same sample; they are often unable to give reliable quantification and are not specific enough to distinguish between degraded and un-degraded compounds present in the same sample. To determine the elementary additive components, atomic absorption and x-ray fluorescence are usually used. These techniques are highly sensitive but not specific, and they are limited to a few set of additives. Recently, the most common way to determine additives in polyolefins has become the use of chromatographic techniques such as gas chromatography and high-performance liquid chromatography, coupled with ultraviolet or evaporative light scattering detection. However, in order to determine the quantity of an additive in a polymer, it is usually necessary to extract it from the polymer quantitatively before analysis. In this regard, three major factors must be taken into account when developing an analytical method for the characterization of polymer additives.[17] The additives themselves are not pure compounds, they are insoluble in the polymer matrix and they are at low concentration. Therefore, the additives must first be separated from the polymer and then the resultant extract must be cleaned to remove any low molecular weight oligomers present and which may interfere with the analysis. To avoid any decomposition of additives, the extract must be handled carefully, because antioxidants are labile, unstable compounds often containing complex decomposition products.[112]

7.3 Extraction Techniques

These can be classified into two categories: the dissolution of polymers and liquid-solid extraction methods.[15]

7.3.1 Dissolution of the polymer

Dissolution and re-precipitation provides an effective method of extraction, whose main advantage is that there is no possibility of any analyte being present in the re-precipitated polymer. The presence of a considerable amount of wax is possible and this should be removed from the solution before further analysis. The disadvantage of this method is that it is considered to be time consuming; hence, some practitioners prefer liquid-solid extraction.[15]

7.3.2 Liquid-solid extraction

Here the separation process takes place by physical means, such as filtration. Such extraction can be carried out by many methods, such as Soxhlet, sonication and shake-flask extraction.[15] The semi-continuous Soxhlet method is most commonly used for the extraction of polymeric additives. In to the Soxhlet procedure, analytes are extracted from solid material by repeated washing with an organic solvent under reflux.[110]

The main advantages of this technique are the reflux of solvent through the sample, displacing the transfer equilibrium, as well as high temperature and the simplicity of the method. The temperature remains high during the process of extraction because heat applied to the distillation flask is spread to the whole system. This method is easy to use and its other advantages are that it requires no filtration after extraction; the sample is placed in a cellulose thimble which efficiently collects dissolved polymer; several samples can be run simultaneously and the equipment is not expensive. It is possible that this non-matrix dependent method might extract more sample by mass than most other modern extraction methods.[110]

Among its disadvantages is the time needed for extraction, which typically varies from 6 hours to 48 hours, and the choice of solvent that affects both extraction time and efficiency. Soxhlet extraction is acknowledged to be efficient, but as mentioned, it is rather slow and

requires large amounts of solvent. This results in dilute solutions requiring further concentration before analysis, which is a time-consuming step during which volatile compounds may be lost. As this method requires large volumes of toxic solvents to be used, it is also potentially environmentally hazardous and expensive. Extracting samples at the boiling point of the solvent for a long period of time brings the risk of thermal-labile analytes being decomposed on extraction. Furthermore, in the conventional Soxhlet method, providing agitation to reduce extraction times is not possible and the technique is restricted in solvent selectivity.[110]

The extraction of additives from PP at room temperature was studied by Spell and Eddy,[15] who found that time required for extraction varied linearly according to polymer density and decreased with increasing particle size. They also found out that there was much variation in extraction time depending on the solvents and additives used. Powdering the polymer to 50 mesh in size allowed 98% extraction of BHT by shaking at room temperature for 30 minutes with carbon disulfide. The same recovery was achieved with isooctane in 125 minutes. The size of the polymer particles is critical. The importance of this issue was further demonstrated by Newton.[15] When ground PP was refluxed with chloroform for 1 hour, complete extraction was achieved. For films, 3 hours were required and for unground granules, 3 hours of extraction time was required to provide an extract for identification purposes only.[15]

A variety of solvents has often been used with Soxhlet extraction. Although this method eventually gives good extraction efficiencies, the extraction rate is slow, as noted above. Furthermore, long extraction times do not necessarily lead to good recovery. For example, only 59% recovery was obtained by Perlstein[15] for extraction of Tinuvin 320 from unground PVC after 16 hours of Soxhlet extraction with diethyl ether. However, recoveries rose to 97% from ground polymer. The extraction time is significantly affected by the choice of solvent.

For example, Wims and Swarin[15] found that talc filled PP needed 72 hours extraction with chloroform, but only 24 hours with THF. Thus, small particles are often essential to complete the extraction in reasonable times, and the solvent must be carefully selected to swell the polymer. It is important to strive to select the most appropriate solvent for extraction, as this will result in savings if the extraction time and the associated solvent usage are reduced.[15]

UAE is very effective in extracting organic and inorganic compounds due to the very high temperatures and pressures achieved and the oxidative power of free radicals. Extraction of additives and other small compounds from polymers is completed in a reasonable time: normally less than 1 hour, if stirred every 10 minutes. The time required for extraction of some additives from polymers such as low density polyethylene or PP is less than 10 minutes. Extraction conditions are extremely dependent on the structure of the desired additives and need to be carefully adjusted for each extraction. The most significant advantages of UAE are that it provides a very efficient extraction of additives from polyolefins without noticeable degradation or need for pre-concentration of the analytes. The principle according to which ultrasonic extraction works is that it agitates the solution and consequent produces cavitation in the liquid. This is expected to enhance the rate of transfer across the polymer/liquid boundary layer, but it will not increase the diffusion of compounds within the polymer.[15]

There are several reports of ultrasonic extraction from polymers. Extraction of a variety of additives from PP, LDPE and HDPE using ultrasonic extraction and MAE was reported by Nielson.[15] The extraction time for all additives was 1 hour with stirring every 10 minutes. Most additives contained in LDPE and PP were extracted within 10 minutes, except for Irganox 1010, which required 1 hour for more than 90% extraction. These results were confirmed by further experiments conducted by Nielson[15] on extraction from HDPE using the same regime. However, the use of DCM-cyclohexane was preferred where phosphate

antioxidants were present, because it prevented hydrolysis of the phosphate by the alcohol. Apart from the speed of ultrasonic extraction from polymers, however, advantages over shaking the sample have not been widely demonstrated.[15]

Several methods of extraction of Tinuvin 770 and Chimassorb 944 from HDPE pellets were compared by Caceres. Less than 20% extraction was achieved by room temperature diffusion into chloroform and ultrasonic extraction. Only 50% extraction resulted from Soxtec extraction with DCM for 4 hours. Dissolution of the polymer in dichlorobenzene at 160 °C for 1 hour followed by re-precipitation of the polymer with propan-2-ol gave 65-70% recovery. Boiling under reflux with toluene at 160 °C for 2-4 hours was the most successful method, extracting 95% of both additives. The large difference in temperature between the boiling solvents causes the poor performance of Soxhlet extraction compared with the reflux method. The pellets were not ground and the size was not specified.[15]

Diffusion to the surface of the polymer is deemed to be one of the limiting steps in extraction; particle size or film thickness is extremely important. Therefore, grinding of the polymer is often an essential step in the analysis. Extraction of thin films and foams is an exception to this point, as the shortest dimension is relatively small. Owing to the heat generated by grinding of polymers, volatile additives might be lost. Before grinding, the polymer must therefore be frozen with liquid nitrogen.[15]

7.4 New developments in additives extraction from polymers

Completing the extraction in less time, using less solvent and also having the possibility of automating the process of analysis have become the principle objectives of any technique to replace traditional extraction methods. Supercritical fluid extraction (SFE), pressurized liquid extraction or microwave-assisted extractions are main techniques that meet these aims.[15] SFE and high-pressure solvent extraction do not guarantee complete recovery of organic additives with high polarity, while antioxidants are extracted with good recoveries in quite a short time

using microwave-assisted extraction (MAE) methods. These are among the recently developed approaches to complete and systematic analysis of organic additives in polyolefins.[17]

The MAE technique, which has become an increasingly commonly used method, consists of heating the extracting solvent or sample with electromagnetic radiation. It provides the user with a homogenous and rapid heating of the sample/solvent system. In MAE, weak hydrogen bonds are broken and dissolved ions facilitate solvent penetration into the matrix, where both enhance solubility of analytes. Any mixture of solvent can be used, as long as it contains at least one microwave-absorbing unit. If MAE is applied to a system with a non-polar solvent, the sample is heated but the solvent remains cold, which could be an advantage when working with thermo-sensitive compounds. MAE can be performed under multimode or fused radiation and in open or closed vessels.[110]

Temperature and pressure can be controlled in closed-vessel MAE. The temperature depends on the microwave power, vessel volume, boiling point of the solvent and the pressure of the solvent used. Solvents can be heated above their atmospheric boiling point, enhancing extraction speed and efficiency. This type of extraction is preferable when working with highly flammable solvents. One advantage is that several samples can be run simultaneously. They are normally placed on a rotating frame in the microwave oven, to provide a homogenous field over the sample during extraction. Cooling the samples to room temperature is extremely important before opening the vessel, so as to prevent problems related to overpressure when working with volatile compounds. Solid residuals must be removed through an additional filtration process or centrifugation.[110]

In cases where open-vessel MAE is used, the process runs at atmospheric pressure and therefore the maximal temperature is the boiling point of the solvent used. Homogenous and efficient heating is provided by focusing the microwaves on the sample in the vessel, whilst

the heated solvent is refluxed through it. An additional filtration step can be avoided by using a Soxhlet-type cartridge vessel. Open-vessel MAE can handle larger sample volumes than closed-vessel MAE and provides safer sample handling. It is considered to be a fast and effective extraction method that requires only a small amount of solvent and can also handle several samples in one extraction. The equipment is quite expensive, however, and some problems concerning reproducibility have been evident. This technique is commonly used in analytical laboratories in the field of sample digestion.[110]

Zlotorzynaski[15] has reviewed the use of microwave radiation in analysis and suggested that microwave extraction is still in initial phases. Reviews of the applications of microwave-assisted sample preparation have recently been published. There are several publications on MAE in environmental analysis, but only a small number of them are concerned with extraction from polymers.[15]

One of the limitations of this technique is that the selected solvent must have a high relative permittivity to be heated by microwaves and accordingly, pure hydrocarbons cannot be used. Acetone-heptane (1+1) was used as a mixture of solvents by Freitag and John[15] to extract some additives such as Irgafos 168, Chimassorb 81 and Irganox 1010 from LDPE, HDPE and PP. The polymers were first ground to 20 mesh in size. The recoveries for all of the extracted additives ranged from 91% to 97% and the extraction time for Irgafos 168 and Chimassorb 81 was 6 minutes from HDPE and 3 minutes from PP and LDPE. The extraction time for Irganox 1010 was longer compared to the other extracted additives, the reason being that the molecular weight had a significant interaction with Irganox 1010. Extraction was achieved in slightly less time using 1,1,1-trichloroethane, but this solvent is environmentally less desirable. The extraction of Iganox 1010 from PP and is easily compared to HDPE, although the scatter of the LDPE results were fairly high. Dissolution of larger particles in toluene-1,2-dichlorobenzene showed good results within only 5 min. However, the dissolution method

gave only 85% recovery of the additives from the PE samples, while the recoveries achieved were fairly high (95%) from PP. Extraction from larger pellets was less efficient. The vessels were pressurized, but the temperatures and pressures reached were not reported.[15]

A comparison between microwave extraction and sonication for HDPE and PP was reported by Nielson.[15] Additives such as BHT, Irganox 1010 and Irganox 1076 were extracted at more than 90% recoveries from ground HDPE in 20 minutes at 50% power. Two solvent systems were used: propan-2-ol-cyclohexane (1+1) and DCM-propan-2-ol (98+2). In each case the prop-2-ol was used to absorb the microwave energy and the other solvent to swell the polymer. The samples were stirred at 5 minutes intervals. The polymer was powdered to 20 mesh in size and 5 g of the polymer sample was used to 50 ml of the solvent. The amount of sample used is much larger than the 50-100 mg typically used in SFE. In case of the PP sample, Irganox 3114, Irganox 1010, Irganox 1076, Irgafos 168 and Tinuvin 3228 were extracted from the ground polymer (20 mesh) [5 g of plastic to 50 ml of solvent, DCM-propan-2-ol (98+2)] in 20 minutes at 20% power, with stirring required every 5 minutes. Only the Irganox 3114 had a low recovery of 79%. Recoveries were also high when larger pellets were used. The only exception was Irganox 1010, for which only 50% recovery was possible without grinding. The vessels were not pressurized and the temperature using the DCM-propan-2-ol mixture did not exceed 50 °C.[15]

The conclusion reached from these examples is that MAE appears to be a rapid and effective technique for additive extraction. Solvent can be selected to swell the polymer, provided that some microwave absorbing solvent is also present. The polymer needs to be ground for efficient extraction. However, too few reports are available for firm conclusions to be drawn.[15]

Different MAE methods have been proposed. Extraction methods from different unground polyolefins matrices were developed by Marcato el al, who utilised microwave energy and

subsequent direct liquid chromatography injection coupled with ultraviolet and evaporative light-scattering detection. Additives such as Irganox 1010, Irganox PS802 and Irgafos 168 contained in LLDPE samples were analyzed. Antioxidants were extracted with a mixture of ethylacetate: n-hexane (75:25) for 15 min at 100 °C. A negligible decomposition of stabilizers was observed in comparison with other traditional extraction such as extraction procedures by refluxing solvent or dissolution polymer-coagulation. Additive extraction from polyolefins using microwave oven and ultrasonic bath techniques for HDPE, LDPE and PP with determination by liquid chromatography were studied by Nielson. The extraction times ranged between 30 and 60 minutes for the ultrasonic bath and shorter times (20 minutes) were needed for microwave, with recoveries higher than 90% for Irganox 1010, Irgafos 168 and Cyasorb UV531. They carried out antioxidant extraction from LDPE within 20 minutes using dichloromethane as extractant, at temperatures lower than 50 °C, which is desirable when volatiles or easily degradable antioxidants such as BHT and phosphite esters are extracted.[20]

Two extraction methods that gave approximately the same yield were compared by Molander *et al*.[20] They comprise of a standard Soxhlet reference method with chloroform (3 h at 40 °C) and an extraction method by microwave energy using acetonitrile (30 min at 120 °C) as pre-treatment of the sample for the study of Irganox 1076 level in LDPE by temperature-programmed packed capillary liquid chromatography coupled to a UV detector.[20]

7.5 Additive stability during extraction

The stability of the additive under extraction conditions needs to be considered by example Irgafos 168 decays via oxidation and less frequently via hydrolysis to give DBP. According to El Mansouri *et al*., who studied the stability of phosphite in polar and polar solvents, the compound was not degraded when polar solvents, dichloromethane and toluene were employed. The evidence was provided by preparing an individual standard solution in DCM

submitted to the process of extraction by microwave energy. Measuring the concentration of the standard by LC before and after extraction did not make a significant difference and the recovery obtained after extracting was 98%, without a signal corresponding to the oxidized Irgafos 168 in the chromatogram. This means that degradation of the antioxidant during the extrusion process or in the life service of the final film is behind the presence of the oxidized Irgafos 168 in the chromatogram, rather than the analytical method.[20]

7.6 Analysis of additives in chromatography techniques

The possibility of compound identification is increased by analysis of polymer additives by mass spectrometry and related techniques. Conventional MS techniques, for example electron-impact ionization, CI, and GC-MS, are not usually suitable for analysis of high-molecular-weight additives of low volatility. Gas and liquid chromatography enables analysis of additives in polymers. GC coupled with MS detection enables both high-resolution chromatographic separation and highly specific and sensitive detection. It is evident that high-boiling-point additives require higher injection and elution temperatures, which can result in analytical artefacts as a result of thermal degradation. In addition, GC analysis of phenol-based flame retardants requires a derivatization step. The chromatographic specificity of LC is often lower than that of GC; and LC detectors are neither specific nor suitable for polar rather than non-polar samples. Most GC-based analytical methods are confined to and optimized for single groups of additives. Recent development in LC-MS techniques based on APCI, however, enable mass-specific detection of hydrophobic compounds, including flame retardants. Pyrolysis-gas chromatography is an important technique for analysis of polymers and large molecules. Mass spectrometry is one of the commonly used detection methods for identification and FID is one of the most frequently used detection techniques for quantitative analysis of pyrolyzates.[111]

Analytes were separated from the polymer matrix by dissolution in xylene then saponified by addition of 0.1 M KOH in methanol in work reported by Faraizadeh.[110] A gas chromatographic technique using a capillary column was presented for determination of Irganox 1010 and 1076 in PE and PP. Saponification products were separated on a Carbowax 20 M capillary column and monitored by FID. 3-(4-hydroxphenyl)propionic acid and acetyl alcohol were used as internal standards to increase the repeatability of the method. The technique was used for deciding antioxidants in the concentration range 0.02-2% in polymer sample. Additives were extracted by dissolving the polymer in boiling xylene and then saponified with methanolic KOH, with simultaneous precipitation of the polymer matrix. The filtrate was acidified and evaporated to dryness after filtration. The residue was then dissolved in xylene and 1 microlitre of this solution was injected into the GC. This method is relatively inexpensive, rapid, and simple in comparison with other methods reported in the literature.[111]

7.7 Optimal Additive Extraction Strategies

The best strategy to achieve the maximum extraction rates with a given solvent is to carry out the extraction in conditions causing the maximum swelling without dissolving the polymer. Extraction is not simple, as many variables need to be considered. The solvent must swell the polymer to dissolve the additives quantitatively. The choice of solvents is critically important: they must be dry and free of stabilizers to avoid any source of contamination, so they should be specified as HPLC grade. All glassware used also needs to be well washed to remove any residual contamination from earlier use. The selection of an extraction procedure depends on many important factors, such as the initial particle size of the samples, the nature of the additive (*M*w, polarity, shape), the stability of the analyte, the chemistry of the additive (interactions between additive and polymeric substrate), the solubility of the additive in the extraction solvent, the migration rate of the additive in the polymer (high molecular weight,

bulky additives diffuse more slowly), the diffusion rate of the solvent into the polymer (a function of density, degree of crystallinity and other factors; it is more difficult to extract additives from HDPE than from LDPE) and the conditions of the extraction process. Such important factors need to be considered if there is to be an effective extraction procedure with no degradation or modification of the extracted additives. Polymers are considered to be nonhomogeneous materials, so that a particle size reduction technique often needs to be applied (not for film) in order to obtain representative samples. It has also been observed that the extraction time increases linearly with polymer density and decreases with smaller particle size, so changing the physical state of the solid samples to provide a larger surface area per unit mass results in complete extraction in a reasonable time. There are many available methods for reducing particle size, such as crushing, cutting and grinding. Some sort of abrasion is involved in all particle size reduction techniques, so contamination by grinding tools is possible and needs to be considered. Great care is also needed during such processes to avoid alteration or loss of a volatile analyte.[119]

7.8 Experimental procedure

7.8.1 Sample preparation and extraction

As noted in the literature review, there are many extraction techniques available and a wide range of equipment on the market from the simplest and cheapest to the most complicated and expensive. Therefore, two different extraction techniques were evaluated in terms of cost and extraction efficiency, in order to decide whether it was possible to meet the requirements or if a combination of techniques would be recommended.

1. In refluxing toluene, with re-precipitation of the polymers by addition of methanol, which is highly recommended by Ciba[120] and,

2. Using an ultrasonic bath as an alternative extraction technique for comparison.

In the latter case, several factors were considered to optimize the extraction efficiency: solvent, temperature, grind (particle) size and extraction time. The extract was analyzed by reversed-phase HPLC using two different columns, different elution gradients and a UV photodiode array detector to identify and quantify the eluted analytes. The chromatogram was calibrated using mixed solutions of additives of known concentrations run under the same condition as the samples, following the internal standardization method for the first procedure (refluxing) and the external standardization method for the second procedure.

7.8.1.1 Refluxing toluene method

About 2 g of the polymer was weighed into a round or flat-bottomed flask. A magnetic stirring bar was added, followed by 48 ml HPLC grade toluene and 2 ml toluene containing Tinuvin 234 (internal standard). The flask was then placed on a reflux condenser and lowered into the heated (130 °C) oil bath to a level just above that of the toluene in the flask. The typical time for dissolution of polymer pellets to form a clear solution was 15 minutes for LLDPE and 30 minutes for HDPE. Once a solution had formed, the flask was lifted above the oil bath and allowed to cool to room temperature without stirring (typically 20 minutes). Next, 50 ml of methanol was added all at once to precipitate the dissolved polymer. The mixture was then shaken by hand until the precipitate was well dispersed (typically three minutes). The solid polymer was then removed by passing through filter paper and sufficient filtrate was collected into a 2 ml vial to be analyzed by reversed-phase HPLC.

7.8.1.2 Ultrasonic method

The polymer was first powdered to 0.2 mm particle size by cooling the sample in enough liquid nitrogen to cover it, topped up until the bubbling stopped. The chips were then added slowly and carefully to the grinder (ZM200) at a speed of 14,000 rpm. After that about 1 g of the powdered polymer was weighed into an HS vial (tightly sealed to avoid solvent loss). Then 10 ml HPLC grade chloroform (or a combination of solvents 75:25 chloroform:

cyclohexane for extraction of Irg. 1010 from HDPE) was added and the sample solution was agitated for 15 minutes using the shaker. Next, the vial containing sample solution was lowered into the ultrasonic bath to a level just above that of the chloroform in the vial and the mixture was shaken by hand every 15 minutes. The typical time for swelling the polymer was 85 minutes. Finally, 2 ml of the sample solution was filtrated through a 0.45 µm disposable syringe filter and collected into a 2 ml vial to be analyzed by reversed-phase HPLC.

7.9 Chromatograph calibration and standard preparation

For the internal standardization method, two stock solutions (A and B) of standards (certified reference materials) IRG 1076, IRG 1010, IRG 168 and Weston 399 in toluene were prepared by weighing about 50 mg of each into a 100 ml serum bottle with 50 g toluene. Using solution A, weighed portions were added by syringe to serum bottles containing 50 ml toluene (with ISTD) and 50 ml methanol: 0.25 g = 250 µg additive (125 ppm polymer basis), 1.00 g = 1000 µg = 500 ppm, 4.0 g = 4000 µg = 2000 ppm. Using solution B, the amounts were: 0.50 g = 500 µg = 250 ppm, 2.00 g = 2000 µg = 1000 ppm.

For the external standardization method, one stock solution of standards (certified reference materials) IRG 1076, IRG 1010, IRG 168 and Weston 399 in chloroform were prepared by weighing about 100 mg of each into a 200 ml serum bottle with 100 ml chloroform. Using the stock solution, 2 ml, 1 ml and 0.5 ml were poured into 10 ml volumetric flasks, which were filled to the mark with chloroform to prepare 2000 ppm, 1000 ppm and 500 ppm samples respectively. Then 2 ml of sample standard solution (1000 ppm) was poured into 10 ml volumetric flask, which was filled to the mark with chloroform to prepare a 100 ppm sample.

7.10 Separation procedure

The separation was performed in two different columns under different elution gradients. The chromatographic experiments were carried out on Waters HPLC system with a gradient pump and automatic injector. For the dissolution method, the analytes were separated using a stainless steel column 4.6 mm x 200 mm packed with C18, 50 µm particle size and the mobile phase were solvent A (75:25) (Methanol/Water) and solvent B (50:50) (Acetonitrile/Ethyl acetate).The chromatographic conditions are summarized in **Table 26** and a LC chromatogram obtained under these conditions is shown in **Fig. 74**.

Table 26 Elution gradient conditions for LC-UV diode-array analysis

Time (min)	Flow rate (ml/min)	Solvent A %	Solvent B%	Description
0	1.5	90	10	analysis
35	1.5	0	100	analysis
37	1.5	90	10	analysis
45	1.5	90	10	post time
50	0	90	10	run end, pump off
55				UV lamp off

A stainless steel column 4.6 mm x 200 mm packed with C18, 50 µm. Flow = 1 Ml min^{-1}. Wavelength = 270 nm. Column oven temperature: 40°C. Injection volume: 20 µL

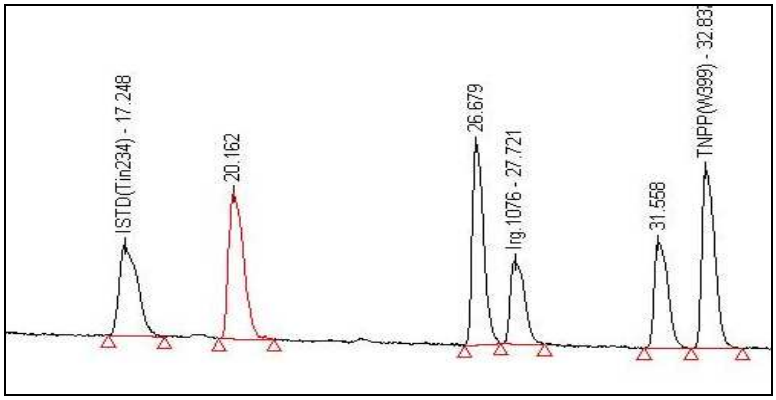

Figure 74 liquid chromatogram of ISTD (Tin234), IRG. 3114, IRG.1010, IRG.1076, Irgf. 168 and W399 (TNPP), respectively, obtained under conditions of Table 19. The x-axis is the retention time (minutes) and plotted on the y-axis a signal (absorbance).

For the Ultrasonic extraction method, the analytes were separated using a stainless steel column 4.6 mm x 150 mm packed with C18, 50 µm particle size and the mobile phase were solvent A (50:50) (Acetonitrile /Water) and solvent B (Acetonitrile). The chromatographic

conditions are summarized in **Table 27** and a LC chromatogram obtained under these conditions is shown in **Fig. 75**.

The signal acquired from the detector was recorded under the Millenium[32] software V.3.2. Quantification was carried out using a calibration plot of external standard for the Ultrasonic extraction method and using a calibration plot of internal standard for the Dissolution method. Calibration curves between 500 and 2000 mg/L were made for all of the additives of interest.

Table 27 Elution gradient conditions for LC-UV diode-array analysis

Time (min)	Flow rate (ml/min)	solvent A %	solvent B%	Description
0	2	80	20	analysis
6	2	0	100	analysis
20	2	0	100	analysis
21	2	80	20	post time
24	0	80	20	run end, pump off
25		80	20	UV lamp off

A stainless steel column 4.6 mm x 150 mm packed with C18, 50 µm. Flow = 2.0 Ml min^{-1}. Wavelength = 210 nm. Column oven temperature: 40°C. Injection volume: 10 µL

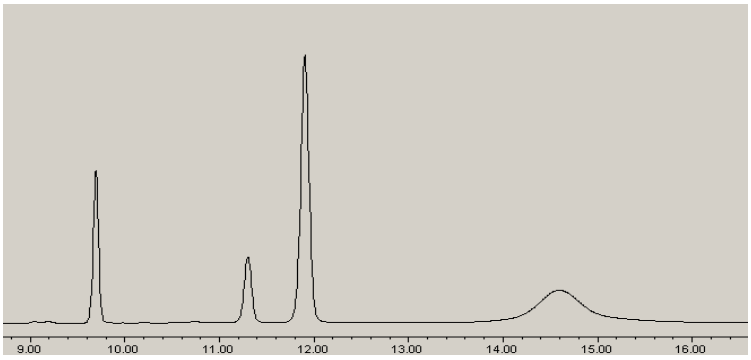

Figure 75 liquid chromatogram of IRG.1010, IRG.1076, IRG. 168 and W399 (TNPP), respectively, obtained under conditions of Table 20. The x-axis is the retention time (minutes) and plotted on the y-axis a signal (absorbance).

7.11 Results and discussion

The first stage was to maximise the extraction efficiency by optimizing the extraction conditions **(Tables 28-29)** for samples of HDPE and LLDPE resins blended in house with known amounts of additives. The results in **Table 28** show that the extraction efficiency was improved considerably from the original conditions (shown in grey). Optimized conditions show a marked increase in the recovery of Irganox 1010 in particular, from 12% recovery originally to 79% recovery optimized. A similar process was employed with LLDPE and **Table 29** shows that the improvement in extraction efficiency was not so marked in this case, as recovery was already around 80%. This initial stage suggests that powdering the polymer to less than 0.5 mm increases the surface in contact with the extracting solvent and raises the extraction yield. Chloroform swells polymers better and a solvent ratio of 75:25 chloroform: cyclohexane was used to extract Irganox 1010 in HDPE. In this combination of solvents, the purpose of the main solvent was to make the polymer swell, while the second solvent was used to complete the extraction and ensure a quantitative solubilisation of the additive in the solvent system. This method showed a marked increase in the recovery of Irganox 1010.

Table 28 Extraction recovery % at different extraction conditions for HDPE using ultrasonic bath

Additive Type			T °C		Particle Size (mm)		Solvent				Times (min)		
IRG 1010	IRG 1076	IRG 168	25	55	0.5	1	DCM	DCM/CH	CF	CF/CH	30	60	120
12	78	62	x			x	x						x
19	73	61	x			x		X					x
21	71	63		x	x			X			x		
23	77	67	x			x				x			x
31	83	74	x			x			x				x
55	75	70	x		x					x			x
61	74	71		x	x					x			x
76	76	68		x	x				x				x
57	87	83	x		x				x				x
68	87	80		x	x				x			x	
79	80	76		x	x					x		x	

Table 29 Extraction recovery % at different extraction conditions for LLDPE using ultrasonic bath

Additive Type			T °C		Particle Size (mm)		Solvent				Times (min)		
IRG 1010	IRG 1076	IRG 168	25	55	0.5	1	DCM	DCM/CH	CF	$CHCL_3$/CH	30	60	120
59	72	73	x			x		X					x
65	76	77	x			x				x			x
61	78	79	x			x	x						x
77	78	70		x	x					x		x	
78	78	70		x	x					x			x
71	82	84	x			x			x				x
92	93	81	x		x				x			x	
92	93	84	x		x				x			x	

The tables below **(Tables 30-38)** show the extraction results for the additives of interest in two different grades of PE samples and PP sample. These were commercial Sabic materials where the value of each additive was already known, allowing us to evaluate the extraction efficiency of both methods. In terms of recovery results, the agreement between the results of both procedures for both polyethylene grades seems very reasonable, while in terms of repeatability, sonication showed much better results. The repeatability of the results of the refluxing experiment was poor because the precipitation step had a quite large influence on the extraction yield. For that reason, the internal standard was used; otherwise the extraction yield might have dropped significantly. As it is not always easy to control this step and make it reproducible, such variation of results may sometimes arise from the difference in sample matrices (PP tends to precipitate in particles, while HDPE forms lumps) or because of the molecular weight and structure of the additives.

Table 30 Extraction of IRG 1010 from HDPE

HDPE	IRG 1010 (µg/g)	
	Refluxing	Ultrasonic bath
Replicate 1	1,282	1,600
Replicate 2	1,142	1,451
Replicate 3	1,641	1,422
Replicate 4	1,549	1,448
Replicate 5	1,227	1,426
Mean	1,368	1,469
STDEV	215	74
RSD	16	5

Table 31 Extraction of TNPP from HDPE

HDPE	TNPP (µg/g)	
	Refluxing	Ultrasonic bath
Replicate 1	859	797
Replicate 2	792	804
Replicate 3	934	805
Replicate 4	1076	875
Replicate 5	849	878
Mean	902	832
STDEV	110	41
RSD	12	5

Table 32 Extraction of IRG 1076 from HDPE

HDPE	IRG 1076 (µg/g)	
	Refluxing	Ultrasonic bath
Replicate 1	1082	1092
Replicate 2	1106	1088
Replicate 3	1178	1115
Replicate 4	1036	1093
Mean	1101	1097
STDEV	59	12
RSD	5	1

Table 33 Extraction of IRG168 from HDPE

HDPE	Irg 168 (µg/g)	
	Refluxing	Ultrasonic bath
Replicate 1	814	820
Replicate 2	765	789
Replicate 3	764	770
Replicate 4	766	794
Mean	777	793
STDEV	25	21
RSD	3	3

Table 34 Extraction of IRG 1076 from LLDPE

LLDPE	IRG 1076 (µg/g)	
	Refluxing	Ultrasonic bath
Replicate 1	665	660
Replicate 2	656	649
Replicate 3	611	646
Replicate 4	560	627
Replicate 5	567	651
Mean	612	647
STDEV	49	12
RSD	8	2

Table 35 Extraction of IRG 1010 from LLDPE

LLDPE	IRG 1010 (µg/g)	
	Refluxing	Ultrasonic bath
Replicate 1	514	556
Replicate 2	552	564
Replicate 3	510	635
Replicate 4	414	610
Replicate 5	470	551
Mean	492	583
STDEV	52	37
RSD	11	6

Table 36 Extraction of TNPP from LLDPE

LLDPE	TNPP (µg/g)	
	Refluxing	Ultrasonic bath
Replicate 1	686	614
Replicate 2	733	574
Replicate 3	784	605
Replicate 4	743	589
Mean	734	596
STDEV	49	18
RSD	7	3

Table 37 Extraction of IRG 168 from LLDPE

LLDPE	IRG 168 (µg/g)	
	Refluxing	Ultrasonic bath
Replicate 1	752	731
Replicate 2	744	714
Replicate 3	807	711
Replicate 4	672	696
Replicate 5	803	732
Mean	756	717
STDEV	55	15
RSD	7	2

Table 38 Extraction of IRG 1010 and IRG 168 from PP (refluxing method)

PP	IRG 1010 (µg/g)	IRG 168 (µg/g)
Replicate 1	215	675
Replicate 2	210	659
Replicate 3	206	636
Replicate 4	210	646
Mean	210	654
STDEV	4	17
RSD	1.8	3

7.12 Conclusion

It may be concluded from the above results that the use of an ultrasonic bath is highly recommended for the extraction of additives of interest from HDPE and LLDPE. It is a very simple, safe and rapid method, using little solvent or reagent, inexpensive in terms of apparatus cost and highly efficient (total extraction); it achieves quantitation without the need for an internal standard and has excellent repeatability. As for the mobile phase, three solvents are used in the method recommended by Ciba,[120] compared to one (acetonitrile) in the second separation method, which reduces the financial and environmental cost of using large volumes of solvents. Grinding PP samples to 0.2 mm particle size was difficult, as the material tends to melt during grinding, so a combination of techniques is recommended if analysis of additives is required for PE and PP samples.

Chapter 8: Conclusions

8.1 Conclusions

The aims of the research discussed in this thesis were: **1.** to establish a reliable characterization method to study the effect of the reaction conditions on the molecular characteristics of PIM-1 made by a series of polymerizations under different reaction conditions and the effect of the nature of the resultant product on its application, such as film forming ability; **2.** to establish fractionation procedure for fractionating the polymer (PIM-1) using solvent/non-solvent mixtures; **3.** to investigate low cost routes to high molar mass PIM-1; and **4.** to establish an inexpensive, rapid and simple method to measure quantitatively the additives contained in different grades of PE and in PP samples.

In conclusion, a reliable GPC method using multiple-detector GPC was successfully established and it was validated. It seems that there is a correlation between low M_w and low polydispersity. However, a significant degree of scatter within sets of replicate polymerizations makes further generalized conclusion on polydispersity difficult. Furthermore replicate syntheses are recommended to improve the statistical significant of the polydispersity data. The procedure to fractionate PIM-1 using chloroform methanol solvent mixtures was successfully established to provide 6 fractions of PDI ranging from 1.3 to 1.7, from an original sample of PDI 2.1 and its repeatability was proved. A low-cost route for the preparation of PIM-1 was successfully established using chloro-monomer. High molecular weight PIM-1 samples showed tailing off , both Mark-Houwink plots and hydrodynamic volume plots showed deviation from linearity at Mw = 200000 g mol^{-1}, which is possibly as a result of side reactions, suggesting that branching or cross-linking had occurred. Making a film from PIM-1 was found to be dependent on the average molecular weight results; 83000 g mol^{-1} is needed to form a very flexible free standing membrane.

For the additives extraction and characterization, the use of an ultrasonic bath is highly recommended for the extraction of additives of interest from HDPE and LLDPE and the refluxing method which is recommended by Ciba[120] could be used for PP samples.

References

1. J. C. Moore, *J. Polym. Sci.*, 1964, **Pt. B 2**, 835-843.

2. www.wikipedia.org, Accessed 15-11-2007

3. H. C. Benoit, *J. Polym. Sci., Part B: Polym. Phys.*, 1996, **34**, 1703-1704.

4. M. D. Zammit and T. P. Davis, *Polymer*, 1997, **38**, 4455-4468.

5. R. P. Chaplin, J. K. Haken and J. J. Paddon, *J. Chromatogr.*, 1979, **171**, 55-61.

6. S. R. Holding, *Endeavour*, 1984, **8**, 17-20.

7. S. Mori and M. Ishikawa, *J. Liq. Chromatogr. Relat. Technol.*, 1998, **21**, 1107-1117.

8. W.-J. Wang, S. Kharchenko, K. Migler and S. Zhu, *Polymer*, 2004, **45**, 6495-6505.

9. J. F. J. Coelho, P. M. F. O. Goncalves, D. Miranda and M. H. Gil, *Eur. Polym. J.*, 2006, **42**, 751-763.

10. P. M. Wood-Adams, J. M. Dealy, A. W. deGroot and O. D. Redwine, *Macromolecules*, 2000, **33**, 7489-7499.

11. C. Kim, J. Sainte Beuve, S. Guilbert and F. Bonfils, *Eur. Polym. J. FIELD Full Journal Title:European Polymer Journal*, 2009, **45**, 2249-2259.

12. M. A. Haney, *J. Appl. Polym. Sci.*, 1985, **30**, 3037-3049.

13. Y. Brun, M. V. Gorenstein and N. Hay, *J. Liq. Chromatogr. Relat. Technol.*, 2000, **23**, 2615-2639.

14. X. Lou, H.-G. Janssen and C. A. Cramers, *J. Microcolumn Sep. FIELD Full Journal Title:Journal of Microcolumn Separations*, 1995, **7**, 303-317.

15. H. J. Vandenburg, A. A. Clifford, K. D. Bartle, J. Carroll, I. Newton, L. M. Garden, J. R. Dean and C. T. Costley, *Analyst (Cambridge, U. K.)*, 1997, **122**, 101R-115R.

16. A. M. Pinto, MSc, Virginia Polytechnic Institute, State University, 1997.

17. B. Marcato and M. Vianello, *J Chromatogr A*, 2000, **869**, 285-300.

18. A. M. Wims and S. J. Swarin, *J. Appl. Polym. Sci.*, 1975, **19**, 1243-1256.

19. M. Thilen and R. Shishoo, *J. Appl. Polym. Sci.*, 2000, **76**, 938-946.

20. M. S. Dopico Garcia, J. M. Lopez V, R. Bouza, M. J. Abad, E. Gonzalez Soto and M. V. Gonzalez Rodriguez, *Anal. Chim. Acta*, 2004, **521**, 179-188.

21. J. Rouquerol, D. Avnir, C. W. Fairbridge, D. H. Everett, J. H. Haynes, N. Pernicone, J. D. F. Ramsay, K. S. W. Sing and K. K. Unger, *Pure Appl. Chem.*, 1994, **66**, 1739-1758.

22. K. S. W. Sing, D. H. Everett, R. A. W. Haul, L. Moscou, R. A. Pierotti, J. Rouquerol and T. Siemieniewska, *Pure Appl. Chem.*, 1985, **57**, 603-619.

23. E. Auer, A. Freund, J. Pietsch and T. Tacke, *Appl. Catal., A*, 1998, **173**, 259-271.

24. U. Mueller, M. Schubert, F. Teich, H. Puetter, K. Schierle-Arndt and J. Pastre, *J. Mater. Chem.*, 2006, **16**, 626-636.

25. S. Sircar, T. C. Golden and M. B. Rao, *Carbon*, 1996, **34**, 1-12.

26. H. Ghobarkar, O. Schaf and U. Guth, *Prog. Solid State Chem.*, 1999, **27**, 29-73.

27. N. B. McKeown and P. M. Budd, *Chem. Soc. Rev.*, 2006, **35**, 675-683.

28. N. B. McKeown, S. Makhseed and P. M. Budd, *Chem. Commun.* 2002, 2780-2781.

29. N. B. McKeown, S. Hanif, K. Msayib, C. E. Tattershall and P. M. Budd, *Chem. Commun.* 2002, 2782-2783.

30. P. M. Budd, B. Ghanem, K. Msayib, N. B. McKeown and C. Tattershall, *J. Mater. Chem.*, 2003, **13**, 2721-2726.

31. P. M. Budd, B. S. Ghanem, S. Makhseed, N. B. McKeown, K. J. Msayib and C. E. Tattershall, *Chem. Commun.*, 2004, 230-231.

32. A. V. Maffei, M. P. Budd and N. B. McKeown, *Langmuir*, 2006, **22**, 4225-4229.

33. N. Du, J. Song, G. P. Robertson, I. Pinnau and M. D. Guiver, *Macromol. Rapid Commun.*, 2008, **29**, 783-788.

34. N. B. McKeown, P. M. Budd, K. J. Msayib, B. S. Ghanem, H. J. Kingston, C. E. Tattershall, S. Makhseed, K. J. Reynolds and D. Fritsch, *Chem.--Eur. J.*, 2005, **11**, 2610-2620.

35. P. M. Budd, N. B. McKeown and D. Fritsch, *Macromol. Symp.*, 2006, **245/246**, 403-405.

36. P. M. Budd, E. S. Elabas, B. S. Ghanem, S. Makhseed, N. B. McKeown, K. J. Msayib, C. E. Tattershall and D. Wang, *Adv. Mater.* 2004, **16**, 456-459.

37. P. M. Budd, N. B. McKeown and D. Fritsch, *J. Mater. Chem.*, 2005, **15**, 1977-1986.

38. P. M. Budd, K. J. Msayib, C. E. Tattershall, B. S. Ghanem, K. J. Reynolds, N. B. McKeown and D. Fritsch, *J. Membr. Sci.*, 2005, **251**, 263-269.

39. H. R. Kricheldorf, D. Fritsch, L. Vakhtangishvili and G. Schwarz, *Macromol. Chem. Phys.*, 2005, **206**, 2239-2247.

40. H. R. Kricheldorf, N. Lomadze, D. Fritsch and G. Schwarz, *J. Polym. Sci., Part A: Polym. Chem.*, 2006, **44**, 5344-5352.

41. H. R. Kricheldorf and G. Schwarz, *Macromol. Rapid Commun.*, 2003, **24**, 359-381.

42. K. J. Reynolds, PhD Thesis, The University of Manchester, 2007.

43. N. B. McKeown, B. Gahnem, K. J. Msayib, P. M. Budd, C. E. Tattershall, K. Mahmood, S. Tan, D. Book, H. W. Langmi and A. Walton, *Angew. Chem., Int. Ed.*, 2006, **45**, 1804-1807.

44. P. J. Flory, *J. Am. Chem. Soc.*, 1936, **58**, 1877-1885.

45. A. D. Jenkins, P. Kratochvil, R. F. T. Stepto and U. W. Suter, *Pure Appl. Chem.*, 1996, **68**, 2287-2311.

46. G. ODIAN, *Principles of polymerization*, Third edn., JOHN WILEY & SONS, INC., United States of America, 1991.

47. P. A. Lovell and R. J. Young, *Introduction to polymers*, Second edn., CRC Press, United States of America, 1991.

48. H. R. Kricheldorf, *Macromol. Symp.*, 2003, **199**, 1-13.

49. K. Kostanski Leopold, M. Keller Douglas and E. Hamielec Archie, *J Biochem Biophys Methods*, 2004, **58**, 159-186.

50. W. W. Yau, J. J. Kirkland and D. D. Bly, *Modern size exclusion liquid chromatography practice of gel permeation and gel filtration chromatography*, John Wiley & Sons Inc., Canada, 1979.

51. J. A. M. Smit, J. A. P. P. Van Dijk, M. G. Mennen and M. Daoud, *Macromolecules*, 1992, **25**, 3585-3590.

52. G. Saunders, *LC-GC Eur.*, 2004, **17**, 650-652, 654-655.

53. P. R. H. K. Robards, P.E. Jackson, *Principles and Practice of Modern Chromatographic Methods*, Academic Press INC.

54. B. Trathnigg, *Prog. Polym. Sci.*, 1995, **20**, 615-650.

55. www.viscotek.com, Accessed 13-11-2007

56. www.waters.com, Accessed 19-11-2007

57. H. G. Barth, *LC-GC Eur.*, 2003, **16**, 46-50.

58. H. G. Barth, B. E. Boyes and C. Jackson, *Anal. Chem.*, 1996, **68**, 445-466.

59. R. Walkenhorst, *LC-GC Eur.*, 2001, **14**, 676-678.

60. T. Mourey, *Int. J. Polym. Anal. Charact.*, 2004, **9**, 97-135.

61. M. G. McKee, S. Unal, G. L. Wilkes and T. E. Long, *Prog. Polym. Sci.*, 2005, **30**, 507-539.

62. Y. Yu, P. J. DesLauriers and D. C. Rohlfing, *Polymer*, 2005, **46**, 5165-5182.

63. C. E. Ioan, T. Aberle and W. Burchard, *Macromolecules*, 1999, **32**, 7444-7453.

64. M. Gaborieau, J. Nicolas, M. Save, B. Charleux, J.-P. Vairon, R. G. Gilbert and P. Castignolles, *J. Chromatogr., A*, 2008, **1190**, 215-223.

65. T. Williams, *J. Mater. Sci.*, 1970, **5**, 811-820.

66. D. W. Shortt, *J. Chromatogr., A, A*, 1994, **686**, 11-20.

67. X. M. Liu, W. Gao, E. P. Maziarz, J. C. Salamone, J. Duex and E. Xia, *J. Chromatogr., A*, 2006, **1104**, 145-153.

68. U. Dayal, *J. Appl. Polym. Sci.*, 1992, **45**, 119-123.

69. B. Coto, J. M. Escola, I. Suarez and M. J. Caballero, *Polym. Test.*, 2007, **26**, 568-575.

70. P. J. Wyatt, *Anal. Chim. Acta*, 1993, **272**, 1-40.

71. Y. Brun, *J. Liq. Chromatogr. Relat. Technol.*, 1998, **21**, 1979-2015.

72. T. Takagi, *J. Chromatogr.*, 1990, **506**, 409-416.

73. T. Xie, J. Penelle and M. Verraver, *Polymer*, 2002, **43**, 3973-3977.

74. M. J. Leamen, N. T. McManus and A. Penlidis, *J. Appl. Polym. Sci.*, 2004, **94**, 2545-2547.

75. R. H. Chen and M. L. Tsaih, *Int. J. Biol. Macromol.*, 1998, **23**, 135-141.

76. www.wyatt.com, Accessed 15-11-2007

77. M. W. Dong, *Modern HPLC for Practicing Scientists*, John Wiley & Sons, INC., United States of America, 2006.

78. P. D. M. Joseph C. Arsenault, *Beginners Guide to Liquid Chromatography*, Waters Corporation, United States of America, 2007.

79. V. R. Meyer, *Practical High-Performance Liquid Chromatography*, Fourth edn., John Wiely & Sons, Great Britain, 2004.

80. www.radleys.co.uk, Accessed 15-05-2009

81. L. E. Grant, PhD, University of Manchester, 2006.

82. O. D. S. J. Throck Watson, *Introduction to Mass spectrometry Instrumentation, Applications and Strategies for Data Interpretation*, Fourth edn., John Wiley & Sons Ltd., Great Britain, 2007.

83. T. Ogawa, S. Tanaka and T. Inaba, *J. Appl. Polym. Sci.*, 1973, **17**, 319-331.

84. M. E. S. Habibe and M. C. A. Esperidiao, *J. Polym. Sci., Part B: Polym. Phys., Part B: Polymer Physics*, 1995, **33**, 759-767.

85. X. M. Liu, E. P. Maziarz and D. J. Heiler, *J. Chromatogr., A*, 2004, **1034**, 125-131.

86. B. S. Ghanem, N. B. McKeown, P. M. Budd, N. M. Al-Harbi, D. Fritsch, K. Heinrich, L. Starannikova, A. Tokarev and Y. Yampolskii, *Macromolecules*, 2009, **42**, 7881-7888.

87. Y. Tezuka, R. Komiya and M. Washizuka, *Macromolecules*, 2003, **36**, 12-17.

88. Y. Tezuka, A. Tsuchitani, Y. Yoshioka and H. Oike, *Macromolecules*, 2003, **36**, 65-70.

89. M. Schappacher and A. Deffieux, *Macromolecules*, 1992, **25**, 6744-6751.

90. B. Lepoittevin and P. Hemery, *J. Polym. Sci., Part A: Polym. Chem.*, 2001, **39**, 2723-2730.

91. J. Roovers and P. M. Toporowski, *J. Polym. Sci., Part B: Polym. Phys.*, 1988, **26**, 1251-1259.

92. A. C. Dagger and J. A. Semlyen, *Polymer*, 1999, **40**, 3243-3245.

93. H. Pasch, A. Deffieux, I. Henze, M. Schappacher and L. Rique-Lurbet, *Macromolecules*, 1996, **29**, 8776-8782.

94. B. Lepoittevin, M.-A. Dourges, M. Masure, P. Hemery, K. Baran and H. Cramail, *Macromolecules*, 2000, **33**, 8218-8224.

95. Y. Mengerink, R. Peters, C. G. deKoster, S. van der Wal, H. A. Claessens and C. A. Cramers, *J. Chromatogr.,* , 2001, **914**, 131-145.

96. W. Lee, H. Lee, H. C. Lee, D. Cho, T. Chang, A. A. Gorbunov and J. Roovers, *Macromolecules*, 2002, **35**, 529-538.

97. H. Oike, T. Mouri and Y. Tezuka, *Macromolecules*, 2001, **34**, 6592-6600.

98. M. T. R. Laguna, R. Medrano, M. P. Plana and M. P. Tarazona, *J. Chromatogr., A*, 2001, **919**, 13-19.

99. L. Guo and D. Zhang, *J. Am. Chem. Soc.*, 2009, **131**, 18072-18074.

100. P. V. Wright, *J. Polym. Sci., Polym. Phys. Ed.*, 1973, **11**, 51-64.

101. K. Dodgson and J. A. Semlyen, *Polymer*, 1977, **18**, 1265-1268.

102. D. E. Niehaus and C. Jackson, *Polymer*, 1999, **41**, 259-268.

103. P. Tackx and J. C. J. F. Tacx, *Polymer*, 1998, **39**, 3109-3113.

104. K. Tribe, G. Saunders and R. Meissner, *Macromol. Symp.*, 2006, **236**, 228-234.

105. J. Pannell, *Polymer*, 1972, **13**, 277-282.

106. K. Miyatake, A. R. Hlil and A. S. Hay, *Macromolecules*, 2001, **34**, 4288-4290.

107. J. Song, N. Du, Y. Dai, G. P. Robertson, M. D. Guiver, S. Thomas and I. Pinnau, *Macromolecules (Washington, DC, U. S.)*, 2008, **41**, 7411-7417.

108. Y. Ye, King III, R.E., in *Polymers, Laminations, Adhesives, Coatings and Extrusions*, TAPPI PLACE Editon edn., 2006.

109. M. A. Farajzadeh, M. Bahram and J. A. Joensson, *Anal. Chim. Acta*, 2007, **591**, 69-79.

110. J. Moeller, E. Stroemberg and S. Karlsson, *Eur. Polym. J.*, 2008, **44**, 1583-1593.

111. M. A. Farajzadeh, A. Nasserzadeh, A. Ranji and E. Feyz, *Chromatographia*, 2007, **65**, 223-227.

112. S. H. Smith and L. T. Taylor, *Chromatographia*, 2002, **56**, 165-169.

113. H. J. Vandenburg, A. A. Clifford, K. D. Bartle, J. Carroll and I. D. Newton, *Analyst*, 1999, **124**, 397-400.

114. N. Haider and S. Karlsson, *Analyst*, 1999, **124**, 797-800.

115. H. El Mansouri, N. Yagoubi and D. Ferrier, *Chromatographia*, 1998, **48**, 491-496.

116. T. Macko, B. Furtner and K. Lederer, *J. Appl. Polym. Sci.*, 1996, **62**, 2201-2207.

117. R. C. Nielson, *J. Liq. Chromatogr.*, 1991, **14**, 503-519.

118. W. Freitag and O. John, *Angew. Makromol. Chem.*, 1990, **175**, 181-185.

119. J. C. J. Bart, *Additives in polymers Industrial analysis and applications*, John Wiley & Sons, Ltd, Chichester, UK, 2005.

120 Confidential Ciba information communicated to SABIC.